
Electronic Thesis and Dissertation Repository

6-8-2015 12:00 AM

Reactivity of the middle cerebral artery to carbon dioxide

Nicole Coverdale, *The University of Western Ontario*

Supervisor: Dr. Kevin Shoemaker, *The University of Western Ontario*

A thesis submitted in partial fulfillment of the requirements for the Doctor of Philosophy degree
in Kinesiology

© Nicole Coverdale 2015

Follow this and additional works at: <https://ir.lib.uwo.ca/etd>



Part of the [Other Physiology Commons](#)

Recommended Citation

Coverdale, Nicole, "Reactivity of the middle cerebral artery to carbon dioxide" (2015). *Electronic Thesis and Dissertation Repository*. 2885.

<https://ir.lib.uwo.ca/etd/2885>

This Dissertation/Thesis is brought to you for free and open access by Scholarship@Western. It has been accepted for inclusion in Electronic Thesis and Dissertation Repository by an authorized administrator of Scholarship@Western. For more information, please contact wlsadmin@uwo.ca.

REACTIVITY OF THE MIDDLE CEREBRAL ARTERY TO CARBON DIOXIDE

(Thesis format: Integrated Article)

by

Nicole Sarah Coverdale

Graduate Program in Kinesiology

A thesis submitted in partial fulfillment
of the requirements for the degree of
Doctor of Philosophy

The School of Graduate and Postdoctoral Studies
The University of Western Ontario
London, Ontario, Canada

© Nicole S. Coverdale, 2015

Abstract

Transcranial Doppler ultrasound (TCD) is used for the assessment of cerebral blood flow velocity (CBFV) at the middle cerebral artery (MCA) with the assumption that diameter of the artery does not change. Thus, CBFV is equivalent to cerebral blood flow (CBF). The purpose of this thesis was determine if the MCA dilates during hypercapnia (HC) and/or constricts during hypocapnia (HO) in healthy young and older adults using 3T magnetic resonance imaging (MRI). We also determined how these changes in MCA cross-sectional area (CSA) influence estimates of CBF and cerebrovascular reactivity (CVR) from TCD in young and older adults. Lastly, we compared whether changes in MCA CSA mimic those at the internal carotid artery (ICA) as assessed with duplex ultrasound during HC and HO. For all studies, HC was induced with 6% carbon dioxide and HO with hyperventilation at 30 breaths per minute, each for five minutes. T2-weighted sagittal images of the MCA were performed with MRI and collection of an image took approximately one minute. When assessing the peak response there was a significant increase in MCA CSA during HC and a decrease during HO. Using these MCA CSA values to calculate CBF resulted in a greater percent change during each protocol compared to CBFV. Changes in MCA CSA were also examined every minute over the five minute periods of HC and HO and significant increases were seen within the first minute of HC while decreases during HO were not evident until minute four. No changes in ICA CSA occurred during HC or HO. Using CBF rather than CBFV to calculate CVR resulted in a greater CVR for each protocol. Finally, when the response to HC was compared between young and older adults the increase in MCA CSA was reduced in older adults compared to young. Cerebrovascular conductance was also reduced in older adults compared to young during HC, while CVR was not different. In summary, the diameter of the MCA changes during manipulations of carbon dioxide and CBFV underestimates CBF and CVR. Also, CVR may not be the best metric to compare the vasodilatory response to HC between groups.

Keywords

Transcranial Doppler ultrasound; Middle cerebral artery; Cerebral blood flow velocity;
Cerebral blood flow; Magnetic resonance imaging; Cerebrovascular reactivity

Co-Authorship Statement

Nicole S. Coverdale was the first author of the three papers that compose the body of this thesis and J. Kevin Shoemaker was the senior author. The co-authors on Chapter 2 were Joseph S. Gati, Oksana Opalevych, and Amanda Perrotta. The co-authors on Chapter 3 were Sophie Lalande and Amanda Perrotta. For Chapter 4 the co-author was Mark B. Badrov.

Specific contributions to the papers are listed as follows:

Conception and design: Nicole S. Coverdale, Joseph S. Gati, and Dr. J. Kevin Shoemaker

Data collection: Nicole S. Coverdale, Oksana Opalevych, Amanda Perrotta, Sophie Lalande, and Mark Badrov

Data analysis and interpretation: Nicole S. Coverdale and Dr. J. Kevin Shoemaker

Writing and revisions: Nicole S. Coverdale with revisions and feedback from all co-authors.

Epigraph

“All research requires patience and inspiration, and the results in themselves are difficult to estimate. They lead to other problems, and may inspire others with new ideas.”

- *Ida Henrietta Hyde*

Dedication

The completion of this thesis required hard work and dedication and this would not have been possible without the help of many people. I must thank my supervisor, Kevin, for setting a superior example of a mentor who is deeply invested in his students and has a passion for science that is highly motivating. I also owe many thanks to Kevin for bringing together a group of people in his lab who have become some of my best friends. Thank you to my lab mates for your constant support in research and in life.

Thank you to my family, Donna, John, and Jessica. Knowing that you are always behind me makes it much easier to dive into new adventures. Finally, to Matti, your unwavering support and belief in me means so much. I can't wait to see what the next chapter brings.

- *Nicole S. Coverdale*

Acknowledgments

I would like to acknowledge the technical assistance of Arlene Fleischhauer for performing phlebotomy for the paper that comprises Chapter 4 and Oksana Opalevych for performing magnetic resonance imaging for all studies.

Table of Contents

Abstract	ii
Co-Authorship Statement.....	iv
Epigraph.....	v
Dedication	vi
Acknowledgments.....	vii
Table of Contents	viii
List of Tables	xi
List of Figures	xii
List of Abbreviations	xiv
Chapter 1	1
1 Introduction	1
1.1 Overview.....	1
1.2 Anatomy of the Cerebral Vasculature.....	4
1.3 Quantification of Cerebral Blood Flow and Transcranial Doppler Ultrasound.....	8
1.3.1 Transcranial Doppler Ultrasound.....	8
1.4 Magnetic Resonance Imaging.....	11
1.5 Regulation of Cerebral Blood Flow	15
1.5.1 Carbon Dioxide	15
1.5.2 Blood Pressure	17
1.5.3 Neural Control	18
1.5.4 Metabolic Control	19
1.6 Cerebrovascular Reactivity and Aging.....	21
1.7 References.....	23
Chapter 2.....	345

2	Cerebral blood flow velocity underestimates cerebral blood flow during modest hypercapnia and hypocapnia	35
2.1	Introduction.....	35
2.2	Materials and Methods.....	36
2.2.1	Experimental Protocols.....	37
2.2.2	Measurements	37
2.2.3	Data Analysis	38
2.2.4	Statistical Analysis.....	39
2.3	Results.....	40
2.4	Discussion	55
2.5	References.....	59
	Chapter 3.....	63
3	Heterogeneous patterns of vasoreactivity in the middle cerebral and internal carotid arteries	63
3.1	Introduction.....	63
3.2	Materials and Methods.....	65
3.2.1	Experimental Protocols.....	65
3.2.2	Measurements	65
3.2.3	Data Analysis	66
3.2.4	Statistical Analysis.....	67
3.3	Results.....	68
3.4	Discussion	82
3.5	References.....	87
	Chapter 4.....	90
4	Role of the middle cerebral artery and grey matter volume in cerebrovascular changes with healthy aging	90
4.1	Introduction.....	90

4.2	Materials and Methods.....	92
4.2.1	Experimental Protocols.....	92
4.2.2	Measurements	93
4.2.3	Data Analysis	94
4.2.4	Statistical Analysis.....	95
4.3	Results.....	95
4.4	Discussion.....	108
4.5	References.....	112
5	General Discussion.....	116
5.1	Perspectives.....	116
5.2	Major Findings.....	116
5.3	Implications for Transcranial Doppler Ultrasound	120
5.4	Conclusions.....	121
5.5	References.....	122
	Appendix A: Ethics Approval.....	123
	Appendix B: Letters of Information and Consent Forms	126
	Appendix C: Rights of Authors of APS Articles	137
	Curriculum Vitae	139

List of Tables

Table 2.1: Physiological results during HC and HO in the lab and MRI.	43
Table 2.2: CBFV during HC and HO obtained from TCD and PC MRI.....	45
Table 3.1: Physiological responses to hypercapnia in the ICA and the MCA over time.	71
Table 3.2: Physiological responses to hypocapnia in the ICA and the MCA over time.....	73
Table 3.3: Physiological variables during hypercapnia and hypocapnia in the MRI session.	75
Table 3.4: Index of wall shear stress (dyn/cm ²) during hypercapnia and hypocapnia in the internal carotid (ICA) and middle cerebral artery (MCA).....	76
Table 4.1: Subject characteristics.	98
Table 4.2: Sex hormones in young and older adults.....	100
Table 4.3: Physiological characteristics at baseline and hypercapnia for Lab and MRI.	101
Table 4.4: Brain volume in young and older adults.....	103

List of Figures

Figure 1.1: The internal carotid and vertebral arteries: right side.....	6
Figure 1.2: The arteries of the base of the brain	7
Figure 1.3: Sagittal image of the spinal column with T ₂ contrast (left side) and T ₁ contrast (right side).....	12
Figure 2.1: Sagittal T2 baseline image through the right middle cerebral artery of a representative subject.....	46
Figure 2.2: Individual and mean changes in the CSA of the middle cerebral artery.....	47
Figure 2.3: Relationship between the change in ETCO ₂ and the change in middle cerebral artery CSA from HO to HC.....	48
Figure 2.4: Bland-Altman and scatter plots comparing TCD and PC CBFV over the range of end-tidal carbon dioxide values	49
Figure 2.5: Bland-Altman and scatter plots comparing TCD and PC CVR over the range of end-tidal carbon dioxide values	51
Figure 2.6: A: CBF during HC and HO calculated by multiplying the cross-sectional area of the MCA by TCD CBFV. B: Percent change in CBFV and CBF during HC and HO.....	53
Figure 2.7: Cerebrovascular reactivity expressed as percent change of CBFV and CBF divided by the change in end tidal carbon dioxide during HC and HO	54
Figure 3.1: Change in MCA and ICA indices during hypercapnia.....	77
Figure 3.2: Change in MCA and ICA indices during HO	79
Figure 3.3: Percent change of Q _{MCA} and MCA _v during changes in ETCO ₂	80
Figure 3.4: Cerebrovascular reactivity (CVR) over five minutes calculated from ICA _v , Q _{ICA} , MCA _v , and Q _{MCA} during manipulations of ETCO ₂	81

Figure 4.1: Middle cerebral artery cross-sectional area (CSA) during hypercapnia in young adults (YA) and older adults (OA).....	104
Figure 4.2: Cerebral blood flow velocity (CBFV) and cerebral blood flow (CBF) during hypercapnia in young adults (YA) and older adults (OA).....	105
Figure 4.3: Mean arterial pressure (A) and cerebrovascular conductance (B) at baseline and hypercapnia in young adults (YA) and older adults (OA).....	106
Figure 4.4: Cerebrovascular reactivity (CVR) at baseline and hypercapnia in young adults (YA) and older adults (OA)	107
Figure 5.1: Change in middle cerebral artery (MCA) cross-sectional area (CSA) during hypercapnia (A) and hypocapnia (B).	119

List of Abbreviations

ACA – Anterior cerebral artery

BP – Blood pressure

CA – Cerebral autoregulation

CBF – Cerebral blood flow

CBF_{GM} – Cerebral blood flow normalized to grey matter volume

CBFV – Cerebral blood flow velocity

CBFV_{GM} – Cerebral blood flow velocity normalized to grey matter volume

CO₂ – Carbon dioxide

CSA – Cross-sectional area

CVC – Cerebrovascular conductance

CVC_{GM} – Cerebrovascular conductance normalized to grey matter volume

CVR – Cerebrovascular reactivity

CVR_{GM} – Cerebrovascular reactivity to grey matter volume

ETCO₂ – End tidal carbon dioxide

GM – Grey matter

HC – Hypercapnia

HDL – High density lipoprotein

HO – Hypocapnia

ICA – Internal carotid artery

ICAv – Internal carotid artery velocity

ICC – Intraclass correlation coefficient

IMT – Intima-media thickness

K⁺ – Potassium

LDL – Low density lipoprotein

MAP – Mean arterial pressure

MCA – Middle cerebral artery

MCAv – Middle cerebral artery velocity

MRI – Magnetic resonance imaging

MoCA – Montreal cognitive assessment

NO – Nitric oxide

O₂ – Oxygen

OA – Older adults

P_aCO₂ – Arterial partial pressure of carbon dioxide

PC – Phase contrast

PCA – Posterior cerebral artery

PO₂ – Partial pressure of oxygen

Q_{ICA} – Internal carotid artery flow

Q_{MCA} – Middle cerebral artery flow

TCD – Transcranial Doppler ultrasound

V_{enc} – Velocity encoding factor

WM – White matter

WSS – Wall shear stress

YA – Young adults

Chapter 1

1 Introduction

1.1 Overview

In order to maintain cerebral function, blood flow is very tightly regulated to ensure adequate delivery of oxygen (O_2) and nutrients and removal of carbon dioxide (CO_2). Over a century of experimentation has contributed to our understanding of measurement and regulation of cerebral blood flow (CBF)(85). Despite these achievements, much work remains and is now potentially more important than ever as cerebrovascular function may play a role in the development of cognitive disorders such as dementia and Alzheimer's disease (86). For example, in the U.S., the prevalence of Alzheimer's disease is estimated to triple by 2050 (37). In this context, development of techniques to accurately quantify CBF and assess cerebrovascular function is vital.

Since its introduction in 1982 (2), transcranial Doppler ultrasound (TCD) has been used widely to quantify cerebral blood flow velocity (CBFV) during many experimental conditions including assessment of autoregulation, metabolic regulation of the cerebral vasculature by CO_2 and O_2 , with exercise, and to assess disease status. With TCD, the middle cerebral artery (MCA) is most commonly insonated. The three main branches coming off of the circle of Willis including the anterior cerebral artery (ACA), middle cerebral or posterior cerebral (PCA) arteries can be insonated with TCD. Transcranial Doppler ultrasound is relatively inexpensive, has excellent time resolution, and is quite user friendly (103) and all of these factors have made it a commonly used tool. With TCD, since the vessel being insonated cannot be visualized, a key assumption is that the diameter of the insonated vessel does not change; this assumption leads to the idea that CBFV estimates CBF.

Since the experiments of Kety and Schmidt (46, 47) the effect of "high CO_2 " or hypercapnia (HC) to increase CBF and "low CO_2 " or hypocapnia (HO) to decrease CBF have been measured and this response is termed cerebrovascular reactivity (CVR). Estimates of CVR have since been used to examine differences between clinical

populations in conditions such as migraine headache (54), diabetes (18) and transient ischemic attack (94), for example, and during healthy aging (107). Transcranial Doppler ultrasound is one method that is used to assess CVR and this estimate is used routinely to predict risk of stroke and transient ischemic events in individuals with carotid artery stenosis (32) and has been associated with all-cause mortality (79). Justification for the use of TCD to provide estimates of CBF during changing levels of end tidal CO₂ (ETCO₂) come from magnetic resonance imaging (MRI) studies at 1.5T which suggested that the MCA diameter does not change during HC or HO (89, 96). However, with a higher resolution MRI (3.0T), MCA dilation can be observed during hypoxia (106). Since the cerebral vasculature is generally more sensitive to the partial pressure of CO₂ (P_aCO₂) than the partial pressure of O₂ (PO₂) this could suggest that at a higher resolution a change in MCA diameter could be detected with MRI during changes in ETCO₂.

Additionally, a change in diameter of the internal carotid artery (ICA), which is the main branch that leads into the MCA, during HO and HC has been documented (104). This is an important finding for two reasons: 1) If the ICA changes diameter during manipulations of ETCO₂ it seems unlikely that the MCA diameter remains constant. 2) The diameter of the ICA can be determined using duplex ultrasound, which is a more readily available technology, whereas MRI is needed to examine MCA diameter. If changes in the ICA diameter mimic those that occur at the MCA then insonation of this vessel could prove useful for supplying a “correction factor” to estimate diameter changes at the MCA with changing ETCO₂. Overall, this assumption that MCA diameter is constant while ETCO₂ changes must be revisited now that advancements in MRI technology are available. This is important to establish first in a young and healthy population and then with a healthy aging and cardiovascular disease model since TCD is often used to estimate CVR in these groups.

The overall objectives of this research were to quantify MCA diameter reactivity, and thereby determine whether or not TCD can adequately quantify CBF and CVR in healthy young and older populations. The **working hypothesis** is that the MCA constricts during HO and dilates during HC, leading to an underestimation of CBF and CVR with TCD.

Study 1. Cerebral blood flow velocity underestimates cerebral blood flow during hypercapnia and hypocapnia.

Purpose: To determine whether the MCA constricts during HO and/or dilates during HC and to quantify the effect of such changes on CBF.

Hypothesis: The cross-sectional area (CSA) of the MCA will change during HO and/or HC.

Study 2. Heterogeneous patterns of vasoreactivity in the middle cerebral and internal carotid arteries.

Purpose: To determine the time course of the change in CSA and flow of the MCA and ICA over 5 minutes of HC and HO in healthy individuals and to study the contributions of MCA CSA data to the estimation of CVR values.

Hypothesis: The change in CSA during HC and HO will lead to an underestimation of CVR as traditionally calculated with CBFV. Additionally, changes in ICA CSA will mimic changes in the MCA during HO and HC.

Study 3. Role of the middle cerebral artery and grey matter volume in cerebrovascular changes with healthy aging.

Purpose: To assess the effect of healthy aging on MCA vasodilation, cerebrovascular reactivity, and cerebrovascular conductance during HC and to normalize these indices to grey matter volume.

Hypothesis: The older adults will have less of a vasodilatory response at the MCA compared to young controls and therefore have decreased CVR and CVC. Cerebral blood flow will be similar between young and older adults when normalized to grey matter volume.

1.2 Anatomy of the Cerebral Vasculature

The brain is supplied by four major arteries which eventually converge to form the circle of Willis. This system is unique to the brain, as opposed to other organs, in that blockade of one of these major arteries does not necessarily mean that adequate perfusion cannot be maintained to the entire brain. Outside of the cerebral circulation, large arteries are generally thought of as conduit vessels and arterioles as the regulator of vascular resistance. In the brain, the larger vessels have more involvement in regulating cerebrovascular resistance (22). For example, moving from the aorta to the pial arteries results in a 50 to 60% reduction in systemic pressure, and estimates suggest that larger cerebral arteries contribute anywhere from 20 to 60% of cerebrovascular resistance (22, 38).

Posteriorly, the two vertebral arteries unite intracranially to form the basilar artery (Figures 1.1 and 1.2). More anteriorly, the carotid arteries contribute the majority of blood supply to the brain, with each contributing approximately 40% to total perfusion (21). From the common carotid artery there is a bifurcation and the external carotid artery supplies blood to the facial region while the ICA enters the cranial cavity (Figure 1.1) and divides into four major branches: the ACA, MCA, anterior choroidal, and the posterior communicating arteries. From the ICA on each side the anterior cerebral arteries are joined by the anterior communicating artery and run parallel to one another to form the rostral portion of the circle of Willis. The posterior communicating arteries are the bridge between the rostral (carotid) circulation and the caudal (basilar) circulation and with the basilar artery forms the caudal portion of the circle of Willis (Figure 1.2). Interestingly, this “normal” layout of the circle of Willis was observed in just over half of human brains in a large sample so this anatomical layout is actually quite variable (4).

The largest branch originating from the basilar artery is the PCA which supplies the inferior and medial aspects of the temporal and occipital lobes (Figure 1.2)(21). The MCA supplies the lateral aspects of each cerebral hemisphere whereas the ACA supplies the medial aspects of the frontal and parietal lobes (21). From these main arteries there is continual branching until the final superficial pial arteries penetrate into the brain matter and are aptly named penetrating arteries (14). These arteries are surrounded by the

Virchow-Robin space and when this space disappears the arterioles are then known as parenchymal and become almost completely surrounded by the end-feet of glial cells known as astrocytes. Astrocytes play a role in the regulation of CBF and will be discussed further below (14).

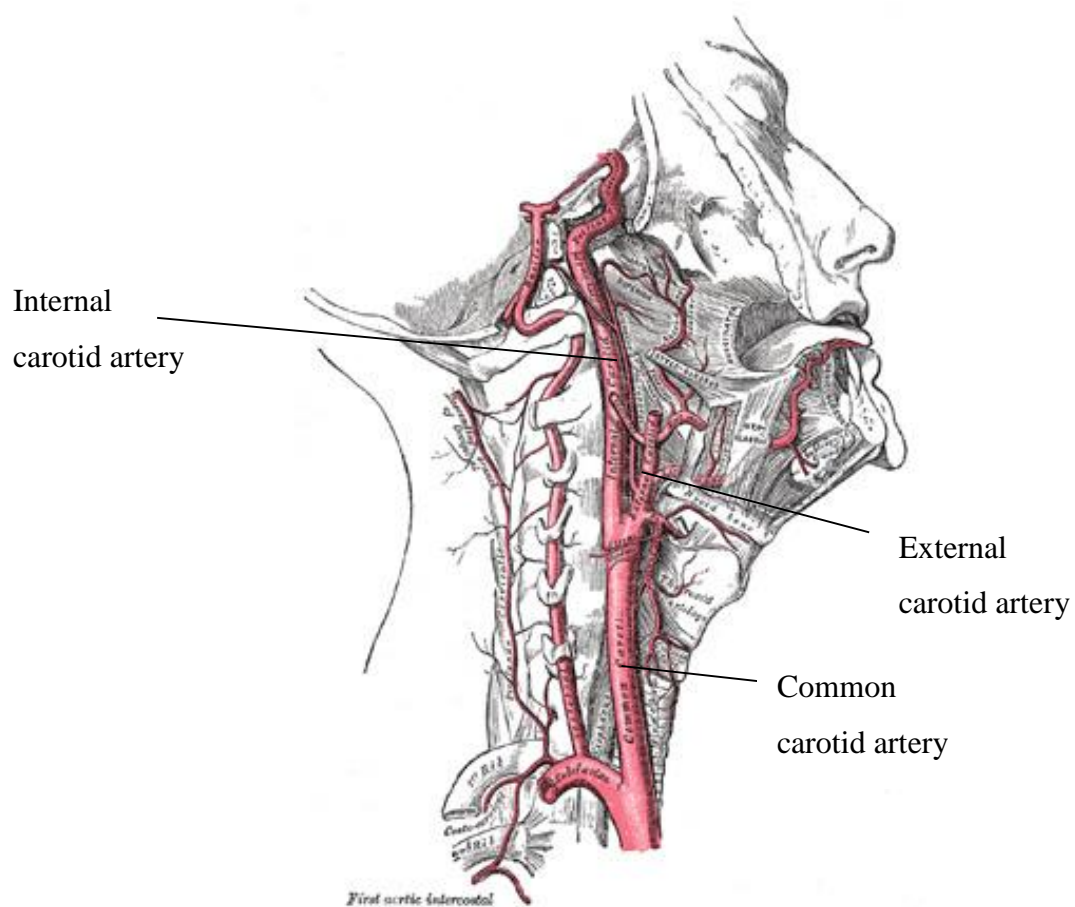


Figure 1.1: The internal carotid and vertebral arteries: right side. Reproduction of a lithograph plate from Gray's Anatomy from the 20th U.S. edition of *Gray's Anatomy of the Human Body*, originally published in 1918.

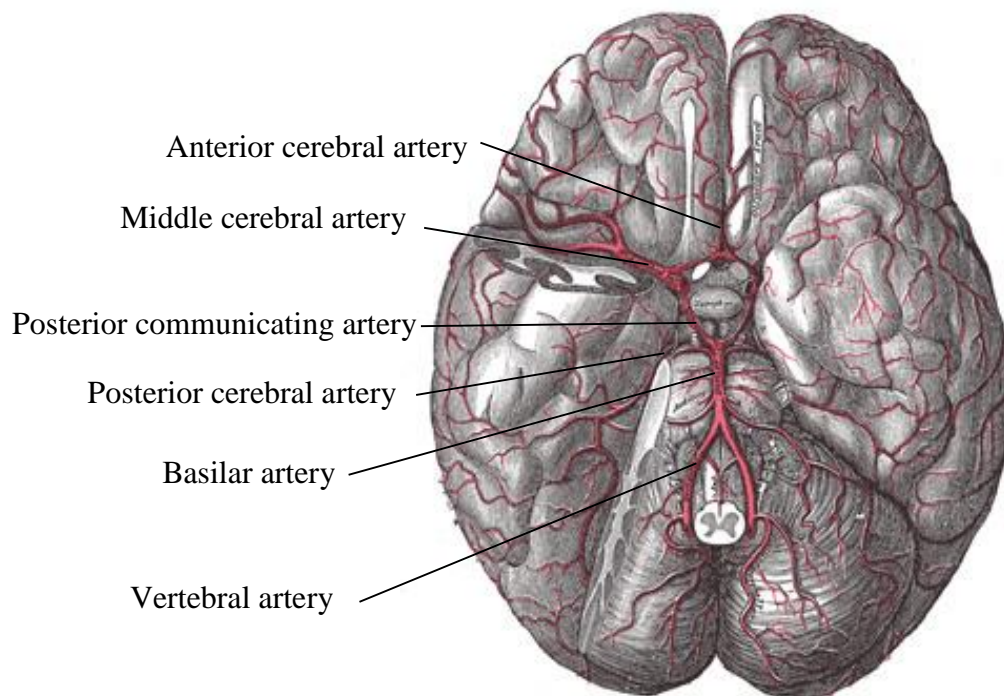


Figure 1.2: The arteries of the base of the brain. The temporal pole of the cerebrum and a portion of the cerebellar hemisphere have been removed on the right side. Reproduction of a lithograph plate from *Gray's Anatomy* from the 20th U.S. edition of *Gray's Anatomy of the Human Body*, originally published in 1918.

1.3 Quantification of Cerebral Blood Flow and Transcranial Doppler Ultrasound

Blood flow can be described by Poiseuille's law [1] and this law applies during laminar flow with Newtonian fluids in a rigid tube, where flow (Q) is proportional to the pressure change across the system (ΔP) and the radius of the tube to the fourth power (r) and is inversely proportional to the length of the tube (L) and viscosity of the fluid (μ). Within a system, during acute changes in Q it is generally assumed that μ and L do not change; thus, Q is determined by the pressure change and the change in r . The effect of r can also be thought of in terms of vascular resistance where Q is inversely proportional to resistance.

[1]

$$Q = \frac{\Delta P \pi r^4}{8 \mu L}$$

Early on, most techniques developed to measure CBF relied on inert or radioactive tracers and a modification of the Fick equation which states that the amount of a tracer taken up by a tissue per unit time is equal to the product of the blood flow through an organ and the arteriovenous difference of the tracer (16). Kety and Schmidt (1946) were the first to use this principle with inert nitrous oxide gas as the tracer (46). Since this time other non-invasive imaging techniques have been established and are used widely.

1.3.1 Transcranial Doppler Ultrasound

The methods discussed above that rely on the Fick equation give an overall estimation of CBF for the brain as a whole. In contrast, transcranial Doppler ultrasound (TCD) measures CBFV at the larger vessels that supply the brain with blood. The premise of Doppler ultrasound is that an ultrasound beam with a known emitted frequency makes contact with a moving red cell and this contact changes the frequency returning to the

receiver. Using this frequency information, which is known as the Doppler shift, the velocity of the red cell can be calculated using the following equation:

[2]

$$v = \frac{f_d \cdot c}{2f_t \cdot \cos \theta}$$

Where v is velocity, f_d is the detected frequency, c is the velocity of a sound wave through tissue, f_t is the transmitted frequency and θ is the angle of insonation (27). This principle was applied to the cerebral circulation as early as 1965 (68), during surgery or in children with open fontanels with the conventionally applied frequency of 5 to 10 MHz (2). This technique was modified to be usable in adults using a frequency of 2 MHz where there is less attenuation of signal by bone and soft tissues. This allows TCD to be applied at windows of the skull where bone is thinner. The most commonly used window is known as the transtemporal window of the temporal bone where TCD can be used to examine CBFV in the ACA, MCA, and PCA which are the three main arteries off of the circle of Willis (2). For the MCA, the first branch off of the circle of Willis (the M1 segment) is most commonly insonated and this is also the case for the A1 branch of the ACA (77). For the posterior circulation, two portions of the PCA can be insonated including P1, which is the segment between the basilar artery and the posterior cerebral collateral artery, and P2, which is the portion distal to the posterior cerebral collateral artery (103). The majority of studies examining the PCA focus on the P1 segment (78, 104). Knowledge of each of the three cerebral arteries average flow velocity, direction of flow, and average depth are used to locate each vessel during a routine TCD examination (103).

Quantification of CBF is possible with duplex ultrasound of the extracranial arteries of the neck as the Doppler signal is used to quantify CBFV and B-mode images are used to determine arterial diameter from which CBF can be calculated (61, 104). With TCD B-mode imaging can be done but it appears to overestimate arterial diameter compared to MRI measurements (106). Often, users of TCD assume that CBFV is equivalent to CBF and this is based on the belief that the diameter of the intracerebral

arteries (mainly the MCA) is constant. This assumption has been examined with MRI during manipulations of ETCO₂ and via direct observation during craniotomy. Two studies have examined MCA diameter at 1.5T during hyperventilatory HO and found no difference in MCA diameter during a decrease from baseline ETCO₂ by ~13 mmHg (89, 96). Serrador et al. (2000) also looked at HC to an ETCO₂ of ~45 mmHg and found no change in diameter (89). In this study, at 1.5 T, the resolution of the magnet was reported to be 0.47 mm. It is possible that changes in MCA diameter were not large enough to be detected at this resolution. When ETCO₂ was manipulated during craniotomy, the diameter change was 1.7% with a sample size of three (28).

Together, these findings described above led most researchers to interpret CBFV as CBF. However, conflicting evidence has been presented. For example, simultaneous recordings of MCA CBFV and venous outflow velocity from the sphenoparietal sinus during HC to ~55 mmHg indicated that venous outflow was higher than MCA CBFV which indicates dilation at the MCA (97). Also, when comparing ¹³³Xe clearance estimates to TCD CBFV during HC with 4 and 6% CO₂ (in O₂) CBF determined with ¹³³Xe clearance was greater than TCD CBFV estimates, inferring vasodilation (15). Lastly, Doppler power can be used to estimate vessel CSA based on the derivation of an equation by Arts and Roelvros (1972) used for determining blood flow (5). At the MCA, when Doppler power was used as an index of CSA during hypercapnic hypoxia (end tidal PO₂ was 50 mmHg and ETCO₂ was 8.5 to 9.5 mmHg above baseline), at the end of the stimulus, a significant increase in Doppler power was noted which the authors suggest is indicative that vasodilation had occurred (80). Notably, in this study neither HC or hypoxia alone had an effect on Doppler power (80). Also, comparison of Doppler power to vessel area in a flow phantom has raised questions as to whether power-based estimates of CSA are justifiable *in vivo* (19). Overall, the fact that some of these findings are inconsistent seems to indicate that the question of whether or not the MCA diameter is constant during HC and/or HO needs to be revisited.

1.4 Magnetic Resonance Imaging

In the context of this thesis, MRI is used for quantification of CBFV, determination of MCA CSA, and estimation of brain volume so the focus will be on details relevant to these techniques.

In the simplest terms, the basis for the MRI signal are the protons that lie within the abundant hydrogen atoms throughout the human body. Hydrogen nuclei intrinsically possess a nuclear spin that gives rise to a magnetic field for each proton. Normally these spins are pointing randomly but within the external magnetic field of the MRI they are all oriented in the same direction to form the net magnetization. The net magnetization is a vector with a transverse component (perpendicular to the magnetic field) and a longitudinal component (parallel or antiparallel to the magnet field). When a person is placed within the MRI, the transverse components cancel out so there is no net transverse magnetization but a longitudinal component is generated because there are more spins parallel to the field than antiparallel. However, no signal is actually generated until these spins are tipped away by what is called a radiofrequency pulse (usually by 90° to tip magnetization from fully longitudinal to fully transverse) from their original orientation; the recovery to their equilibrium state is where the MRI signal comes from. When magnetization is in the transverse direction the spins produce an oscillating electric current so signal is produced. After the spins have been tipped, the recovery of the longitudinal magnetization is described by a time constant known as T_1 . In the transverse direction, the spins lose coherence (are out of phase with one another) and the magnetization decays; this process is described by the time constant T_2 . An image is formed because different types of tissue have different T_1 and T_2 values (83). In T_2 -weighted images tissues with long T_2 values give the largest signal intensity so they appear to be bright. Fluids have the longest T_2 while water-based tissues have longer T_2 values than fat-based tissues (Figure 1.3)(65). In images with predominantly T_1 contrast, long T_1 tissues give the weakest signal so in this case, the brightest pixels are associated with short T_1 values. Any tissues with more water (and thus more protons) will appear dark and this type of scan is useful for showing anatomy (Figure 1.3) (65).



Figure 1.3: Sagittal image of the spinal column with T₂ contrast (left side) and T₁ contrast (right side). Image courtesy of GE Healthcare.

Phase contrast (PC) imaging can be used to determine CBFV and was first described by Moran in 1982 (70). This type of MRI is based on the principle that applied magnetic gradients introduce a phase shift in moving protons that is proportional to fluid velocity (9). With PC MRI two acquisitions need to be performed because the phase of the signal can depend on many factors. Therefore, it is necessary to collect one acquisition with a pulse sequence that is relatively insensitive to flow followed by one that is sensitive to flow over a particular range of velocities so that the two acquisitions can be subtracted. This should remove the effect of any dephasing due to other factors. The phase is unchanged for any protons that are not moving, thus the subtraction also suppresses any signal from background tissue (102). The maximum measurable velocity is a parameter selected by the operator, known as the encoding velocity (V_{enc}), which corresponds to a phase shift of 180° (69).

Estimates of CBFV derived from TCD have been compared to PC derived estimates, although few studies have looked at agreement between the two modalities beyond calculation of a correlation coefficient which is useful for detection of random error but does not detect systematic biases (62). Baledent et al. (2006) found small to moderate correlations between PC and TCD for peak systolic and end diastolic velocities in the MCA and absolute values for TCD were higher than for PC (9). Valdueza et al. (1997) also reported higher values of CBFV at rest and during hyperventilation with TCD (96). In the only examination to date looking at CVR to HC (from 40 mmHg at baseline to 45 mmHg) with PC MRI and TCD it was again reported that CBFV and CVR values derived from TCD were slightly higher and proportional bias was present where there was a larger difference between the two modalities at higher velocities (57). It remains to be seen how TCD and PC MRI may compare when velocities are examined over a wider range of $ETCO_2$.

MRI can also be used to examine structural properties of the cerebral blood vessels with angiography (magnetic resonance angiography). Magnetic resonance angiography relies on changes in the signal due to the flow of blood through or within the image plane. If, after the 90° pulse, another 180° pulse is applied then an image with T_2 contrast can be generated that has what is known as “black blood contrast” where the

blood appears dark and there is good contrast between the blood vessel walls and the blood (83). In contrast, if this 180° pulse is not applied, then the signal from flowing blood is visible and appears bright. This is the basis for time-of-flight magnetic resonance angiography (12).

Brain volume quantification is a technique used to detect structural differences of different brain tissues (grey matter, white matter, etc.) while discounting differences in positioning and larger scale differences in volume (6). The steps for determination of brain volume involve spatially normalizing a T_1 -weighted image of an individual brain to the group template. This process is a registration so that local areas stretch and compress with respect to one another to match the template image. The image is then segmented into tissue classes (gray matter, white matter and cerebrospinal fluid) and smoothed. This type of analysis has been applied to many areas of research. For example, the negative linear association grey matter volume and age has been characterized with this methodology (31).

1.5 Regulation of Cerebral Blood Flow

The regulation of CBF is complex and is dependent on many factors including the perfusion pressure of the brain, arterial blood gases, metabolic factors involved with neurovascular coupling, and the autonomic nervous system (105).

1.5.1 Carbon Dioxide

It is well established that alterations in $P_a\text{CO}_2$ have an effect on cerebral vessels that is unique to the cerebral circulation (3). Increased $P_a\text{CO}_2$ results in decreased tone in all cerebral vessels with the smaller vessels being most responsive. Hypocapnia causes a similar increase in tone in cerebral vessels of all sizes (100). Hypercapnia produces an increase in CBF that was first reported to be approximately 75% during inhalation of 5 to 7% CO_2 (47). Conversely, a decrease in $P_a\text{CO}_2$ causes a decrease in CBF which was first documented to be 32% during active hyperventilation (46). In general, during HO CBF decreases 2 to 3% per mmHg decrease in $P_a\text{CO}_2$ to a minimum level of ~10 to 15 mmHg. During HC the increase in CBF is approximately 3 to 4 % per mmHg increase in $P_a\text{CO}_2$ with its highest level at 10 to 20 mmHg above baseline (13). It was originally unclear whether $P_a\text{CO}_2$ itself was the stimulus for the change in CBF or whether the accompanying pH change initiated the response. Human studies ruled out the effect of arterial pH on vessel diameter (36, 53). Direct observation of pial arterioles in an anesthetized cat model have shown that the effect of CO_2 is mediated by a change in pH of the extracellular fluid (cerebrospinal fluid) rather than a change in $P_a\text{CO}_2$ (51).

The mechanism through which CO_2/pH affects vessel tone is not entirely clear and this is probably due to redundancy in the regulatory mechanisms. An inhibitory effect of protons on voltage dependent calcium channels has been suggested whereby their activation prevents calcium entry into the vascular smooth muscle cell (101). Additionally, potassium (K^+) channels have been proposed to play a role where their activation leads to hyperpolarization of the membrane, inhibition of calcium channels and vasodilation (73). Based on animal work, four types of K^+ channels have been identified on cerebral vessels including inward rectifier K^+ channels, delayed rectifier K^+ channels, ATP-sensitive K^+ channels, and calcium-sensitive K^+ channels (50). Of these, ATP-

sensitive K^+ channels and calcium activated K^+ channels likely play a major role (59). In animal studies, only combined inhibition of ATP-sensitive K^+ channels and calcium activated K^+ channels abolished hypercapnic vasodilation (59).

In addition to a direct action on various ion channels, it is possible that CO_2/pH exerts effects on cerebral vessels through vasoactive mediators. Nitric oxide (NO) likely plays a role in the flow response to HC since its blockade reduces the response (88, 99). Exogenous administration of a NO donor also increases the response to HC and diminishes the response to HO in humans (55). It appears that the source of NO, at least in a rodent model, is neuronal NO synthase, rather than the endothelium (58). However, there are also contradictory data that minimize the role that NO plays on CVR to CO_2 . Ide et al. (2007) reported that blockade of NO had no effect on the CBFV response to HC (42). It is possible that this is due to compensatory dilatory mechanisms that are upregulated when NO is blocked. Additionally, when nitrite and nitrate levels were examined (as surrogate estimates of NO), along with CVR, there was no correlation between the measurements (66).

Evidence from pigs suggests that prostenoids may play a permissive role during HC-induced increases in flow but on their own they are not likely the necessary mediator for vasodilation (56). Also, in humans, administration of the cyclooxygenase inhibitor indomethacin, reduces the CBFV response to HC (10). The conclusion from the bulk of this evidence is that we have some ideas as to how CO_2 exerts its effects on the cerebral circulation but there are still many questions that remain unanswered.

The vasoactive response in the brain to HC and HO has been utilized to estimate CVR and characterize cerebrovascular health. As stated previously, CVR is the change in CBFV or CBF to a change in P_aCO_2 and is generally quantified as the absolute or percent change in CBF (or CBFV) per change in P_aCO_2 (or $ETCO_2$). Cerebrovascular reactivity is thought to be an indicator of overall cerebral health and decreased CVR is associated with several pathological states including ischemic stroke in those with carotid occlusion (92), sleep-related disordered breathing (71), hypertension (90), multiple sclerosis (63), Alzheimer's disease (67), preeclampsia (87), and mortality in general (79).

Commonly, HO CVR is assessed during hyperventilation that reduces $P_a\text{CO}_2$. Alternatively, within the literature there are varying methodologies employed to increase $P_a\text{CO}_2$ including rebreathing (30), breath holding (45, 81), inhalation of 2 to 6% CO_2 in air (10, 84), inhalation of 5% CO_2 in 95% O_2 (referred to as carbogen) (44), and administration of acetazolamide (98), which increases $P_a\text{CO}_2$ by inhibiting the enzyme carbonic anhydrase. Benefits and drawbacks of each of these are summarized in a review by Fierstra et al. (2013)(23) and the authors conclude that the best option is CO_2 as a stimulus to examine CVR.

1.5.2 Blood Pressure

In general, cerebral perfusion pressure can be defined as the difference between mean arterial pressure (MAP) and intracranial pressure. For decades, students of physiology have been taught that CBF is protected against changes in MAP over the pressure range of approximately 60 to 150 mmHg and this concept is known as cerebral autoregulation (CA). Autoregulation can be examined in terms of the steady state relationship between CBF and MAP over minutes or hours and this is known as static CA (105). Alternatively the capacity of the cerebrovasculature to regulate the pressure-flow relationship to transient changes in MAP over several seconds or heart beats is known as dynamic CA (105). Based on an amalgamation of studies in patients, the concept of autoregulation was developed and only recently has it been questioned since studies in healthy humans do not support a system where CBF is completely protected against fluctuations in MAP (61). Not until technology was available in the 1980s to examine beat-by-beat measurements of MAP and CBF was it possible to examine more transient effects of MAP on CBF. Aaslid (1989) developed a thigh cuff method where occlusion of the thigh with rapid cuff release induced transient hypotension and it was observed that CBFV tracked the drop in MAP but recovered more quickly (1). This finding with others led to the development of the concept that CA acts as a high pass filter where higher frequency BP fluctuations are transferred to the cerebral circulation whereas the circulation is buffered against slower changes in MAP (108).

It should be noted that static versus dynamic CA are experimental rather than physiological classifications and it is likely that the mechanisms for static and dynamic

CA are similar. A close matching in the percent change in cerebrovascular resistance to slower, drug-induced changes in pressure and those that occur during the drop in MAP during thigh-cuff release has been described (95). The mechanisms through which cerebrovascular resistance is modified to maintain cerebral perfusion pressure are unclear at this time but likely include a combination of neurogenic, myogenic and possibly endothelial responses (93, 105). Interestingly, based on animal studies, it has been estimated that larger cerebral arteries contribute anywhere from 20 to 60% of cerebrovascular resistance at rest (22, 38).

Additionally, it is important to remember that factors like BP and CO₂ do not exert their effects on the cerebral blood vessels independently. There is an interplay between the role of MAP and CO₂ on the cerebral vasculature. This was first established in dogs where animals with a MAP of 100 mmHg had a less pronounced reaction to HC and HO than normotensive animals and at a MAP of 50 mmHg there was no change in CBF with HC or HO (35). Also, using CO₂ as a stimulus to examine CVR may also increase systemic MAP and possibly perfusion pressure. Battisti-Charbonney et al. (2011) observed that below a threshold ET_{CO}₂, MAP changed little, but above this, MAP increased linearly with ET_{CO}₂ (11). Therefore, it is important to report cerebrovascular conductance (CVC) in an attempt to account for the effect of MAP changes during a CVR test.

1.5.3 Neural Control

The cerebral vessels are densely innervated and the sources of innervation differ depending on the location of the vessel. The larger blood vessels that run along the surface of the brain are said to be innervated extrinsically by the superior cervical ganglion, the sphenopalatine and otic ganglia, and the trigeminal ganglion (33). The superior cervical ganglion provides sympathetic innervation and releases norepinephrine and neuropeptide Y. The sphenopalatine and otic ganglia are responsible for parasympathetic innervation and releases vasoactive intestinal polypeptide, NO, acetylcholine, among others. Lastly, the trigeminal ganglion is a source of sensory nerves that contain calcitonin gene-related polypeptide, substance P, neurokinin A, and others (33). The role of extrinsic sympathetic innervation in the brain is somewhat unclear as the

results of blockade studies in humans have been equivocal (41, 75). In contrast, ganglionectomy in patients with pathological conditions has resulted in increased CBF in the majority of studies (43, 91) though it is unclear how these findings may apply in a healthy population (48). In addition, the general consensus based on the body of literature suggests that sympathetic innervation may serve as a protective mechanism to shift the autoregulatory curve to higher pressure. This mechanism would protect the brain against increased pressure with sympathetic activation (33). For example, when norepinephrine was infused to raise pressure the change in cerebrovascular resistance that occurred was not present when phentolamine, which is a non-selective α -receptor blocker, was infused. Additionally, CBFV increased when norepinephrine and phentolamine were infused together indicating that CA was impaired (49).

As pial arteries enter the brain cortical tissue they lose this extrinsic nerve supply and receive inputs from neurons within the brain itself and this is termed “intrinsic innervation.” These smaller vessels receive nerve afferents from areas such as the locus coeruleus, raphe nucleus, and basal forebrain (14). However, this innervation does not interact directly with the vessel but is instead in contact with astrocytes surrounding the blood vessel (14). The best studied pathways involved in intrinsic innervation include release of acetylcholine from the nucleus basalis, norepinephrine from the locus coeruleus, and serotonin from the raphe nucleus (33). Receptors for these neurotransmitters are located on both astrocytes and on smooth muscle and/or endothelial cells of blood vessels (33). Complete description of these pathways is beyond the scope of this review but it should be noted that literature in this area focuses, out of necessity, on animal models and in some cases on brain slices. In this type of experimental set-up blood vessels are not pressurized and do not have intraluminal flow (33). This is a valuable experimental design to answer some questions about intrinsic innervation but applicability to the intact human cerebrovasculature is unclear.

1.5.4 Metabolic Control

Within the brain, blood flow increases to areas that are neuronally active and this relationship is termed neurovascular coupling. The distribution of CBF is coordinated to increase when activity in a certain brain region increases and this response is known as

functional hyperemia. The hyperemic response occurs within seconds and is very specific to the region that is neuronally active (17, 74). There is a close association between neurons, astrocytes and blood vessels within the cortex and together, these three components comprise the neurovascular unit. Functionally, this association allows delivery of substrates to support neuronal activation and removal of metabolic by-products (40).

The mechanisms that are involved neurovascular regulation are still a topic of study but it is clear that there is involvement by neurons, astrocytes and vascular cells (40). Initially, it was proposed that a reduction in glucose or oxygen triggered by neuronal activation may trigger the blood flow response. However, further research indicated that it is likely synaptic signaling and not an energy deficit that triggers the flow response (7). There are several chemical mediators that have been proposed to be involved in stimulating the functional hyperemic response and this list includes ions, neurotransmitters, vasoactive factors that are released in response to neurotransmitters, and metabolic by-products (29). However, in blockade experiments, inhibiting one candidate mediator does not completely inhibit the response which indicates that there may be mechanistic redundancy or that some combination of the proposed mediators are involved in the response (40). One mechanism that is fairly well established to play a role in the hyperemic response is activation of glutamate receptors through synaptic transmission that initiates release of NO (39) and increases calcium in astrocytic end-feet that leads to release of other vasoactive mediators including prostenoids (40), of which some derivatives lead to vasodilation while others cause constriction (39). Which pathway predominates at any given time remains unclear but is likely regulated by another mediator such as lactate, adenosine, or the level of oxygen (39). From the local area where there is an up regulation in flow associated with neuronal activation upstream arteries also dilate to prevent a drop in microvascular pressure and avoid a 'steal' from adjacent areas (22). Overall, the mechanisms involved in neurovascular coupling remain unclear and require further study, especially in humans. The issue is further complicated because the mechanisms of functional hyperemia may differ from one brain location to another (40). For example, in the cerebellum CBF increases are highly dependent on NO

synthase but in the somatosensory cortex NO synthase-related mechanisms play a less prominent role (20).

1.6 Cerebrovascular Reactivity and Aging

As mentioned previously, CVR is decreased with many pathological conditions. However, the evidence related to healthy aging and CVR is mixed with some studies reporting that CVR is reduced with healthy aging (10, 25, 60), maintained (26, 72), increased (109), or different between sexes (44, 64). These differences likely are due to a number of factors including the age range of the subject pool, the stimulus used to assess CVR, sex differences, and possibly the way that the data are presented.

A large scale epidemiological study was conducted by Bakker et al. (2004) that examined CVR in adults grouped by decade up until the age of 90 reported a 0.08% per mmHg decrease per year (8). Therefore, studies that use an older population are probably more likely to find a difference in CVR compared to a young group. Additionally, the literature on CVR is complicated by the use of 5% CO₂ in 95% oxygen (known as carbogen) as a stimulus (8, 44, 60). This is problematic because a constrictive effect from the hyperoxia may counteract vasodilation due to HC (24). For example, when CVR was determined by two imaging methods, using the blood oxygen level dependent signal and arterial spin labelling, there was agreement between methods when CO₂ in air was the stimulus and agreement with blood oxygen level dependent imaging carbogen estimates of CVR. However, the CVR values determined with arterial spin labelling and carbogen did not agree with other estimates (34). Lastly, when CO₂ in air is used as the stimulus, different percentages of CO₂ have been used in the literature ranging from 2% to 7% (10, 72, 76, 82, 107). This difference makes comparison between studies more challenging.

Some studies have reported that there are sex differences in CVR. Bakker et al. (2004) examined CVR in older adults aged 55 years and older and found that CVR was greater in men (8). Additionally, declining CVR in women with age but no effect in men has been reported (44). Similarly, Matteis et al. (1998) reported that CVR, as assessed by the breath-holding index, was lower in post-menopausal women compared to younger

premenopausal women and young and older men (64). Significant differences in CVR have also been reported across the menstrual cycle (52) yet very few studies take this into account when choosing young female subjects.

The reporting of CVR in terms of absolute values or percent change further complicates study findings. For example, Oudegeest-Sander et al. (2014) examined CVR in young, elderly, and older elderly groups and found no difference in CVR expressed in relative terms but a difference in absolute values (76). Since there is no standardized metric that is preferred then both absolute and relative CVR should be presented. Lastly, the majority of studies described here have utilized TCD, and therefore, have measured CBFV not CBF. If the MCA dilates during HC and/or constricts during HO to a different extent in young and older subjects then using CBFV alone may disguise any differences between the groups. In summary, the question of whether or not aging is related to diminished CVR should be revisited due to the limitations in the previous research described above.

1.7 References

1. Aaslid R, Lindegaard K, Sorteberg W, Nornes H. Cerebral autoregulation dynamics in humans. *Stroke* 20: 45–52, 1989.
2. Aaslid R, Markwalder TM, Nornes H. Noninvasive transcranial Doppler ultrasound recording of flow velocity in basal cerebral arteries. *J Neurosurg* 57: 769–774, 1982.
3. Ainslie PN, Ashmead JC, Ide K, Morgan BJ, Poulin MJ. Differential responses to CO₂ and sympathetic stimulation in the cerebral and femoral circulations in humans. *J Physiol* 566: 613–624, 2005.
4. Alpers B, Berry R, Paddison R. Anatomical studies of the circle of Willis in normal brain. *Arch Neurol Psychiatry* 81: 409–418, 1959.
5. Arts M, Roelvros J. On the instantaneous measurement of blood flow by ultrasonic means. *Med Biol Eng* 10: 23–34, 1972.
6. Ashburner J, Friston KJ. Why voxel-based morphometry should be used. *Neuroimage* 14: 1238–1243, 2001.
7. Attwell D, Iadecola C. The neural basis of functional brain imaging signals. *Trends Neurosci* 25: 621–625, 2002.
8. Bakker SL, de Leeuw FE, den Heijer T, Koudstaal PJ, Hofman A, Breteler MM. Cerebral haemodynamics in the elderly: the rotterdam study. *Neuroepidemiology* 23: 178–184, 2004.
9. Baledent O, Fin L, Khuoy L, Ambarki K, Gauvin AC, Gondry-Jouet C, Meyer ME. Brain hydrodynamics study by phase-contrast magnetic resonance imaging and transcranial color doppler. *J Magn Reson Imaging* 24: 995–1004, 2006.

10. Barnes JN, Schmidt JE, Nicholson WT, Joyner MJ. Cyclooxygenase inhibition abolishes age-related differences in cerebral vasodilator responses to hypercapnia. *J Appl Physiol* 112: 1884–1890, 2012.
11. Battisti-Charbonney A, Fisher J, Duffin J. The cerebrovascular response to carbon dioxide in humans. *J Physiol* 589: 3039–3048, 2011.
12. Biglands JD, Radjenovic A, Ridgway JP. Cardiovascular magnetic resonance physics for clinicians: Part II. *J Cardiovasc Magn Reson* 14: 66, 2012.
13. Brugniaux J, Hodges A, Hanly P, Poulin M. Cerebrovascular responses to altitude. *Respir Physiol Neurobiol* 158: 212–223, 2007.
14. Cipolla J. The Cerebral Circulation. San Rafael, CA: Morgan & Claypool Life Sciences, 2009.
15. Clark JM, Skolnick BE, Gelfand R, Farber RE, Stierheim M, Stevens WC, Beck G, Lambertsen CJ. Relationship of ^{133}Xe cerebral blood flow to middle cerebral arterial flow velocity in men at rest. *J Cereb blood flow Metab* 16: 1255–1262, 1996.
16. Coles JP. Imaging of cerebral blood flow and metabolism. *Curr Opin Anaesthesiol* 19: 473–480, 2006.
17. Cox SB, Woolsey TA, Rovainen CM. Localized dynamic changes in cortical blood flow with whisker stimulation corresponds to matched vascular and neuronal architecture of rat barrels. *J Cereb Blood Flow Metab* 13: 899–913, 1993.
18. Dandona P, James IM, Newbury PA, Woollard ML, Beckett AG. Cerebral blood flow in diabetes mellitus: evidence of abnormal cerebrovascular reactivity. *Br Med J* 2: 325–326, 1978.
19. Deverson S, Evans D. Using doppler signal power to detect changes in vessel size: a feasibility study using a wall-less flow phantom. *Ultrasound Med Biol* 26: 593–602, 2000.

20. Drake CT, Iadecola C. The role of neuronal signaling in controlling cerebral blood flow. *Brain Lang* 102: 141–52, 2007.
21. Edvinsson L, Krause D. *Cerebral Blood Flow and Metabolism*. 2nd ed. Philadelphia, PA: Lippincott Williams & Wilkins, 2002.
22. Faraci FM, Heistad DD. Regulation of large cerebral arteries and cerebral microvascular pressure. *Circ Res* 66: 8–17, 1990.
23. Fierstra J, Sobczyk O, Battisti-Charbonney A, Mandell DM, Poublanc J, Crawley AP, Mikulis DJ, Duffin J, Fisher JA. Measuring cerebrovascular reactivity: what stimulus to use? *J Physiol* 591: 5809–5821, 2013.
24. Floyd TF, Clark JM, Gelfand R, Detre JA, Ratcliffe S, Guvakov D, Lambertsen CJ, Eckenhoff RG. Independent cerebral vasoconstrictive effects of hyperoxia and accompanying arterial hypocapnia at 1 ATA. *J Appl Physiol* 95: 2453–2461, 2003.
25. Fluck D, Beaudin AE, Steinback CD, Kumarpillai G, Shobha N, McCreary CR, Peca S, Smith EE, Poulin MJ. Effects of aging on the association between cerebrovascular responses to visual stimulation, hypercapnia and arterial stiffness. *Front Physiol* 5: 49, 2014.
26. Galvin SD, Celi LA, Thomas KN, Clendon TR, Galvin IF, Bunton RW, Ainslie PN. Effects of age and coronary artery disease on cerebrovascular reactivity to carbon dioxide in humans. *Anaesth Intensive Care* 38: 710–717, 2010.
27. Gill RW. Measurement of blood flow by ultrasound: accuracy and sources of error. *Ultrasound Med Biol* 11: 625–641, 1985.
28. Giller CA, Bowman G, Dyer H, Mootz L, Krippner W. Cerebral arterial diameters during changes in blood pressure and carbon dioxide during craniotomy. *Neurosurgery* 32: 732–737, 1993.
29. Girouard H, Iadecola C. Neurovascular coupling in the normal brain and in hypertension, stroke, and Alzheimer disease. *J Appl Physiol* 100: 328–335, 2006.

30. Glodzik L, Rusinek H, Brys M, Tsui WH, Switalski R, Mosconi L, Mistur R, Pirraglia E, de Santi S, Li Y, Goldowsky A, de Leon MJ. Framingham cardiovascular risk profile correlates with impaired hippocampal and cortical vasoreactivity to hypercapnia. *J Cereb blood flow Metab* 31: 671–689, 2011.
31. Good CD, Johnsrude IS, Ashburner J, Henson RN, Friston KJ, Frackowiak RS. A voxel-based morphometric study of ageing in 465 normal adult human brains. *Neuroimage* 14: 21–36, 2001.
32. Gupta A, Chazen JL, Hartman M, Delgado D, Anumula N, Shao H, Mazumdar M, Segal AZ, Kamel H, Leifer D, Sanelli PC. Cerebrovascular reserve and stroke risk in patients with carotid stenosis or occlusion: a systematic review and meta-analysis. *Stroke* 43: 2884–2891, 2012.
33. Hamel E. Perivascular nerves and the regulation of cerebrovascular tone. *J Appl Physiol* 100: 1059–1064, 2006.
34. Hare HV, Germuska M, Kelly ME, Bulte DP. Comparison of CO₂ in air versus carbogen for the measurement of cerebrovascular reactivity with magnetic resonance imaging. *J Cereb Blood Flow Metab* 33: 1799–1805, 2013.
35. Harper AM, Glass HI. Effect of alterations in the arterial carbon dioxide tension on the blood flow through the cerebral cortex at normal and low arterial blood pressures. *J Neurol Neurosurg Psychiatry* 28: 449–452, 1965.
36. Harper AM, Bell RA. The effect of metabolic acidosis and alkalosis on the blood flow through the cerebral cortex. *J Neurol Neurosurg Psychiatry* 26: 341–344, 1963.
37. Hebert L, Weuve J, Scherr P, Evans D. Alzheimer disease in the United States (2010-2050) estimated using the 2010 census. *Neurology* 80: 1778–1783, 2013.
38. Heistad DD, Marcus ML, Abboud FM. Role of large arteries in regulation of cerebral blood flow in dogs. *J Clin Invest* 62: 761–768, 1978.

39. Howarth C. The contribution of astrocytes to the regulation of cerebral blood flow. *Front Neurosci* 8: 1–9, 2014.
40. Iadecola C. Neurovascular regulation in the normal brain and in Alzheimer's disease. *Nat Rev Neurosci* 5: 347–360, 2004.
41. Ide K, Secher NH. Cerebral blood flow and metabolism during exercise. *Prog Neurobiol* 61: 397–414, 2000.
42. Ide K, Worthley M, Anderson T, Poulin MJ. Effects of the nitric oxide synthase inhibitor L-NMMA on cerebrovascular and cardiovascular responses to hypoxia and hypercapnia in humans. *J Physiol* 584: 321–332, 2007.
43. Jeng JS, Yip PK, Huang SJ, Kao MC. Changes in hemodynamics of the carotid and middle cerebral arteries before and after endoscopic sympathectomy in patients with palmar hyperhidrosis: preliminary results. *J Neurosurg* 90: 463–467, 1999.
44. Kastrup A, Dichgans J, Niemeier M, Schabet M. Changes of cerebrovascular CO₂ reactivity during normal aging. *Stroke* 29: 1311–1314, 1998.
45. Kastrup A, Kru G, Neumann-Haefelin T, Moseley ME. Assessment of cerebrovascular reactivity with functional magnetic resonance imaging : comparison of CO₂ and breath holding. *Magn Reson Imaging* 19: 13–20, 2001.
46. Kety SS, Schmidt CF. The effects of active and passive hyperventilation on cerebral blood flow, cerebral oxygen consumption, cardiac output, and blood pressure of normal young men. *J Clin Invest* 25: 107–119, 1946.
47. Kety SS, Schmidt CF. The effects of altered arterial tensions of carbon dioxide and oxygen on cerebral blood flow and cerebral oxygen consumption of normal young men. *J Clin Invest* 27: 484–492, 1948.

48. Kimmerly DS, Shoemaker JK. Hypovolemia and MSNA discharge patterns: assessing and interpreting sympathetic responses. *Am J Physiol Heart Circ Physiol* 284: H1198–204, 2003.
49. Kimmerly DS, Tutungi E, Wilson TD, Serrador JM, Gelb a. W, Hughson RL, Shoemaker JK. Circulating norepinephrine and cerebrovascular control in conscious humans. *Clin Physiol Funct Imaging* 23: 314–319, 2003.
50. Kitazono T, Faraci F, Taguchi H, Heistad DD. Role of potassium channels in cerebral blood vessels. *Stroke* 26: 1713–1723, 1995.
51. Kontos HA, Raper AJ, Patterson JL. Analysis of vasoactivity of local pH, PCO₂ and bicarbonate on pial vessels. *Stroke* 8: 358–360, 1977.
52. Krejza J, Rudzinski W, Arkuszewski M, Onuoha O, Melhem ER. Cerebrovascular reactivity across the menstrual cycle in young healthy women. *Neuroradiol J* 26: 413–419, 2013.
53. Lambertsen CJ, Semple SJ, Smyth MG, Gelfand R. H and pCO₂ as chemical factors in respiratory and cerebral circulatory control. *J Appl Physiol* 16: 473–484, 1961.
54. Lauritzen M, Olsen TS, Lassen NA, Paulson OB. Regulation of regional cerebral blood flow during and between migraine attacks. *Ann Neurol* 14: 569–572, 1983.
55. Lavi S, Egbarya R, Lavi R, Jacob G. Role of nitric oxide in the regulation of cerebral blood flow in humans: chemoregulation versus mechanoregulation. *Circulation* 107: 1901–1905, 2003.
56. Leffler C, Mirro R, Pharris L, Shibata M. Permissive role of prostacyclin in cerebral vasodilation to hypercapnia in newborn pigs. *Am J Physiol* 267: H285–H291, 1994.
57. Leung J, Behpour A, Sokol N, Mohanta A, Kassner A. Assessment of intracranial blood flow velocities using a computer controlled vasoactive stimulus: a

- comparison between phase contrast magnetic resonance angiography and transcranial Doppler ultrasonography. *J Magn Reson Imaging* 38: 733–738, 2013.
58. Lindauer U, Kunz A, Schuh-Hofer S, Vogt J, Dreier JP, Dirnagl U. Nitric oxide from perivascular nerves modulates cerebral arterial pH reactivity. *Am J Physiol Circ Physiol* 281: H1353–1363, 2001.
 59. Lindauer U, Vogt J, Schuh-Hofer S, Dreier JP, Dirnagl U. Cerebrovascular vasodilation to extraluminal acidosis occurs via combined activation of ATP-sensitive and Ca^{2+} -activated potassium channels. *J Cereb Blood Flow Metab* 23: 1227–1238, 2003.
 60. Lipsitz LA, Mukai S, Hamner J, Gagnon M, Babikian V. Dynamic regulation of middle cerebral artery blood flow velocity in aging and hypertension. *Stroke* 31: 1897–1903, 2000.
 61. Liu J, Zhu YS, Hill C, Armstrong K, Tarumi T, Hodics T, Hynan LS, Zhang R. Cerebral autoregulation of blood velocity and volumetric flow during steady-state changes in arterial pressure. *Hypertension* 62: 973–979, 2013.
 62. Ludbrook J. Comparing methods of measurements. *Clin Exp Pharmacol Physiol* 24: 193–203, 1997.
 63. Marshall O, Lu H, Brisset J-C, Xu F, Liu P, Herbert J, Grossman RI, Ge Y. Impaired cerebrovascular reactivity in multiple sclerosis. *JAMA Neurol* 71: 1275–1281, 2014.
 64. Matteis M, Troisi E, Monaldo BC, Caltagirone C, Silvestrini M. Age and sex differences in cerebral hemodynamics: a transcranial Doppler study. *Stroke* 29: 963–967, 1998.
 65. McRobbie D, Moore E, Graves M, Prince M. *MRI From Picture to Proton*. 2nd ed. Cambridge: Cambridge University Press, 2007.

66. Meadows GE, Kotajima F, Vazir A, Kostikas K, Simonds AK, Morrell MJ, Corfield DR. Overnight changes in the cerebral vascular response to isocapnic hypoxia and hypercapnia in healthy humans: protection against stroke. *Stroke* 36: 2367–2372, 2005.
67. Meel-van den Abeelen A, Lagro J, Beek A, Claassen J. Impaired Cerebral Autoregulation and Vasomotor Reactivity in Sporadic Alzheimer's Disease. *Curr Alzheimer Res* 11: 11–17, 2014.
68. Miyazaki M, Kato K. Measurement of cerebral blood flow by ultrasonic doppler technique. *Jpn Circ J* 29: 375–382, 1965.
69. Miyazaki M, Lee VS. Nonenhanced MR angiography. *Radiology* 248: 20–43, 2008.
70. Moran PR. A flow velocity zeugmatographic interlace for NMR imaging in humans. *Magn Reson Imaging* 1: 197–203, 1982.
71. Morgan BJ, Reichmuth KJ, Peppard PE, Finn L, Barczi SR, Young T, Nieto FJ. Effects of sleep-disordered breathing on cerebrovascular regulation: a population-based study. *Am J Respir Crit Care Med* 182: 1445–1452, 2010.
72. Murrell CJ, Cotter JD, Thomas KN, Lucas SJ, Williams MJ, Ainslie PN. Cerebral blood flow and cerebrovascular reactivity at rest and during sub-maximal exercise: effect of age and 12-week exercise training. *Age* 35: 905–920, 2013.
73. Nelson MT, Quayle JM. Physiological roles and properties of potassium channels in arterial smooth muscle. *Am J Physiol* 268: C799–822, 1995.
74. Ngai A, Ko K, Morii S, Winn H. Effect of sciatic nerve stimulation on pial arterioles in rats. *Am J Physiol Heart Circ Physiol* 254: 133–139, 1988.
75. Ohta S, Hadeishi H, Suzuki M. Effect of stellate ganglion block on cerebral blood flow in normoxemic and hyperoxemic states. *J Neurosurg Anesthesiol* 2: 272–279, 1990.

76. Oudegeest-Sander MH, van Beek AHEA, Abbink K, Olde Rikkert MGM, Hopman MTE, Claassen JAHR. Assessment of dynamic cerebral autoregulation and cerebrovascular CO₂ reactivity in ageing by measurements of cerebral blood flow and cortical oxygenation. *Exp Physiol* 99: 586–598, 2014.
77. Park K-I, Kang D-W, Roh J-K. Interpretation of Increased Anterior Cerebral Artery Flow Velocity on Transcranial Doppler Ultrasound. *Cerebrovasc Dis* 14: 61–63, 2002.
78. Phillips AA, Warburton DER, Ainslie PN, Krassioukov AV. Regional neurovascular coupling and cognitive performance in those with low blood pressure secondary to high-level spinal cord injury: improved by alpha-1 agonist midodrine hydrochloride. *J Cereb Blood Flow Metab* 34: 794–801, 2014.
79. Portegies ML, de Bruijn RF, Hofman A, Koudstaal PJ, Ikram MA. Cerebral vasomotor reactivity and risk of mortality: the Rotterdam Study. *Stroke* 45: 42–47, 2014.
80. Poulin M, Robbins P. Indexes of flow and cross-sectional area of the middle cerebral artery using Doppler ultrasound during hypoxia and hypercapnia in humans. *Stroke* 27: 2244–2250, 1996.
81. Ratnatunga C, Adiseshiah M. Increase in middle cerebral artery velocity on breath holding: a simplified test of cerebral perfusion reserve. *Eur J Vasc Surg* 4: 519–523, 1990.
82. Reich T, Rusinek H. Cerebral cortical and white matter reactivity to carbon dioxide. *Stroke* 20: 453–457, 1989.
83. Ridgway JP. Cardiovascular magnetic resonance physics for clinicians: part I. *J Cardiovasc Magn Reson* 12: 71, 2010.
84. Ringelstein EB, Sievers C, Ecker S, Schneider PA, Otis SM. Noninvasive assessment of CO₂-induced cerebral vasomotor response in normal individuals and patients with internal carotid artery occlusions. 19: 963–969, 1988.

85. Roy C, Sherrington C. On the regulation of the blood supply of the brain. *J Physiol* 11: 85–158, 1890.
86. Sabayan B, Jansen S, Oleksik AM, van Osch MJP, van Buchem MA, van Vliet P, de Craen AJM, Westendorp RGJ. Cerebrovascular hemodynamics in Alzheimer's disease and vascular dementia: a meta-analysis of transcranial Doppler studies. *Ageing Res Rev* 11: 271–277, 2012.
87. Sariri E, Vahdat M, Behbahani AS, Rohani M, Kashanian M. Cerebro vascular reactivity (CVR) of middle cerebral artery in response to CO₂ 5% inhalation in preeclamptic women. *J Matern Fetal Neonatal Med* 26: 1020–1023, 2013.
88. Schmetterer L, Findl O, Strenn K, Graselli U, Kastner J, Eichler H, Wolzt M. Role of NO in the O₂ and CO₂ responsiveness of cerebral and ocular circulation in humans. *Am J Physiol Integr Comp Physiol* 273: R2005–R2012, 1997.
89. Serrador JM, Picot PA, Rutt BK, Shoemaker JK, Bondar RL. MRI measures of middle cerebral artery diameter in conscious humans during simulated orthostasis. *Stroke* 31: 1672–1678, 2000.
90. Serrador JM, Sorond FA, Vyas M, Gagnon M, Iloputaife ID, Lipsitz LA. Cerebral pressure-flow relations in hypertensive elderly humans: transfer gain in different frequency domains. *J Appl Physiol* 98: 151–159, 2005.
91. Shenkin H, Cabieses F, Van den Noordt G. The effect of bilateral stellectomy upon the cerebral circulation of man. *J Clin Invest* 30: 90–93, 1951.
92. Silvestrini M, Vernieri F, Pasqualetti P, Matteis M, Passarelli F, Troisi E, Caltagirone C. Impaired cerebral vasoreactivity and risk of stroke in patients with asymptomatic carotid artery stenosis. *JAMA* 283: 2122–2127, 2000.
93. Tan CO, Taylor JA. Integrative physiological and computational approaches to understand autonomic control of cerebral autoregulation. *Exp Physiol* 99: 3–15, 2014.

94. Thompson SW. Reactivity of cerebral blood flow to CO₂ in patients with transient cerebral ischemic attacks. *Stroke* 2: 273–278, 1971.
95. Tiecks F, Lam A, Aaslid R, Newell D. Comparison of static and dynamic cerebral autoregulation measurements. *Stroke* 26: 1014–1019, 1995.
96. Valdueza JM, Balzer JO, Villringer A, Vogl TJ, Kutter R, Einhaupl KM. Changes in blood flow velocity and diameter of the middle cerebral artery during hyperventilation: assessment with MR and transcranial Doppler sonography. *AJNR American J Neuroradiol* 18: 1929–1934, 1997.
97. Valdueza JM, Draganski B, Hoffmann O, Dirnagl U, Einhaupl KM. Analysis of CO₂ vasomotor reactivity and vessel diameter changes by simultaneous venous and arterial Doppler recordings. *Stroke* 30: 81–86, 1999.
98. Vorstrup S, Brun B, Lassen N. Evaluation of the cerebral vasodilatory capacity by the acetazolamide test before EC-IC bypass surgery in patients with occlusion of the internal carotid artery. *Stroke* 17: 1291–1298, 1986.
99. Wang Q, Paulson OB, Lassen NA. Effect of nitric oxide blockade by N^G-Nitro-L-Arginine on cerebral blood flow response to changes in carbon dioxide tension. *J Cereb blood flow Metab* 12: 947–953, 1992.
100. Wei E, Kontos H, Patterson JJ. Dependence of pial arteriolar response to hypercapnia on vessel size. *Am J Physiol* 238: 697–703, 1980.
101. West GA, Leppla DC, Simard JM. Effects of external pH on ionic currents in smooth muscle cells from the basilar artery of the guinea pig. *Circ Res* 71: 201–209, 1992.
102. Wheaton AJ, Miyazaki M. Non-contrast enhanced MR angiography: physical principles. *J Magn Reson Imaging* 36: 286–304, 2012.
103. Willie CK, Colino FL, Bailey DM, Tzeng YC, Binsted G, Jones LW, Haykowsky MJ, Bellapart J, Ogoh S, Smith KJ, Smirl JD, Day TA, Lucas SJ, Eller LK, Ainslie

- PN. Utility of transcranial Doppler ultrasound for the integrative assessment of cerebrovascular function. *J Neurosci Methods* 196: 221–237, 2011.
104. Willie CK, Macleod DB, Shaw AD, Smith KJ, Tzeng YC, Eves ND, Ikeda K, Graham J, Lewis NC, Day TA, Ainslie PN. Regional brain blood flow in man during acute changes in arterial blood gases. *J Physiol* 590: 3261–3275, 2012.
 105. Willie CK, Tzeng YC, Fisher JA, Ainslie PN. Integrative regulation of human brain blood flow. *J Physiol* 592: 841–859, 2014.
 106. Wilson MH, Edsell ME, Davagnanam I, Hirani SP, Martin DS, Levett DZ, Thornton JS, Golay X, Strycharczuk L, Newman SP, Montgomery HE, Grocott MP, Imray CH, Group CXER. Cerebral artery dilatation maintains cerebral oxygenation at extreme altitude and in acute hypoxia--an ultrasound and MRI study. *J Cereb Blood Flow Metab* 31: 2019–2029, 2011.
 107. Yamamoto M, Meyer JS, Sakai F, Yamaguchi F. Aging and cerebral vasodilator responses to hypercarbia: responses in normal aging and in persons with risk factors for stroke. *Arch Neurol* 37: 489–496, 1980.
 108. Zhang R, Zuckerman JH, Giller CA, Levine BD. Transfer function analysis of dynamic cerebral autoregulation in humans. *Am J Physiol Heart Circ Physiol* 43: 233–241, 1998.
 109. Zhu YS, Tarumi T, Tseng BY, Palmer DM, Levine BD, Zhang R. Cerebral vasomotor reactivity during hypo- and hypercapnia in sedentary elderly and Masters athletes. *J Cereb Blood Flow Metab* 33: 1190–1196, 2013.

Chapter 2

2 Cerebral blood flow velocity underestimates cerebral blood flow during modest hypercapnia and hypocapnia

(Published in J Appl Physiol 117:1090-1096, 2014. Used with permission – see Appendix C)

2.1 Introduction

The responsiveness of the cerebral circulation to altered carbon dioxide (CO₂) partial pressures has long been recognized (12) and is the basis of one method to assess cerebrovascular health (9, 14). Alterations in vessel diameter have been observed with in vitro preparations or craniotomy with changes in inspired CO₂ at the level of the smaller cerebral arteries including the anterior cerebral artery, the M2 segment of the middle cerebral artery (MCA) and the intraparenchymal cerebral arterioles (1, 7). Whether or not larger cerebral arteries constrict and/or dilate in conscious humans is important because the standard tool for measuring cerebral hemodynamics, transcranial Doppler ultrasound (TCD), measures cerebral blood flow velocity (CBFV) which is used as a surrogate for cerebral blood flow (CBF). However, the change in CBFV is equivalent to the change in CBF only if the diameter of the insonated vessel does not change. This assumption is particularly relevant to the M1 segment of the MCA, as it is the cerebral vessel that is most often studied using TCD. Early studies used magnetic resonance imaging (MRI) and reported that MCA diameter did not change in response to manipulations of end-tidal CO₂ (ETCO₂) (22, 25). Serrador et al. examined MCA diameter during hypercapnia (HC) at an ETCO₂ of approximately 45 mmHg and during hypocapnia (HO) at 24 mmHg in 6 subjects and found no change in either condition (22). The voxel dimensions in this case were 0.47 x 0.47 x 5.0 mm. Valdueza et al. had 7 subjects hyperventilate to an ETCO₂ of 27 mmHg and no change in MCA diameter was detected with a voxel size of 0.8 x 0.4 x 3.0 mm (25). Both of these investigations were performed at 1.5 T with limited spatial resolution relative to higher field systems currently available.

In contrast to MRI data (22, 25), indirect measures suggest that MCA diameter does change across levels of ETCO_2 . For example, combined measures of the hypercapnia-induced flow difference between CBFV in the MCA and the sphenoparietal sinus (which drains the MCA) indicated a greater increase on the venous side (26). The authors attributed this observation to MCA vasodilation (26).

Measures of CBFV as an index of CBF are challenged not only by the assumption of constant MCA diameter, but also velocity errors. A problem inherent to the Doppler signal is overestimation of peak values due to spectral broadening, which has a greater impact as the angle of insonation increases (11). Spectral broadening occurs intrinsically due to the nature of transmitting and receiving acoustic energy (8) and has been documented with other types of Doppler ultrasound systems (11). In addition to TCD, MRI-based phase contrast (PC) imaging can estimate CBFV based on the principle that applied magnetic gradients induce a phase shift in moving protons that is proportional to fluid velocity. Phase contrast imaging has been validated against a flow phantom for estimation of total CBF through the basilar artery and internal carotid arteries and has been used to estimate MCA CBFV (2, 15, 23). Leung et al. reported that PC-based estimates were lower than those measured by TCD with the error attributed to Doppler spectral broadening (15). Overall, the agreement between TCD and PC estimates of CBFV requires further study.

The primary purpose of this study was to determine if the MCA constricts during HO and/or dilates during HC and to quantify the impact of such changes on CBF. A secondary purpose was to compare velocity measures from TCD to velocity measures collected with PC MRI over a range of ETCO_2 values.

2.2 Materials and Methods

In total, nineteen subjects (24 ± 2 years, 8 males) participated in this study. Subjects were not on any medications and were non-smokers with no history of cardiovascular disease. All subjects gave informed consent and the protocol was approved by the Health Sciences Research Ethics Board at Western University.

2.2.1 Experimental Protocols

Subjects participated in two testing sessions including an MRI day and a physiological data collection (Lab) day that were matched for time of day. Subjects were asked to refrain from alcohol, caffeine and physical activity for 12 hours prior to testing. The protocol consisted of 5 minutes of baseline measures followed by 5 minutes of HC or HO (assigned randomly) then a 3-4 minute recovery period. The CO₂ manipulation that had not yet been performed (HC or HO) was then completed for 5 minutes after another 5 minute baseline. To induce HC the subjects breathed air that consisted of 6% CO₂, 21% oxygen, and balanced nitrogen. For HO, participants breathed at a rate of 30 breaths per minute guided by a metronome. The protocols were designed to increase ETCO₂ by approximately 10 mmHg during HC and decrease ETCO₂ by approximately 15 mmHg during HO.

2.2.2 Measurements

2.2.2.1 Lab Session

Heart rate was acquired from standard ECG. Finger arterial blood pressure (BP) was measured continuously and the brachial waveform (Finometer, Finapres Medical Systems BV, Amsterdam, The Netherlands) was corrected to brachial sphygmomanometric values. End-tidal CO₂ (CO2100C analyzer, Biopac, CA, USA) and breathing frequency (respiratory strain gauge) were measured continuously. Cerebral blood flow velocity of the MCA was measured in a supine position using a 2-MHz pulsed transcranial Doppler ultrasound probe (Neurovision system, Multigon Industries, Elmsford, CA, USA). The average depth of the ultrasound beam was 5.0 ± 0.4 cm.

2.2.2.2 MRI Session

A 3T MRI (Magnetom TIM TRIO, Siemens Medical Solutions, Erlangen, Germany) was used for data collection. A 3D time of flight sequence was used to select the location on the M1 segment of the right MCA to apply a T2 fast spin echo sequence and a PC sequence that were used to determine the vessel cross-sectional area (CSA) and CBFV, respectively. Both T2 and PC sequences were applied during baseline conditions (Pre HC and Pre HO) and each experimental condition (HC and HO) for 9 subjects (25 ± 2 years,

5 males). In each condition, two T2 image acquisitions were performed (approximately 1 minute per acquisition) followed by one PC acquisition (approximately 2 minutes) followed by two more T2 acquisitions. In the MRI session for the remaining subjects 2 to 5 T2 images were taken at baseline and during HC and HO for assessment of MCA CSA. For T2 images, used to calculate MCA CSA, (8 slices, repetition time (TR) = 3000 ms, echo time (TE) = 100 ms, flip angle = 120° , voxel dimensions $0.4 \times 0.4 \times 2.0 \text{ mm}^3$), the pulse sequence was gated to the peak of the pulse wave from the continuous signal derived from an MRI-compatible pulse oximeter (8600FO MRI, Nonin Medical Inc., Plymouth, MN, USA) as measured at the right third finger.

For the PC acquisition, which was used to determine CBFV, (TR = 24.75 ms, TE = 6.01 ms, flip angle = 15° , voxel dimensions $0.7 \times 0.7 \times 3.0 \text{ mm}^3$) 25 phases were retroactively gated to the signal from the pulse oximeter. The velocity-encoding factor (V_{enc}), which is the maximum measurable velocity, was individually determined since setting the V_{enc} too low can result in aliasing (18). The V_{enc} for Pre HC and Pre HO conditions was, on average, $111 \pm 14 \text{ m/s}$, $145 \pm 13 \text{ m/s}$ for HC, and $98 \pm 14 \text{ m/s}$ for HO. Respiration was collected with a strain gauge around the upper abdomen.

2.2.3 Data Analysis

2.2.3.1 Lab Data

Values of heart rate, BP, breathing frequency, and mean CBFV were averaged for the 5 minute baseline periods. These measures were averaged every minute during HC and HO and the value reported corresponds to when the maximal and minimal CSA measurements from the MRI were recorded.

2.2.3.2 MRI Data

Figure 2.1 shows a representative baseline T2 image. Using Osirix imaging software (Pixmeo, Bernex, Switzerland) the CSA of each MCA image was measured in triplicate by two blinded observers. The MCA was assumed to be circular but rather than fitting a circle to the vessel we chose to outline the lumen manually point by point for the best fit and this was done at each operator's discretion after training by the same investigator. An

intra-class correlation coefficient (ICC) was calculated to examine the agreement between the two observers. The ICC between the two observers was 0.92; thus, the average CSA between the two observers is reported. The HC and HO CSAs are reported as the maximal CSA for HC and the minimal CSA for HO as well as the average of all CSAs during HC and HO. The diameter was then determined as the square root of CSA divided by π multiplied by 2.

An index of vascular reactivity was assessed relative to the corresponding baseline as the $\Delta\text{CSA}/\Delta\text{ETCO}_2$ during each of HC and HO. Cerebral blood flow was calculated ($\text{CSA} \times \text{CBFV}$) using TCD CBFV as the basis for CBF calculations unless otherwise noted. Percent change ($\%\Delta$) from baseline was calculated for CBF and CBFV. Cerebrovascular reactivity (CVR) for CBF and CBFV was calculated as both absolute and relative change ($\Delta\text{CBF}/\Delta\text{ETCO}_2$, $\Delta\text{CBFV}/\Delta\text{ETCO}_2$, $\%\Delta\text{CBF}/\Delta\text{ETCO}_2$, $\%\Delta\text{CBFV}/\Delta\text{ETCO}_2$).

Phase contrast data were assessed using cvi⁴² (Circle Cardiovascular Imaging, Calgary, AB, Canada). Phases were quantified into velocities based on the V_{enc} . The lumen of the MCA was identified and the mean velocity for each voxel was determined over the 25 phases. To coincide with the TCD analysis, a peak velocity for each of the 25 images was determined from the voxel with the highest velocity within the MCA and these values were averaged over the cardiac cycle. The analysis was performed by two blinded observers and values were averaged. The ICC between the two observers was 1.0 ($p < 0.001$).

2.2.4 Statistical Analysis

Data are presented as mean \pm standard deviation unless otherwise indicated. SigmaStat12.0 was used for statistical analysis. All comparisons were made with a paired t-test. Average and maximal/minimum data are reported for HC and HO. The maximum/minimum CSA were the main outcome of interest because this represents the maximum to which CSA changes may impact TCD estimates of CBFV. Therefore, all calculations relating to the change in CSA relate to the maximal CSA during HC and the minimum during HO. Bland-Altman analysis was performed to examine the spread of

differences between PC and TCD for estimates of CBFV and CVR. The differences between the two estimates were plotted against the corresponding means and fixed and/or proportional biases were assessed. A one sample t-test was performed on the difference values between the two observers, and between PC and TCD difference values, to test for fixed bias since the differences should be equal to zero if no fixed bias exists (3). The regression between the differences and corresponding means was plotted and a slope different from zero was used to indicate the presence of proportional bias (3). The ICC was also calculated to examine the agreement between PC and TCD and a value greater than 0.8 was considered to indicate good agreement.

Cohen's d was calculated for the change in CSA during HC and HO to provide an estimate of the effect size. Additionally, a post hoc power analysis was performed for the change in CSA during each of the HO and HC conditions using GPower 3.1 (6) specifying two tails, an α -value of 0.05, the sample size, and the effect size of Cohen's d .

2.3 Results

T2 images were collected for 19 subjects and analysis of CSA was performed on images from 15 subjects for HO and on 13 subjects for HC for whom image quality provided clear MCA edges. Phase contrast images of sufficient quality to determine CBFV were obtained in 7 of 9 individuals for both the HC and HO trials and TCD CBFV was collected in these same subjects. The average time between the Lab and MRI session was 53 ± 58 days. This estimate is variable because 13 subjects had their Lab and MRI sessions within 29 days of one another while the other 6 had 3 to 4 months between test dates due to the reduced availability of the MRI.

Table 2.1 illustrates the physiologic responses to HC and HO in both the laboratory and MRI sessions. End-tidal CO_2 increased during HC and decreased during HO in each session ($p < 0.01$ for all cases). Breathing rate was not different during HC in the MRI or in the Lab session. By design, breathing rate was elevated compared to baseline during HO in each session ($p < 0.001$). Additionally, heart rate increased during both HC and HO in the MRI and Lab sessions ($p < 0.05$ for all cases). Blood pressure was measured only in the Lab session and during HC, SBP and MAP increased above

baseline ($p < 0.05$ for both cases) while DBP remained unchanged. During HO, SBP increased above baseline ($p < 0.01$) while MAP and DBP remained unchanged.

During HC, CSA of the MCA increased from 5.6 ± 0.8 at baseline to a maximal CSA of $6.5 \pm 1.0 \text{ mm}^2$ ($p < 0.001$; Figure 2.2A) and an average CSA of $6.3 \pm 0.9 \text{ mm}^2$ ($p < 0.001$). During HO, the CSA decreased from 5.8 ± 0.9 at baseline to a minimum of $5.3 \pm 0.9 \text{ mm}^2$ ($p < 0.001$; Figure 2.2B) and an average CSA of $5.5 \pm 0.9 \text{ mm}^2$ ($p = 0.01$). For HC, Cohen's d was 0.94 and the achieved power was 0.87. For HO, Cohen's d was 0.50 and achieved power was 0.44. Figure 2.2 illustrates the individual patterns of response showing a homogeneous dilatory response for all subjects during HC and heterogeneous vasoconstriction during HO where 6 participants showed less than a 5% change in MCA CSA. Figure 2.3 shows the mean and individual data for the relationship between ETCO_2 and CSA. The average increase during HC was $0.11 \pm 0.07 \text{ mm}^2/\text{mmHg}$ while the average decrease during HO was $0.04 \pm 0.03 \text{ mm}^2/\text{mmHg}$.

Both PC and TCD methods produced similar significant changes in CBFV during both HC and HO stimuli. Overall, there was a strong linear association between TCD and PC estimates of CBFV ($r = 0.71$, $p < 0.001$; Figure 2.4B). The limits of agreement with Bland-Altman analysis were at -27 and 20 on the y-axis (Figure 2.4A) and 1 value fell outside this range at approximately $y = 23$. Bland-Altman analysis revealed no significant fixed (mean difference -3.56 cm/s ; $p = 0.13$) or proportional biases ($r = 0.01$; $p = 0.98$). However, the spread of the differences between PC and TCD produced limits of agreement with a wide range. The ICC for CBFV was 0.83 ($p < 0.001$).

There were no differences in CVR between CBFV estimates obtained by TCD and PC for HC or HO (TCD: $2.42 \pm 3.98 \text{ cm/s/mmHg}$; PC: $2.87 \pm 1.63 \text{ cm/s/mmHg}$, for HC $p = 0.33$ and TCD: $-1.67 \pm 1.37 \text{ cm/s/mmHg}$; PC: $-0.92 \pm 1.17 \text{ cm/s/mmHg}$, for HO $p = 0.14$). There was a strong linear association between TCD and PC CVR ($r = 0.81$, $p < 0.001$; Figure 2.5B). Bland-Altman analysis for CVR (Figure 2.5A) revealed one point that fell outside the limits of agreement of -3.6 and 4.8. No fixed bias (mean difference 0.6 cm/s/mmHg ; $p = 0.10$) was observed; however, the slope of the regression line was

different from zero ($r=0.57$; $p=0.032$), indicating proportional bias was present. The ICC for CVR was 0.86 ($p<0.001$).

Cerebral blood flow, calculated from TCD CBFV and MCA CSA, increased from baseline during HC and decreased during HO ($p<0.01$ for each; Figure 2.6A). The $\% \Delta$ was greater for CBF than for CBFV during HC and HO ($p<0.001$ for each comparison; Figure 2.6B). There was also a significant change from baseline during HC (from 219 ± 38 to 333 ± 68 ml/min; $p=0.001$) and HO (from 211 ± 34 to 156 ± 13 ml/min; $p=0.007$) when CBF was calculated from PC CBFV and MCA CSA. Cerebrovascular reactivity calculated from CBF was 19 ± 23 ml/min/mmHg for HC and -8 ± 6 ml/min/mmHg for HO. Comparing $\% \Delta$ CBFV CVR to $\% \Delta$ CBF CVR revealed that the reactivity to HC and HO was greater for $\% \Delta$ CBF CVR than $\% \Delta$ CBFV CVR ($p<0.05$ for both cases; Figure 2.7).

Table 2.1: Physiological results during HC and HO in the lab and MRI.

	Pre HC	HC	Pre HO	HO
<i>MRI</i>				
End tidal carbon dioxide (mmHg)	37 ± 3	$46 \pm 5^*$	36 ± 4	$23 \pm 3^\dagger$
Breathing rate (breaths per minute)	13 ± 3	15 ± 3	13 ± 4	$28 \pm 1^\dagger$
Heart rate (beats per minute)	63 ± 6	$67 \pm 7^*$	67 ± 11	$76 \pm 12^\dagger$
<i>Lab</i>				
End tidal carbon dioxide (mmHg)	39 ± 3	$49 \pm 5^*$	36 ± 4	$25 \pm 9^\dagger$
Breathing rate (breaths per minute)	14 ± 2	16 ± 3	14 ± 3	$29 \pm 1^\dagger$
Heart rate (beats per minute)	61 ± 9	$65 \pm 6^*$	64 ± 9	$69 \pm 7^\dagger$
Systolic blood pressure (mmHg)	107 ± 11	$112 \pm 13^*$	110 ± 8	$114 \pm 9^\dagger$
Diastolic blood pressure (mmHg)	69 ± 8	70 ± 10	69 ± 8	70 ± 8
Mean arterial pressure (mmHg)	82 ± 9	$86 \pm 10^*$	84 ± 7	85 ± 7

Values are means \pm SD. * $p < 0.05$ for Pre HC versus HC. † $p < 0.05$ for Pre HO versus HO. MRI: HC n=13, HO n=15. Lab: HC and HO n=7. HC = hypercapnia; HO = hypocapnia.

Table 2.2: CBFV during HC and HO obtained from TCD and PC MRI.

	Pre HC	HC	Pre HO	HO
TCD CBFV (cm/s)	68 ± 9	85 ± 15*	69 ± 8	55 ± 16†
PC CBFV (cm/s)	64 ± 10	85 ± 15*	61 ± 8	51 ± 8†

Values are means ± SD. *p<0.05 for Pre HC versus HC. †p<0.05 for Pre HO versus HO. TCD and PC: HC n=7 and HO n=7. CBFV = cerebral blood flow velocity; HC = hypercapnia; HO = hypocapnia; PC = phase contrast; TCD = transcranial Doppler ultrasound.

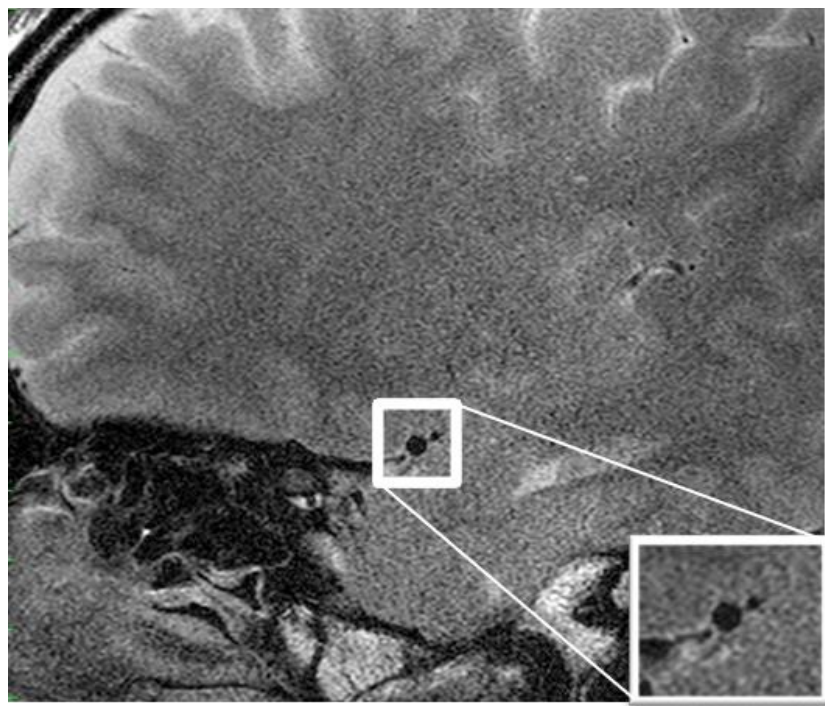


Figure 2.1: Sagittal T2 baseline image through the right middle cerebral artery of a representative subject.

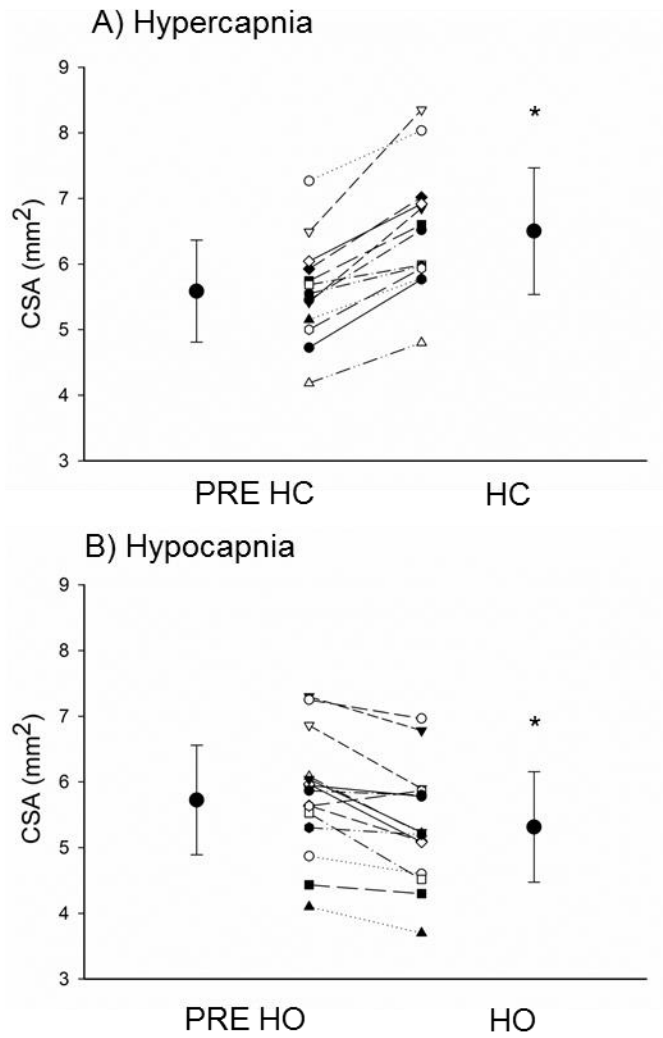


Figure 2.2: Individual and mean changes in the CSA of the middle cerebral artery. A: HC (n=13). B: HO (n=15). CSA = cross-sectional area; HC = hypercapnia; HO = hypocapnia.

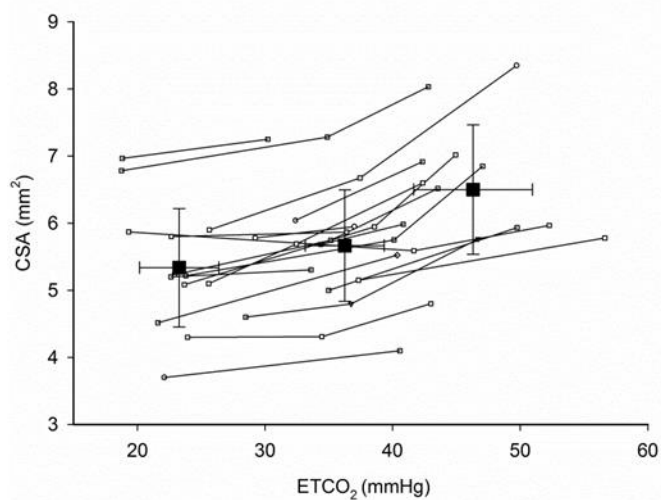


Figure 2.3: Relationship between the change in ETCO₂ and the change in middle cerebral artery CSA from HO to HC. Filled squares represent mean data with standard deviation bars and unfilled squares show individual data (n=19; n=9 with data points for HO and HC, n=6 for HO alone, and n=4 for HC alone). CSA = cross-sectional area; ETCO₂ = end-tidal carbon dioxide; HC = hypercapnia; HO = hypocapnia.

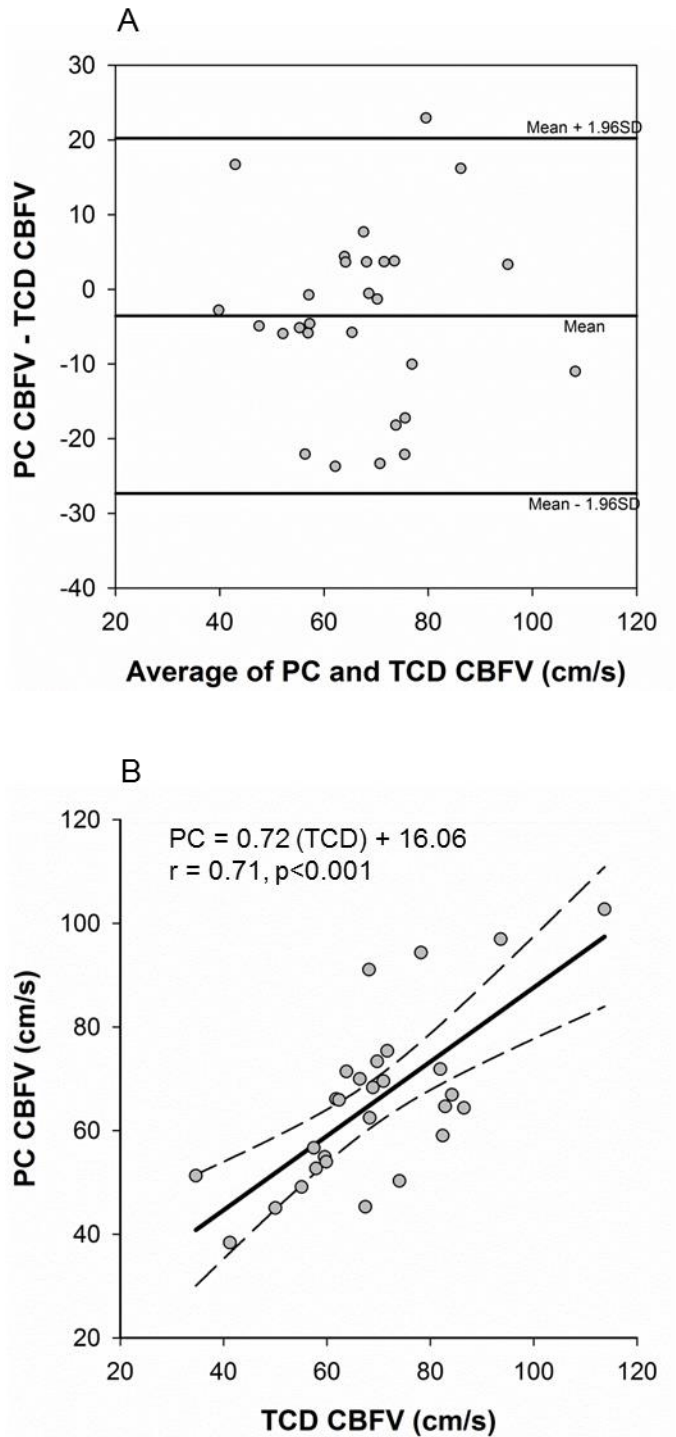


Figure 2.4: Bland-Altman and scatter plots comparing TCD and PC CBFV over the range of end-tidal carbon dioxide values. Pre HC, HC, Pre HO and HO are represented for 7 subjects for a total of 28 data points. A: Bland-Altman plot of CBFV. B: Scatter plot

with the regression line (solid line) and 95% confidence intervals (dashed lines) for CBFV. CBFV = cerebral blood flow velocity; PC = phase contrast; TCD = transcranial Doppler ultrasound.

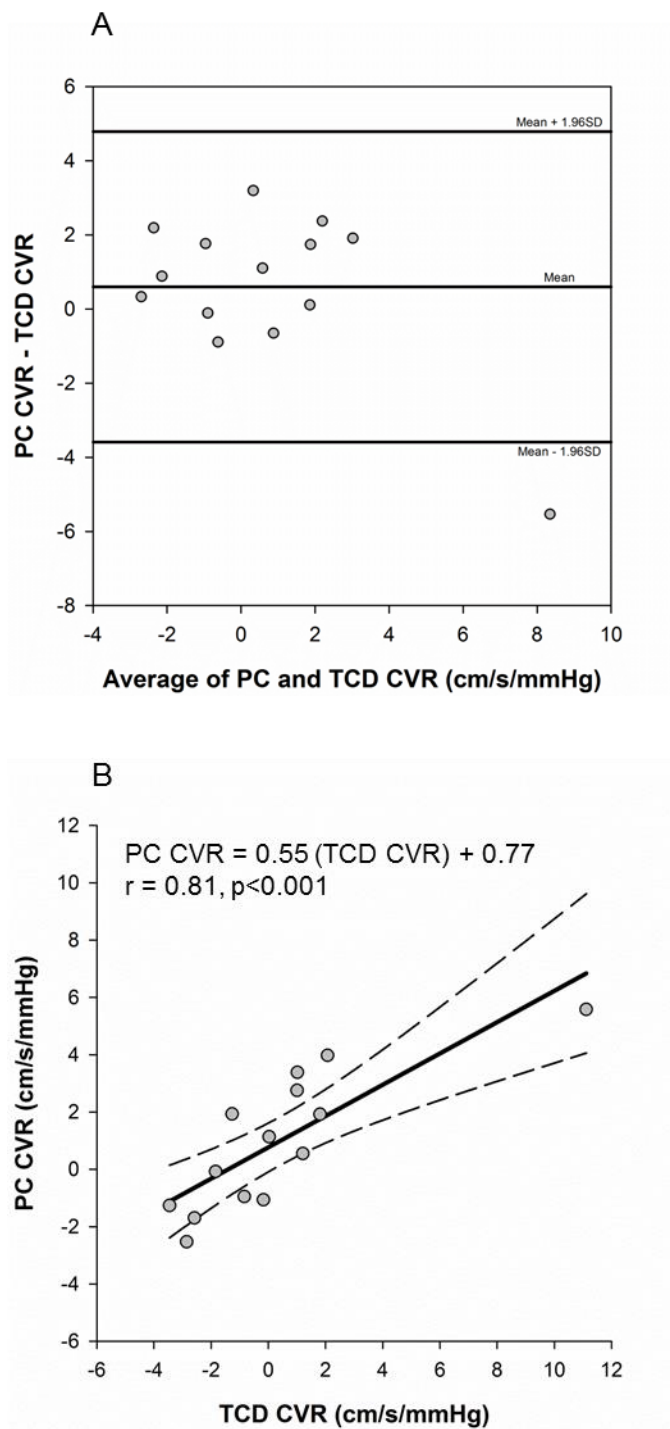


Figure 2.5: Bland-Altman and scatter plots comparing TCD and PC CVR over the range of end-tidal carbon dioxide values. The change from Pre HC to HC and Pre HO to HO are represented for 7 subjects for a total of 14 data points. A: Bland-Altman plot of CVR. B: Scatter plot with the regression line (solid line) and 95% confidence intervals (dashed

lines) for CVR. CVR= cerebrovascular reactivity; PC = phase contrast; TCD = transcranial Doppler ultrasound.

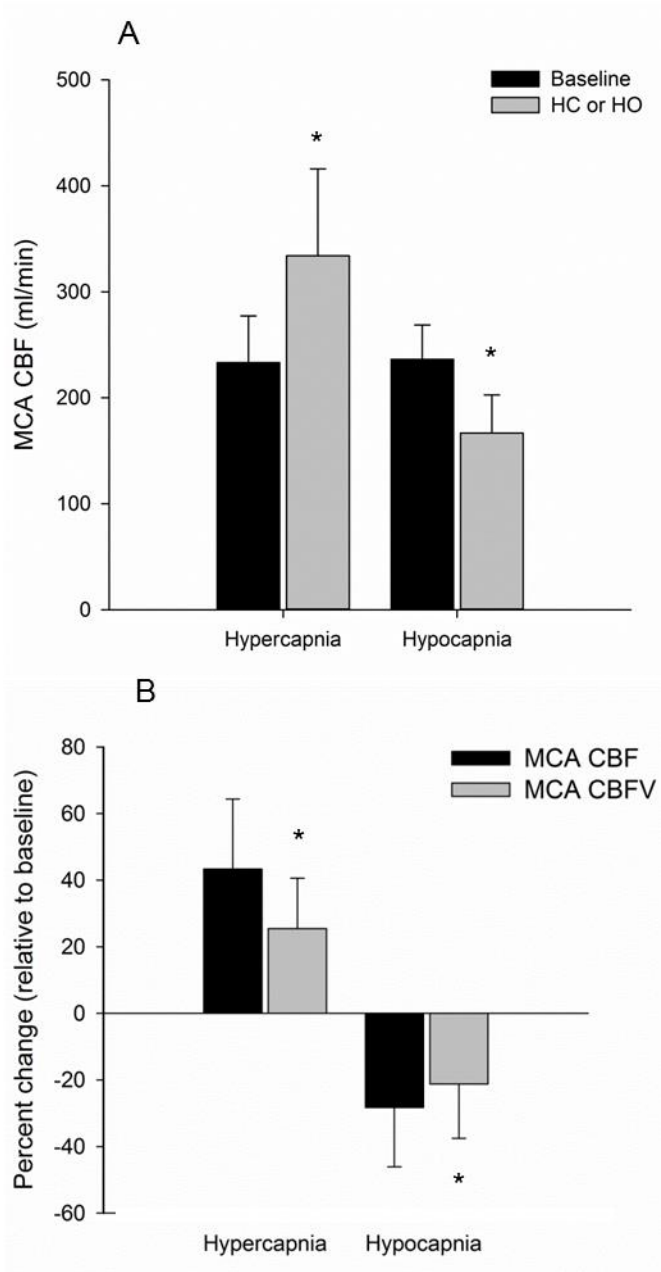


Figure 2.6: A: CBF during HC and HO calculated by multiplying the cross-sectional area of the MCA by TCD CBFV. B: Percent change in CBFV and CBF during HC and HO. * $p < 0.05$. CBF = cerebral blood flow; CBFV = cerebral blood flow velocity; HC = hypercapnia; HO = hypocapnia; MCA = middle cerebral artery; TCD = transcranial Doppler ultrasound. $n=7$ for all conditions.

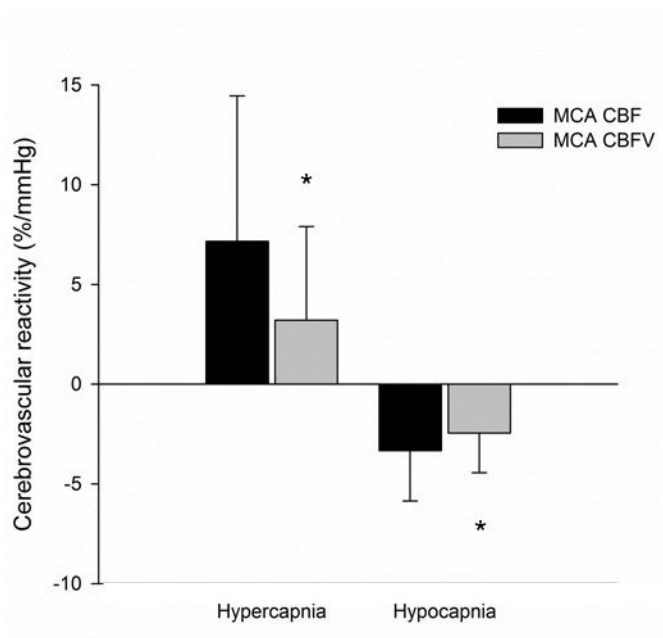


Figure 2.7: Cerebrovascular reactivity expressed as percent change of CBFV and CBF divided by the change in end tidal carbon dioxide during HC and HO.* $p < 0.05$. CBF = cerebral blood flow; CBFV = cerebral blood flow velocity; CVR = cerebrovascular reactivity; HC = hypercapnia; HO = hypocapnia; MCA = middle cerebral artery; TCD = transcranial Doppler ultrasound. $n=7$ for all conditions.

2.4 Discussion

This study was the first to show that MCA CSA increases by $16 \pm 7\%$ and decreases by $8 \pm 6\%$ during HC and HO, respectively. Thus, using CBFV as an estimate of flow underestimated true flow changes in the MCA. Cerebrovascular reactivity was also lower when using CBFV compared to CBF. Additionally, there was some variability between TCD and PC estimates of CBFV during both HC and HO conditions which was evident by the wide limits of agreement produced from Bland Altman analysis despite the strong ICC value.

Overall, MCA diameters calculated from measures of CSA in the current study (2.66 ± 0.21 to 2.87 ± 0.21 mm for HC and 2.69 ± 0.20 to 2.59 ± 0.21 with HO) are comparable to values of 2.23 mm (24) to 3.4 mm (10, 21, 22, 25, 28) from other studies that have employed MRI. In the current analysis, the percent change in diameter with HC was $8 \pm 3\%$ over an average change in ETCO_2 of 9 ± 4 mmHg whereas diameter decreased $4 \pm 4\%$ during an ETCO_2 decrease of 13 ± 5 mmHg. Willie et al. (2012) reported a change in the diameter of the internal carotid artery of approximately 20% over a PaCO_2 range of 50 mmHg (27). Thus, the current data produced a rate of diameter change (approximately 0.4%/mmHg) over a physiologically-relevant range of ETCO_2 that is consistent with that of the internal carotid artery (approximately 0.6%/mmHg) observed over a much wider range of ETCO_2 .

Previously, MCA diameter was observed not to change across a similar range of ETCO_2 examined in the current study (22, 25). However, Serrador et al. (2000) used 1.5 T MRI with a voxel size of $0.47 \times 0.47 \times 5.00$ mm giving a total voxel volume of 1.11 mm^3 (22). In the current study, the resolution of the 3T system was greater with a voxel size of $0.4 \times 0.4 \times 2.0$ mm for a voxel volume of 0.32 mm^3 . The voxel volume affects not only the resolution but also the impact of partial volume effects. In particular, the smaller voxel volume of the 3T system used here will reduce the presence of two or more types of tissue in one voxel where signal from one would “water down” signal from the second. With the larger voxel volume in the previous study partial volume effects may have minimized any detectable change (22). In addition, a higher signal-to-noise ratio was

achieved with the 32 channel head coil and the signal-to-noise ratio is inherently two times greater at 3 T compared to 1.5 T (4). Some variability in MCA CSA was observed across subjects in the current study, especially during HO. The observation of a greater dilatory response to HC versus constrictor response to HO is consistent with previous observations of the internal carotid artery (27). We observed high between-subject variability in the constrictor response to HO which suggests either varying sensitivity to CO₂ or that the MCA exists in a constricted state at baseline. Giller et al. (1993) also observed variability in the response to HO upon direct observation of the MCA during craniotomy (7). We speculate that the brain could be protected from inappropriate vasoconstriction which could lead to damaging ischemia, particularly if it involves the major arteries at the base of the brain. In this context, baseline flow may be the regulated variable in the brain as opposed to the P_aCO₂.

In the current study no significant biases were observed when comparing TCD and PC estimates of CBFV. Additionally, the ICC was strong indicating that variation between the two methods in the same subject was minimal compared to variation between subjects. However, the variability in the differences between the two methods produced quite a spread of data, resulting in wide limits of agreement. Leung et al. observed proportional bias with less agreement between the two methods at high levels of CBFV during HC (15). However, in this study, proportional bias was observed only with CVR due to one data point where CVR was highest. This indicates that TCD and PC may not provide similar estimates of CBFV in individuals who express a large CVR response to HC. Leung et al. suggested that one way to reduce this variability between the two methods may be to compare the mean CBFV signal instead of the peak signal which may reduce partial volume effects (15).

The increase in MCA CSA with HC may be influenced by the concurrent rise in BP. In this study, mean arterial pressure increased during HC by approximately $5 \pm 3\%$. Under conditions of normal ETCO₂ a change in BP should have minimal effect on CBF due to intact cerebral autoregulation. However, under hypercapnic conditions dynamic cerebral autoregulation is impaired (19). Thus, it is possible that the cerebral circulation may respond passively to small BP changes leading to an effect on the CSA of the MCA

during HC. Indeed, pharmacological studies indicate that larger cerebral vessels, such as the internal carotid artery, can change diameter passively during changes in BP (16). Based on these earlier data (16), the change in diameter in internal carotid artery diameter that could be expected with our change in BP is approximately 3% (16) which is less than the 8% diameter change observed. However, the study of Liu et al. was performed under conditions of normocapnia so it is unclear how HC may affect these results (16).

This study is limited by the fact that MCA CSA and TCD measurements were collected on different days that were, on average, 53 days apart. We attempted to decrease day to day variability by performing data collection at the same time of day in the separate sessions. Despite this limitation, studies suggest that TCD and PC estimates of CBFV are reproducible over a week in the case of TCD and over 72 days for PC (5, 23). These studies are limited by the fact that they examined repeatability under conditions of normocapnia. Few studies that have assessed the reproducibility of cerebrovascular reactivity to carbon dioxide have produced variable findings. McDonnell et al. found the ICC between two estimates of TCD-based CBFV change during HC performed a week apart to be fairly strong ($ICC=0.73$) in one rater who had more recently been trained, but much weaker in the other rater ($ICC=0.08$) (17). Additionally, BP measurements were not taken during the MRI session.

Another limitation of the current study was that P_aCO_2 was not measured. Previous studies indicate that $ETCO_2$ overestimates P_aCO_2 during HC but not HO (20, 27). Regardless, $ETCO_2$ was used in all cases so any overestimation was comparable between TCD and PC.

Lastly, it must be noted that in a minimal number of T2 images the vessel borders were unclear and as result were not analyzed. Respiratory-induced motion artifacts can be problematic and were a concern for this study. All images used in this study were carefully monitored for significant motion problems like blurring or ghosting. It is unlikely that the image quality could be significantly improved through the use of respiratory gating for the following reasons: (1) the significant increase in scan time during the T2 turbo spin echo sequence used in this study could potentially introduce

patient movement artifacts other than respiration itself, and (2) the potentially large variation between TR periods in this acquisition would significantly alter the spin history and introduce other unwanted magnitude and phase variances and therefore image artifacts.

In summary, the present data support the conclusion that the CSA of the MCA changes in response to changes in ETCO_2 . The response was more homogeneous across participants during HC than HO. These data contribute to emerging evidence that alterations in CBF due to manipulations of the arterial partial pressure of CO_2 and/or the arterial partial pressure of oxygen are not solely due to changes in the smaller arterioles (27, 28). Therefore, caution must be applied when using CBFV as a surrogate for CBF during conditions that manipulate concentrations of arterial gases.

2.5 References

1. Atkinson JL, Anderson RE, Sundt TM. The effect of carbon dioxide on the diameter of brain capillaries. *Brain Res* 517: 333-340, 1990.
2. Baledent O, Fin L, Khuoy L, Ambarki K, Gauvin AC, Gondry-Jouet C, Meyer ME. Brain hydrodynamics study by phase-contrast magnetic resonance imaging and transcranial color doppler. *J Magn Reson Imaging* 24: 995-1004, 2006.
3. Bland JM, Altman DG. Statistical methods for assessing agreement between two methods of clinical measurement. *Lancet* 1: 307-310, 1986.
4. Campeau NG, Huston J, Bernstein MA, Lin C, Gibbs GF. Magnetic resonance angiography at 3.0 Tesla: initial clinical experience. *Top Magn Reson Imaging* 12: 183-204, 2001.
5. Demolis P, Chalon S, Giudicelli JF. Repeatability of transcranial Doppler measurements of arterial blood flow velocities in healthy subjects. *Clin.Sci* 84: 599-604, 1993.
6. Faul F, Erdfelder E, Lang AG, Buchner A. G*Power 3: a flexible statistical power analysis program for the social, behavioral, and biomedical sciences. *Behav Res Methods* 39: 175-191, 2007.
7. Giller CA, Bowman G, Dyer H, Mootz L, Krippner W. Cerebral arterial diameters during changes in blood pressure and carbon dioxide during craniotomy. *Neurosurgery* 32: 737-41, 1993.
8. Guidi G, Licciardello C, Falteri S. Intrinsic spectral broadening (ISB) in ultrasound Doppler as a combination of transit time and local geometrical broadening. *Ultrasound Med Biol* 26: 853-862, 2000.
9. Gur AY, Bova I, Bornstein NM. Is impaired cerebral vasomotor reactivity a predictive factor of stroke in asymptomatic patients? *Stroke* 27: 2188-2190, 1996.

10. Hansen JM, Pedersen D, Larsen VA, Sanchez-del-Rio M, Alvarez Linera JR, Olesen J, Ashina M. Magnetic resonance angiography shows dilatation of the middle cerebral artery after infusion of glyceryl trinitrate in healthy volunteers. *Cephalalgia* 27: 118-127, 2007.
11. Hoskins PR. Accuracy of maximum velocity estimates made using Doppler ultrasound systems. *Br J Radiol* 69: 172-177, 1996.
12. Kety SS, Schmidt CF. The effects of altered arterial tensions of carbon dioxide and oxygen on cerebral blood flow and cerebral oxygen consumption of normal young men. *J Clin Invest* 27: 484-492, 1948.
13. Krejza J, Rudzinski W, Pawlak MA, Tomaszewski M, Ichord R, Kwiatkowski J, Gor D, Melhem ER. Angle-corrected imaging transcranial doppler sonography versus imaging and nonimaging transcranial doppler sonography in children with sickle cell disease. *AJNR Am J Neuroradiol* 28: 1613-1618, 2007.
14. Lavi S, Gaitini D, Milloul V, Jacob G. Impaired cerebral CO₂ vasoreactivity: association with endothelial dysfunction. *Am J Physiol Heart Circ Physiol* 291: H1856-61, 2006.
15. Leung J, Behpour A, Sokol N, Mohanta A, Kassner A. Assessment of intracranial blood flow velocities using a computer controlled vasoactive stimulus: a comparison between phase contrast magnetic resonance angiography and transcranial Doppler ultrasonography. *J Magn Reson Imaging* 38: 733-738, 2013.
16. Liu J, Zhu YS, Hill C, Armstrong K, Tarumi T, Hodics T, Hynan LS, Zhang R. Cerebral autoregulation of blood velocity and volumetric flow during steady-state changes in arterial pressure. *Hypertension* 62: 973-979, 2013.
17. McDonnell MN, Berry NM, Cutting MA, Keage HA, Buckley JD, Howe PR. Transcranial Doppler ultrasound to assess cerebrovascular reactivity: reliability, reproducibility and effect of posture. *PeerJ* 1: e65, 2013.
18. Miyazaki M, Lee VS. Nonenhanced MR angiography. *Radiology* 248: 1: 20-43, 2008.

19. Panerai RB, Deverson ST, Mahony P, Hayes P, Evans DH. Effects of CO₂ on dynamic cerebral autoregulation measurement. *Physiol Meas* 20: 265-275, 1999.
20. Peebles K, Celi L, McGrattan K, Murrell C, Thomas K, Ainslie PN. Human cerebrovascular and ventilatory CO₂ reactivity to end-tidal, arterial and internal jugular vein PCO₂. *J Physiol* 584: 347-357, 2007.
21. Schreiber SJ, Gottschalk S, Weih M, Villringer A, Valdueza JM. Assessment of blood flow velocity and diameter of the middle cerebral artery during the acetazolamide provocation test by use of transcranial Doppler sonography and MR imaging. *AJNR Am J Neuroradiol* 2: 1207-1211, 2000.
22. Serrador JM, Picot PA, Rutt BK, Shoemaker JK, Bondar RL. MRI measures of middle cerebral artery diameter in conscious humans during simulated orthostasis. *Stroke* 31: 1672-1678, 2000.
23. Spilt A, Box FM, van der Geest RJ, Reiber JH, Kunz P, Kamper AM, Blauw GJ, van Buchem MA. Reproducibility of total cerebral blood flow measurements using phase contrast magnetic resonance imaging. *J Magn Reson Imaging* 16: 1-5, 2002.
24. Tarasow E, Abdulwahed Saleh Ali A, Lewszuk A, Walecki J. Measurements of the middle cerebral artery in digital subtraction angiography and MR angiography. *Med Sci Monit* 13: 65-72, 2007.
25. Valdueza JM, Balzer JO, Villringer A, Vogl TJ, Kutter R, Einhaupl KM. Changes in blood flow velocity and diameter of the middle cerebral artery during hyperventilation: assessment with MR and transcranial Doppler sonography. *AJNR Am J Neuroradiol* 18: 1929-1934, 1997.
26. Valdueza JM, Draganski B, Hoffmann O, Dirnagl U, Einhaupl KM. Analysis of CO₂ vasomotor reactivity and vessel diameter changes by simultaneous venous and arterial Doppler recordings. *Stroke* 30: 81-86, 1999.

27. Willie CK, Macleod DB, Shaw AD, Smith KJ, Tzeng YC, Eves ND, Ikeda K, Graham J, Lewis NC, Day TA, Ainslie PN. Regional brain blood flow in man during acute changes in arterial blood gases. *J Physiol* 590: 3261-3275, 2012.
28. Wilson MH, Edsell ME, Davagnanam I, Hirani SP, Martin DS, Levett DZ, Thornton JS, Golay X, Strycharczuk L, Newman SP, Montgomery HE, Grocott MP, Imray CH for Caudwell Xtreme Everest Research Group. Cerebral artery dilatation maintains cerebral oxygenation at extreme altitude and in acute hypoxia-an ultrasound and MRI study. *J Cereb Blood Flow Metab* 31: 2019-2029, 2011.

Chapter 3

3 Heterogeneous patterns of vasoreactivity in the middle cerebral and internal carotid arteries

(Published in Am J Physiol Heart Circ Physiol. 2015 Feb 27;ajpheart.00761.2014. doi: 10.1152/ajpheart.00761.2014. [Epub ahead of print]. Used with permission – see Appendix C)

3.1 Introduction

It is well known that the cerebral vessels demonstrate high sensitivity to levels of carbon dioxide (CO₂) (7) but the exact mechanisms of this reactivity have yet to be elucidated (1, 13, 20). The relative change in flow or flow velocity to a given change in end tidal CO₂ (ETCO₂) is a standard measurement known as cerebrovascular reactivity (CVR) that reflects the health of the cerebrovascular system (11) and the risk for a future ischemic event (15). The relative contributions of subcortical and intraparenchymal vessels to estimates of CVR remain unknown and the reactivity is generally attributed to the pial or intraparenchymal vessels. Yet, estimates based on the fall in pressure from the aorta indicate that the large subcortical or cerebral arteries contribute as much as 50 to 60% to cerebrovascular resistance (5). Thus, understanding their reactivity to changes in CO₂ has important implications for determining cerebrovascular health.

The contribution of the conduit vessels to CVR remains unclear in intact humans due to lack of access to direct *in vivo* assessment of these vessels. This limitation has led to reliance on transcranial Doppler ultrasound (TCD) to assess cerebral vasomotor control, a method that is applied easily and provides excellent temporal resolution of cerebral blood flow velocity (CBFV). Although the total power of the Doppler signal has been used to account for possible changes in middle cerebral artery (MCA) cross-sectional area (CSA) (12), TCD cannot quantify cerebral blood flow (CBF) because the CSA of the insonated vessel cannot be visualized directly. Thus, CBFV is accepted as a suitable analog of CBF. This supposition is supported by earlier magnetic resonance imaging (MRI) studies in which changes in MCA diameter were not observed during

hypocapnia (HO: hyperventilation to 24 mmHg (14) and 27 mmHg (18)) or hypercapnia (HC: ETCO_2 increased to 45 mmHg (14)).

Recently, we used 3T MRI and a 32 channel head-coil to enhance resolution and observed a statistically significant change in MCA diameter of $8 \pm 3\%$ during HC (ETCO_2 increased 9 mmHg above baseline) and a decrease in diameter of $4 \pm 4\%$ during HO (ETCO_2 decreased by 13 mmHg) (4). Thus, concurrent measures of CBFV alone using phase contrast imaging or TCD, underestimated the true CBF by as much as 20% (4). These observations were based on assessment of the maximal CSA during five minute periods of HC and the minimal CSA during hyperventilatory HO. These MCA diameter changes were replicated at 7T during HC by an independent group who reported a $7 \pm 3\%$ diameter change when ETCO_2 was kept constant at 15 mmHg above each subject's baseline (19). The time course of dilation and the contribution of the MCA to changes in CVR remain fundamental to gaining greater understanding of the contributions of these vessels versus downstream segments of the vascular tree to cerebrovascular control.

The internal carotid artery (ICA) diameter changes by approximately 20% over a range of partial pressures of CO_2 (P_aCO_2) from 15 to 65 mmHg while the partial pressure of oxygen (PO_2) was clamped (21). However, the timing of this response is unknown as the diameter measures were made after 12 to 15 minutes of CO_2 stimulus. Since the ICA can be insonated by the more cost-effective and accessible method of ultrasound it would be useful to determine if the changes in the ICA CSA during HC and HO mimic the changes in the MCA.

The purposes of this study were to determine the time course of the change in CSA and flow of the MCA and ICA over 5 minutes of HC and HO in healthy individuals and to study the contributions of MCA CSA data to the estimation of CVR values. We also estimated wall shear stress (WSS) in order to quantify how flow-mediated effects may contribute to the vascular responses.

3.2 Materials and Methods

Fourteen subjects (23 ± 3 years, 7 females) gave informed consent to participate in this study that was approved by the Health Sciences Research Ethics Board at Western University and performed in accordance with the Declaration of Helsinki. Subjects were non-smokers, were not on any medications, and had no history of cardiovascular disease.

3.2.1 Experimental Protocols

Subjects participated in two test days: 1) a Lab day where TCD of the MCA and duplex imaging of the ICA were performed and 2) a separate MRI day. The Lab and MRI days were matched for time of day. Subjects were asked to refrain from alcohol, caffeine and physical activity for 12 hours prior to testing. The protocol on each test day consisted of 5 minutes of baseline measures (Pre HC and Pre HO) followed by 5 minutes of hypercapnia (HC) or hypocapnia (HO) (the order of which was counterbalanced across participants) then a 3 to 4 minute recovery period to allow ETCO_2 levels to return to normal. The PO_2 was not clamped during the ETCO_2 manipulations. Another 5 minute baseline was then performed followed by the ETCO_2 manipulation that had yet to be performed. For HC, subjects breathed air composed of 6% CO_2 , 21% oxygen, and 72% nitrogen. Hypocapnia was induced by hyperventilation at 30 breaths per minute guided by a metronome. Previous use of these protocols in our lab suggested that ETCO_2 levels remain fairly constant (within $\sim 1\text{-}2$ mmHg) over the 5 minutes during each manipulation (23).

3.2.2 Measurements

3.2.2.1 Lab Session

Heart rate was acquired from standard ECG. Finger arterial blood pressure (BP) was measured continuously (Finometer, Finapres Medical Systems BV, Amsterdam, The Netherlands). The brachial BP waveform was corrected to brachial sphygmomanometric values. Breathing frequency and ETCO_2 were monitored continuously with a respiratory strain gauge and a gas analyzer (ML206, ADInstruments, Colorado Springs, CO, USA) respectively. Right middle cerebral artery velocity (MCAv) was measured in a supine

position (2 MHz pulsed wave TCD probe; Neurovision, Multigon Industries, Elmsford, CA, USA). The average depth of insonation was 4.8 ± 0.3 cm.

Duplex ultrasound imaging was used to record the right ICA flow velocity (ICAv) (Doppler ultrasound, 4.7 MHz probe) continuously while a longitudinal image of the vessel was taken every minute during baseline and each protocol (10 MHz probe; Vivid 7 system, GE Healthcare Canada, Mississauga, ON, Canada). The ICA recording site was at least 1 cm superior to the carotid sinus. Velocity waveforms were processed to produce an analog signal of the instantaneous weighted mean flow velocity. The 2D echo ultrasound images were stored for analysis with EchoPAC software (GE Healthcare Canada, Mississauga, ON, Canada).

3.2.2.2 MRI Session

A 3T MRI (Magnetom Prisma, Siemens Medical Solutions, Erlangen, Germany) was used to image the MCA. A 3D time of flight pulse sequence was used to identify the M1 segment location for application of a T2 fast spin echo sequence (8 slices, repetition time = 3000 ms, echo time = 96 ms, flip angle = 120° , voxel dimensions = $0.4 \times 0.4 \times 2.0$ mm³) for image acquisition. Collection of an image took approximately one minute and was gated to the peak of the pulse wave at the finger derived from an MRI-compatible pulse oximeter (8600FO MRI, Nonin Medical Inc., Plymouth, MN, USA) as measured at the right third finger. Respiration was monitored with a strain gauge around the upper abdomen and ETCO₂ data were collected as described during the Lab session.

3.2.3 Data Analysis

Three systolic and three diastolic diameters were measured for each ICA image by a blinded observer and an average of the three was taken. The accuracy of measurement was confirmed by a second blinded observer using images from four participants across the range of image quality (a total of 92 images) producing an intraclass correlation coefficient (ICC) of 0.89 ($p < 0.001$). A mean diameter was then calculated as: mean diameter (mm) = $(2/3 * \text{diastolic diameter (mm)}) + (1/3 * \text{systolic diameter (mm)})$. Internal carotid artery flow (Q_{ICA}) was determined as: Q_{ICA} (ml/min) = ICAv (cm/s) $[\pi * (\text{mean diameter (cm)} / 2)^2] * 60$ (s/min).

From the sagittal images, the MCA CSA was measured manually in triplicate by each of two blinded observers using Osirix imaging software (Pixmeo, Bernex, Switzerland) (ICC of 0.96; $p < 0.001$) and the data from both observers were averaged and reported. An estimate of blood flow in the MCA (Q_{MCA}) was determined as: Q_{MCA} (ml/min) = $MCAv$ (cm/s) * CSA (cm²) * 60 (s/min). The reproducibility of MCA flow velocity responses to HC and HO has been established in our hands under laboratory and MRI conditions, albeit with separate modalities (i.e., TCD and phase contrast imaging) (4). Therefore, Q_{MCA} data were based on $MCAv$ and CSA data that were collected on separate days. When reported, the MCA diameter was calculated from the measured CSA value. The percent change (% Δ) in CSA between baseline and HC or HO time points was also calculated for the ICA and the MCA.

Flow indices for each vessel are reported both as absolute values and as % Δ to account for differences in baseline flow. Cerebrovascular conductance (CVC) was calculated for the ICA and the MCA as the quotient of flow and mean arterial pressure (MAP). CVR was calculated for both arteries as the % Δ in flow from baseline per mmHg change in $ETCO_2$ at each minute of the 5 minute period during HC and HO. Wall shear stress was calculated for the MCA and the ICA at baseline and each minute of HC and HO as: WSS (τ , dyn/cm²) = $4 * \eta * Q / r^3 * \pi$, where η is the blood viscosity (0.009 Poise), Q is flow (ml/min) and r is the radius of the inside of the artery (cm) (3).

All variables were similar in the baseline periods of the Lab and MRI sessions so an average of this five minute period is reported for heart rate, BP, breathing frequency, $ETCO_2$, $MCAv$, $ICAv$, Q_{ICA} , Q_{MCA} , CVC, CVR and WSS indices. The values during HC and HO are reported for each minute over the 5 minute period.

3.2.4 Statistical Analysis

The effect of HC or HO on the time course of MCA and ICA changes in CSA , with the corresponding $ETCO_2$, heart rate and respiration outcomes, were characterized first using one-way repeated measures ANOVAs (main effect of time) (SigmaStat 12.0, Systat Software, San Jose, CA, USA). Subsequently, the effects of HC and HO on MCA and ICA over time were assessed using a general linear mixed ANOVA model (main effects

of artery). Additionally, comparisons between Lab values of ETCO_2 , heart rate, and respiration to MRI values over time were performed with general linear mixed ANOVA (main effect of experimental session). The effect of HC and HO on the index of WSS was examined using one-way repeated measures ANOVA. The probability level for statistical significance was $p < 0.05$ and significant main effects or interactions were assessed using Tukey's post hoc test. A post-hoc power analysis was performed with G*Power 3.1 (31) specifying two tails, an α -value of 0.05, the sample size and the effect size (Cohen's d).

3.3 Results

Clear MCA images and complete data for MCA_V and Q_{ICA} were obtained from 11 participants (23 ± 3 years, 5 females) during HC at baseline and sample sizes at each of the 5 time points were: 9, 10, 9, 9, and 8, respectively. The Pre HO sample size was 9 (23 ± 3 years, 4 females) and the sample sizes at each of the 5 time points were 8, 9, 8, 9, and 5, respectively.

During HC there was a main effect of time for all BP variables, heart rate, respiration rate, ETCO_2 , and CVC but there was no effect of artery (Table 3.1). Thus, the experimental stimuli and conditions were replicated for each of the two protocols within the same session that studied the MCA and the ICA responses. When the MCA, ICA and MRI protocols were compared there was a trend for a main effect of experimental session for respiration rate ($p = 0.06$) and no differences for ETCO_2 or heart rate.

Compared with baseline, a main effect of time was observed during HO for heart rate, respiration rate, and ETCO_2 but not for BP variables and there was no effect of artery for any of these variables when the ICA and MCA protocols were compared (Table 3.2). However, main effects of time and artery were observed for CVC where constriction of the downstream vascular bed was observed in both vessels but overall levels were greater in the ICA. During HO, there was a main effect of experimental session when comparing the MCA, ICA and MRI protocols for ETCO_2 ($p = 0.05$) and no differences in heart rate or respiration rate.

Table 3.3 shows the changes in heart rate and respiration rate during HC and HO in the MRI session. In the MRI during HC, heart rate was increased compared to baseline at minutes 2 to 5 of HC ($p<0.05$). Additionally, respiration rate was increased at minutes 4 and 5 compared to minute 1 of HC ($p=0.04$ for each). Compared to baseline, heart rate was elevated at all time points of HO ($p<0.05$) except minute 5. By design, breathing rate was elevated at all time points in HO ($p<0.001$).

Figure 3.1A shows the time course of the MCA CSA response to HC. The MCA CSA increased progressively above baseline over the five minutes of HC ($p<0.05$). Compared to baseline ($5.8 \pm 1.1 \text{ mm}^2$), the largest MCA CSA ($6.8 \pm 1.3 \text{ mm}^2$; $+14 \pm 8\%$) occurred at four minutes of HC. A main effect for time ($p=0.05$) was observed for the ICA CSA response to HC (Figure 3.1B) but no pairwise comparisons reached significance despite ETCO_2 levels that were greater than baseline at each time point ($p<0.001$). Main effects of time ($p<0.001$) and artery ($p<0.001$) were observed for $\%\Delta\text{ICA}$ and $\%\Delta\text{MCA CSA}$ (Figure 3.1C). In terms of Q_{ICA} and Q_{MCA} a main effect of time ($p<0.001$) and a trend for a difference between arteries ($p=0.07$) were observed during HC (Figure 3.1D). The $\%\Delta Q_{\text{MCA}}$ and $\%\Delta Q_{\text{ICA}}$ increased similarly with time ($p<0.001$) in each artery (Figure 3.1E).

Figure 3.2A illustrates the change in MCA CSA during HO. Compared to baseline, the MCA CSA was reduced from baseline ($5.9 \pm 0.8 \text{ mm}^2$) only at minutes four ($p=0.01$ versus baseline and $p=0.003$ versus HO min 1) and five ($5.1 \pm 0.5 \text{ mm}^2$ at HO5; $6 \pm 6\%$; $p=0.03$ versus baseline and $p=0.008$ versus HO min 1). The ICA CSA was not different from baseline at any time point during HO despite significant and rapid reductions in ETCO_2 (Figure 3.2B). A main effect of time ($p=0.02$) was observed for $\%\Delta\text{CSA}$ of the ICA and MCA during HO (Figure 3.2C). Main effects of time ($p<0.001$) and artery ($p=0.006$) were observed for absolute Q_{ICA} and Q_{MCA} values during HO (Figure 3.2D) but not for $\%\Delta$ of either value (Figure 3.2E).

During HC, a time x method interaction was observed such that the $\%\Delta\text{MCAv}$ was less than $\%\Delta Q_{\text{MCA}}$ and this effect was present after three minutes of HC ($p<0.02$;

Figure 3.3A). During HO, a main effect for time ($p<0.001$) was observed indicating similar relative reductions in both MCAv and Q_{MCA} .

Compared with baseline, MCA WSS was elevated at all HC time points ($p<0.01$), and time points 2, 4, and 5 were greater than 1 ($p<0.03$; Table 3.4). Compared with baseline, MCA WSS was reduced at all HO time points ($p<0.05$). In the ICA, wall shear stress increased progressively during HC with time points 2 to 5 minutes being different from baseline ($p<0.001$) and time points 4 and 5 minutes being greater than the first minute of HC ($p<0.05$). During HO the ICA WSS was reduced compared to baseline at all time points except minute five ($p<0.05$).

The contributions of changes in CSA to the overall CVR outcome was examined by using MCAv and Q_{MCA} to calculate CVR. After five minutes, CVR was 3.13 ± 1.55 %/mmHg when MCAv was used and 4.88 ± 2.46 %/mmHg using Q_{MCA} (Figure 3.4A). This is a difference of $58 \pm 25\%$ in CVR. Using ICAv and Q_{ICA} to calculate CVR during HC resulted in very similar estimates to those calculated from Q_{MCA} after five minutes, although the pattern of response appears to be different (using ICAv: 4.56 ± 2.02 %/mmHg and using Q_{ICA} : 4.70 ± 1.93 %/mmHg at minute five; Figure 3.4A). Hypocapnia elicited a similar CVR value at five minutes when it was calculated using ICAv, Q_{ICA} and MCAv despite a different response pattern between MCAv and estimates based on ICAv. Additionally, CVR calculated using Q_{MCA} was smaller than any of the other estimates indicating that failure to account for MCA CSA changes leads to an underestimation of CVR to HO (Figure 3.4B).

Table 3.1: Physiological responses to hypercapnia in the ICA and the MCA over time.

Time		Pre	1	2	3	4	5	P-value	
Sample		(11)	(9)	(10)	(9)	(9)	(8)	Time	Artery
SBP	ICA	112 ± 10	114 ± 12	115 ± 11	116 ± 13	116 ± 12	118 ± 14	<0.001	0.97
(mmHg)	MCA	111 ± 12	114 ± 12	116 ± 13	117 ± 14	116 ± 13	118 ± 13		
DBP	ICA	68 ± 10	66 ± 6	67 ± 6	67 ± 8	68 ± 9	70 ± 9	0.021	0.94
(mmHg)	MCA	66 ± 8	66 ± 8	67 ± 8	67 ± 9	68 ± 9	70 ± 9		
MAP	ICA	82 ± 8	83 ± 7	84 ± 6	85 ± 8	86 ± 9	87 ± 9	<0.001	0.94
(mmHg)	MCA	82 ± 8	83 ± 9	84 ± 8	84 ± 9	86 ± 9	86 ± 9		
HR	ICA	60 ± 7	63 ± 6	66 ± 8	64 ± 11	66 ± 11	62 ± 9	<0.001	0.48
(bpm)	MCA	62 ± 11	67 ± 11	67 ± 9	68 ± 10	70 ± 11	66 ± 8		

Resp	ICA	15 ± 3	15 ± 3	15 ± 2	16 ± 2	16 ± 2	16 ± 1	<0.001	0.50
(breaths/min)	MCA	14 ± 3	15 ± 2	15 ± 2	15 ± 3	15 ± 2	16 ± 2		
ETCO ₂	ICA	39 ± 5	48 ± 3	49 ± 4	49 ± 5	49 ± 4	49 ± 5	<0.001	0.55
(mmHg)	MCA	40 ± 4	49 ± 4	50 ± 4	51 ± 5	51 ± 5	50 ± 5		
CVC	ICA	4.0 ± 1.2	4.3 ± 1.3	4.7 ± 1.3	5.0 ± 1.6	5.5 ± 2.2	4.9 ± 1.4	<0.001	0.12
(ml/min/ mmHg)	MCA	3.0 ± 1.0	3.8 ± 1.4	4.0 ± 1.2	4.4 ± 1.3	4.4 ± 1.3	3.9 ± 1.3		

Values are mean ± standard deviation. Sample sizes are shown in brackets. No time x artery interactions were present. CVC = cerebrovascular conductance; DBP = diastolic blood pressure; ETCO₂ = end tidal carbon dioxide; HR = heart rate; ICA = internal carotid artery; MAP = mean arterial pressure; MCA = middle cerebral artery; Resp = respiration rate; SBP = systolic blood pressure. Values for ICA and MCA were obtained during separate trials of the same session, acquired in varied order.

Table 3.2: Physiological responses to hypocapnia in the ICA and the MCA over time.

Time		Pre	1	2	3	4	5	P-value	
Sample		(9)	(8)	(9)	(8)	(9)	(5)	Time	Artery
SBP	ICA	119 ± 9	120 ± 12	121 ± 12	119 ± 15	118 ± 12	120 ± 13	0.35	0.70
(mmHg)	MCA	118 ± 12	116 ± 13	118 ± 12	116 ± 11	117 ± 13	117 ± 4		
DBP	ICA	69 ± 10	69 ± 12	71 ± 11	70 ± 12	69 ± 11	71 ± 11	0.19	0.85
(mmHg)	MCA	69 ± 9	67 ± 9	68 ± 10	68 ± 9	69 ± 9	70 ± 8		
MAP	ICA	87 ± 9	87 ± 11	89 ± 11	88 ± 13	87 ± 11	88 ± 11	0.14	0.70
(mmHg)	MCA	86 ± 9	84 ± 10	85 ± 10	84 ± 9	85 ± 10	87 ± 4		
HR	ICA	60 ± 12	66 ± 10	62 ± 12	66 ± 12	65 ± 12	64 ± 11	<0.001	0.95
(bpm)	MCA	60 ± 11	65 ± 13	65 ± 14	66 ± 15	65 ± 13	62 ± 9		
Resp	ICA	15 ± 3	29 ± 1	28 ± 3	29 ± 2	29 ± 2	28 ± 5	<0.001	0.93
(breaths/min)	MCA	14 ± 3	29 ± 2	29 ± 2	30 ± 1	28 ± 2	28 ± 2		

ETCO ₂	ICA	39 ± 3	31 ± 4	30 ± 3	29 ± 4	29 ± 3	28 ± 2	<0.001	0.47
(mmHg)	MCA	39 ± 5	30 ± 4	29 ± 5	28 ± 5	27 ± 5	25 ± 4		
CVC (ml/min/ mmHg)	ICA	3.4 ± 0.7	2.8 ± 0.3	2.5 ± 0.3	2.7 ± 0.3	2.8 ± 0.7	2.5 ± 0.4	<0.001	0.023
	MCA	2.7 ± 0.7	2.4 ± 0.7	2.2 ± 0.7	2.2 ± 0.5	2.0 ± 0.6	2.0 ± 0.7		

Values are mean ± standard deviation. Sample sizes are shown in brackets. No time x artery interactions were present. CVC = cerebrovascular conductance; DBP = diastolic blood pressure; ETCO₂ = end tidal carbon dioxide; HR = heart rate; ICA = internal carotid artery; MAP = mean arterial pressure; MCA = middle cerebral artery; Resp = respiration rate; SBP = systolic blood pressure. Values for ICA and MCA were obtained during separate trials of the same session, acquired in varied order.

Table 3.3: Physiological variables during hypercapnia and hypocapnia in the MRI session.

	Pre	1	2	3	4	5
Hypercapnia	(11)	(9)	(10)	(9)	(9)	(8)
Heart rate (bpm)	59 ± 8	62 ± 10	66 ± 12*	67 ± 10*	68 ± 10*	69 ± 10*
Respiration rate (breaths/minute)	13 ± 3	13 ± 3	13 ± 3	14 ± 2	15 ± 2†	14 ± 3†
End tidal carbon dioxide (mmHg)	37 ± 3	52 ± 2*	52 ± 2*	53 ± 2*	53 ± 2*	52 ± 1*
Hypocapnia	(9)	(8)	(9)	(8)	(9)	(5)
Heart rate (bpm)	61 ± 9	70 ± 10*	68 ± 11*	67 ± 11*	67 ± 11*	67 ± 4
Respiration rate (breaths/minute)	14 ± 3	29 ± 1*	29 ± 1*	29 ± 1*	29 ± 1*	28 ± 1*
End tidal carbon dioxide (mmHg)	37 ± 4	24 ± 5*	25 ± 6*	24 ± 6*	24 ± 6*	25 ± 6*

Values are mean ± SD. *p<0.05 compared to Pre. †p<0.05 compared to time 1. Sample sizes are in brackets.

Table 3.4: Index of wall shear stress (dyn/cm²) during hypercapnia and hypocapnia in the internal carotid (ICA) and middle cerebral artery (MCA).

		Pre	1	2	3	4	5
Hypercapnia	ICA	3.6 ± 1.4	4.2 ± 1.6	4.7 ± 1.7*	4.8 ± 1.7*	5.0 ± 1.8*†	4.0 ± 1.0*†
	MCA	19 ± 5.6	20 ± 4.4*	23 ± 6.4*†	22 ± 4.6*	23 ± 4.9*†	23 ± 6.1*†
Hypocapnia	ICA	3.0 ± 0.9	2.5 ± 0.6*	2.3 ± 0.7*	2.5 ± 0.6*	2.5 ± 1.0*	2.6 ± 0.8
	MCA	17 ± 4.8	15 ± 4.9*	14 ± 5.1*	15 ± 5.4*	14 ± 5.6*	16 ± 6.9*

Values are mean ± SD. *p<0.05 compared to Pre. †p<0.05 compared to time point 1.

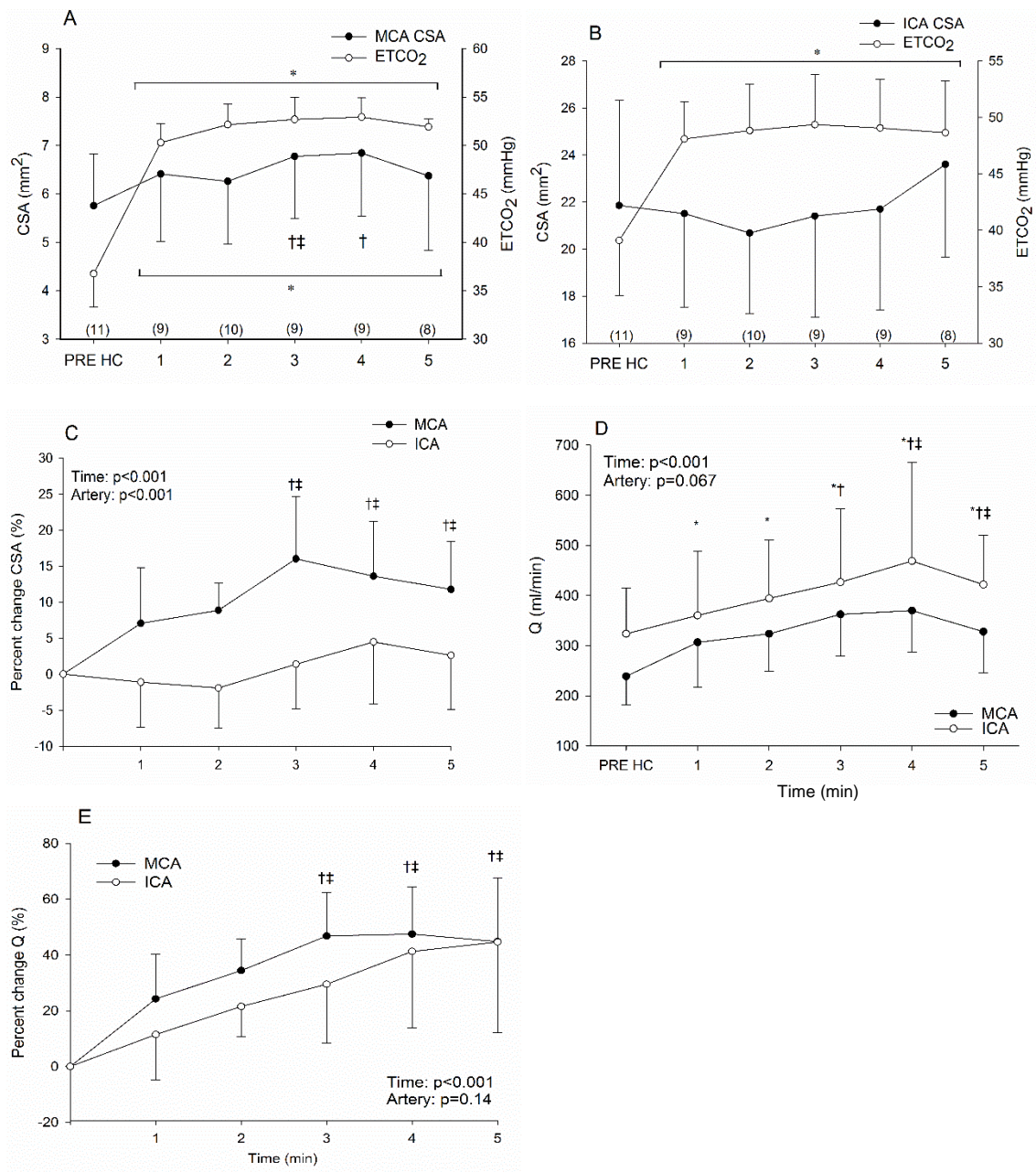


Figure 3.1: Change in MCA and ICA indices during hypercapnia. Sample sizes at each time point are in brackets along the x-axis. A: MCA CSA. B: ICA CSA. There was a main effect of time ($p=0.045$) but no significant pairwise comparisons. C: Percent change in CSA from baseline. D: Absolute Q. E: Percent change in Q from baseline. CSA = cross-sectional area; CVR = cerebrovascular reactivity; ET_{CO}2 = end tidal carbon

dioxide; HC = hypercapnia; HO = hypocapnia; ICA = internal carotid artery; MCA = middle cerebral artery; Q = flow. * $p < 0.05$ compared to Pre; † $p < 0.05$ compared to time 1; ‡ $p < 0.05$ compared to time 2.

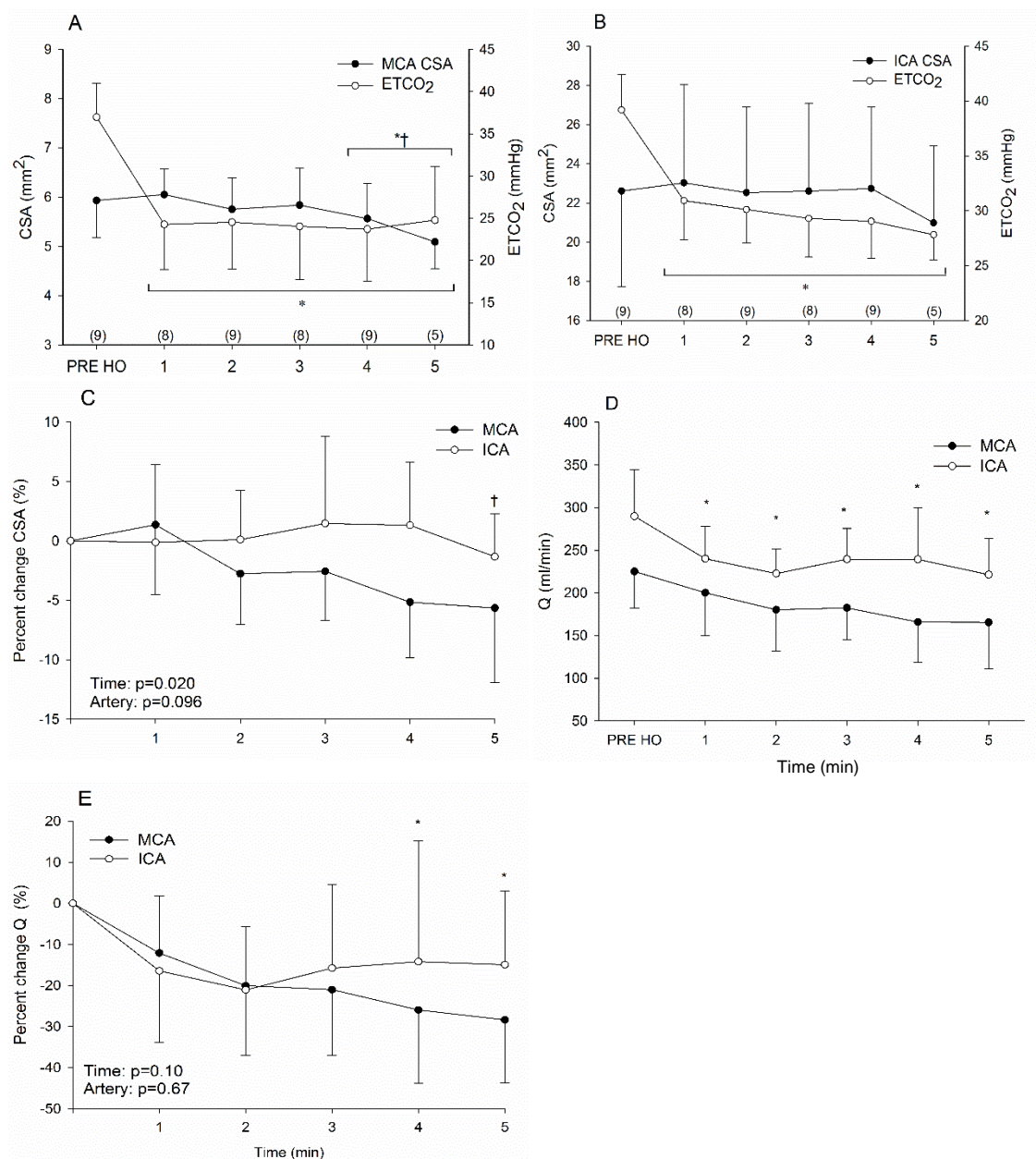


Figure 3.2: Change in MCA and ICA indices during HO. Sample sizes at each time point are in brackets along the x-axis. A: MCA CSA. B: ICA CSA. C: Percent change in CSA from baseline. D: Absolute Q. E: Percent change in Q from baseline. CSA = cross-sectional area; CVR = cerebrovascular reactivity; ETCO₂ = end tidal carbon dioxide; HC = hypercapnia; HO = hypocapnia; ICA = internal carotid artery; MCA = middle cerebral artery; Q = flow. *p<0.05 compared to Pre; †p<0.05 compared to time 1.

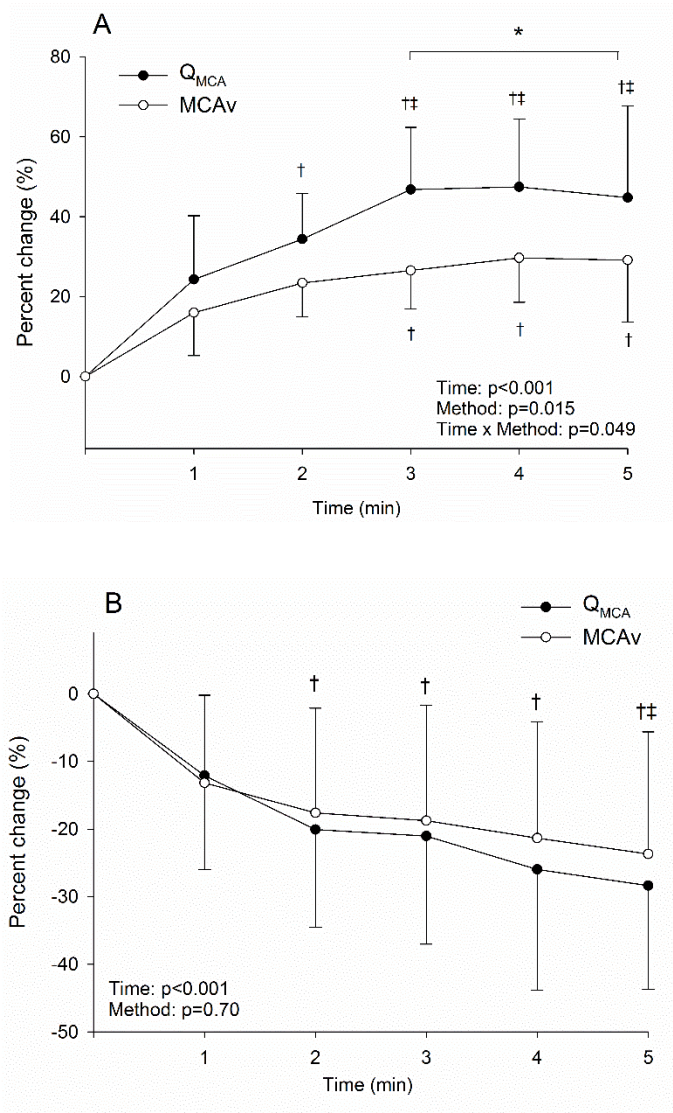


Figure 3.3: Percent change of Q_{MCA} and MCAv during changes in $ETCO_2$. A: Hypercapnia. B: Hypocapnia. $ETCO_2$ = end tidal carbon dioxide; MCAv = middle cerebral artery flow velocity; Q_{MCA} = middle cerebral artery flow. * $p < 0.05$ for Q_{MCA} versus MCAv; † $p < 0.05$ compared to time 1; ‡ $p < 0.05$ compared to time 2.

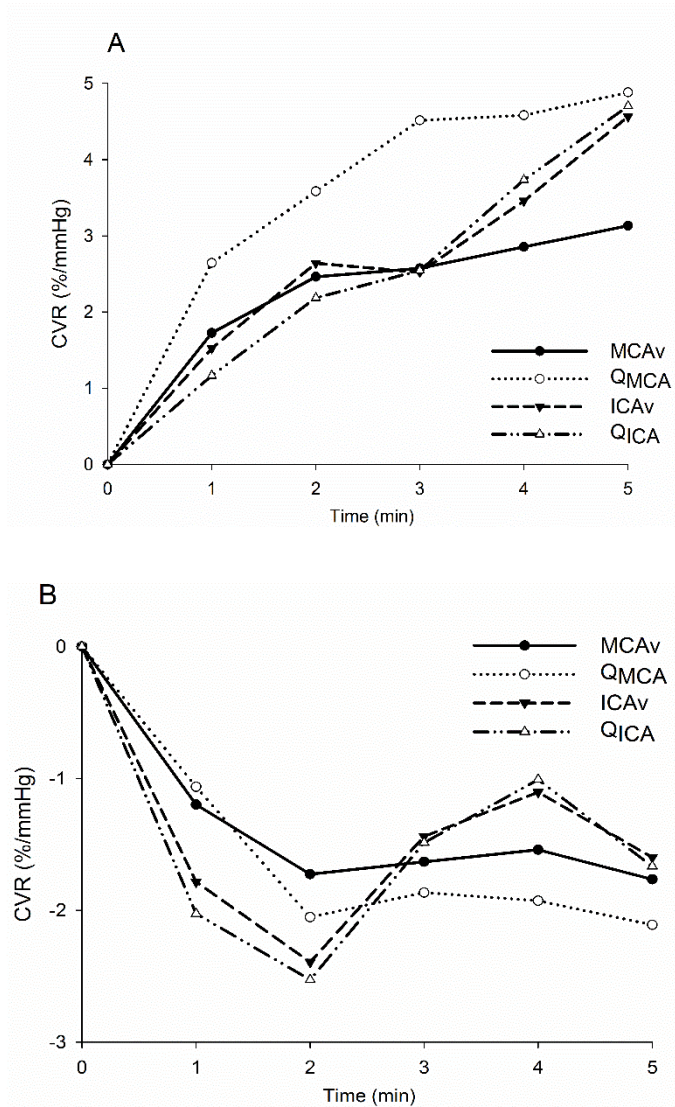


Figure 3.4: Cerebrovascular reactivity (CVR) over five minutes calculated from ICAv, QICA, MCAv, and QMCA during manipulations of ET_{CO}₂. A: Hypercapnia. Standard deviation ranges are as follows: MCAv 1.02 to 1.55 %/mmHg; QMCA 1.33 to 2.46 %/mmHg; ICAv 1.39 to 2.04 %/mmHg; QICA 0.92 to 2.10 %/mmHg. B: Hypocapnia. MCAv -1.22 to -1.65 %/mmHg; QMCA -1.11 to -1.71 %/mmHg; ICAv -1.98 to -2.92 %/mmHg; QICA -2.05 to -3.18 %/mmHg. ET_{CO}₂ = end tidal carbon dioxide; ICAv = internal carotid artery flow velocity; MCAv = middle cerebral artery flow velocity; QICA = internal carotid artery flow; QMCA = middle cerebral artery flow.

3.4 Discussion

The main findings of this study are as follows: 1) The CSA of the MCA increased by the first minute during HC, while a decrease in MCA CSA was not observed until the fourth minute during HO. 2) No change was observed in ICA CSA during these HC or HO stimuli despite large changes in Q, flow velocity and WSS in each vessel and condition. 3) The corresponding relative changes in Q_{MCA} and Q_{ICA} were similar for both HC and HO. 4) The percent change in $MCAv$ was less than the percent change in Q_{MCA} during HC but not HO. 5) Failure to account for MCA dilation during HC underestimated CVR by 58%. These results indicate that the subcortical vessels dilate rapidly, contribute significantly to the change in cerebral vascular conductance during HC, and are important to the normal CVR response during HC. Additionally, the relative change in ICA flow corresponded well to the ipsilateral change in MCA flow rate as would be expected. Overall, the data illustrate a greater vasoreactivity of the MCA versus the ICA in response to changes in $ETCO_2$.

The baseline MCA CSA values observed in this study ($5.8 \pm 1.1 \text{ mm}^2$), using a different complement of participants, are nearly identical to those observed in our previous work ($5.9 \pm 0.8 \text{ mm}^2$) (4). Also, the $8 \pm 3\% \Delta$ in MCA diameter during HC, and $4 \pm 4\% \Delta$ during HO, of the previous study are very similar to the respective values of $8 \pm 4\%$ and $3 \pm 2\%$ in the current study. Similarly, the average ICA baseline diameter of $5.2 \pm 0.5 \text{ mm}$ is comparable to the values reported by Willie et al. of $5.2 \pm 0.6 \text{ mm}$ (21) and Liu et al. of $4.7 \pm 0.7 \text{ mm}$ (9).

An important observation of the current study was that the rapid change in MCA CSA following an increase in $ETCO_2$ was not matched by concurrent ICA dilation. The lack of change in ICA dimensions stands in contrast to the findings of Willie et al., who observed both a dilation during iso-oxic HC and constriction during iso-oxic HO (21). This between-study difference likely reflects the shorter stimulus used in the current study. Specifically, ICA diameter measurements were made during the first five minutes of the CO_2 challenge of the current study but after at least 12 minutes in the Willie et al. study. Also, the magnitude of the HC stimulus was ~30% greater (65 mmHg) in the

Willie et al. study. Thus, the MCA appears to exert greater sensitivity to changes in ETCO_2 than the ICA.

The current observations have important implications for the study of CVR, a measurement used often as an index of cerebrovascular health (11, 15). Many studies of CVR take advantage of the accessible TCD method to study MCA CBFV responses to HC (see Topicuoglu (16); Tsivgoulis et al (17) for review). A long-standing assumption of TCD is that the diameters of the large subcortical vessels being interrogated change little so that flow velocity is proportionate to changes in total flow. Whereas this assumption found support using earlier MRI devices operating at 1.5 T (14, 18), the improved resolution of current MRI technology exposed the reactivity of this conduit vessel to changes in ETCO_2 . Thus, reliance on CBFV data underestimates the true change in CBF and this, of course, would underestimate the true values of CVR during both HC and HO. The magnitude of this error will depend on the vasodilatory sensitivity of the MCA that may vary with age, sex, disease, etc. Further, the combined data from the current study, our previous report (4), and that of Willie et al. (21), suggest that the magnitude of this error may change over the duration, and possibly dose, of the ETCO_2 challenge. These observations highlight the need for caution when interpreting CVR outcomes.

In contrast to the findings during HC, MCA_V did not underestimate Q_{MCA} during HO as we previously reported (4). The current data indicate that this constrictor pattern was delayed, relative to the more rapid dilation, not being observed until the fourth minute of HO (Figure 3B) and even then there was not a significant difference between the percent change in MCA_V and Q_{MCA} . The slower and smaller effect of HO suggests that the MCA exists at a heightened level of contractile state at baseline levels of ETCO_2 such that its sensitivity for further constriction is diminished. This interpretation is consistent with the exponential nature of increase in CBF during the transition from HO to HC (4, 21). The variability in findings between studies may be due to the approach that highlighted the peak response in our earlier report versus the time course pattern in the current analysis. Also, inter-individual variability and the overall smaller response to HO will add to between-study variations. Another source of variability could be the

difference in ETCO_2 between the Lab and MRI sessions. In the future, this issue could be resolved with clamping of ETCO_2 levels to ensure that the same stimulus was attained on both the Lab and MRI day.

In the current approach, the changes in flow observed in the ICA were driven primarily by the changes in CBFV that, in turn, resulted from dilation or constriction of the downstream vessels. Conversely, the changes in flow at the MCA resulted from a combination of the change in velocity (reflecting changes in downstream vascular conductance) and the change in MCA CSA. Thus, five important conclusions relevant to CVR assessment can be made from the current observations. First, use of velocity data alone underestimates the change in Q_{MCA} . Second, measures of ICA flow reflect more accurately the CVR outcome with HC than MCA mean flow velocity and CVR calculated using Q_{ICA} provides a similar estimate to that calculated from Q_{MCA} when MRI technology is not available, at least within the timeframe of the current paradigm. Third, the subcortical cerebral vessels, such as the MCA, contribute importantly to the CVR outcome. Fourth, reactivity of cerebrovascular segments appears to increase when moving from the ICA to the MCA and possibly beyond. Fifth, CVR appears to change over time during application of a five minute stimulus and this should be considered when quantifying CVR.

This project provides, to our knowledge, the first insight into ETCO_2 -induced changes in WSS in the M1 segment of the MCA and in the ICA of humans. Of course, calculating WSS using a derivation of the Hagen-Poiseuille equation in human pulsatile flow ignores assumptions of laminar Newtonian fluid flowing through straight rigid cylindrical tubes. Also, the values presented here are calculated from flow data that are averaged over time and cannot be used to consider peak and nadir values observed during systole and diastole. Therefore, the values of WSS presented here must be considered to be approximates only and qualitative in nature. With these constraints, WSS increased during HC by ~40% in the ICA and 15% in the MCA. Thus, the dilatory response in the MCA appears to have prevented the large increase in shear stress that was present in the ICA. Likely, a hypercapnia induced increase in flow in blood vessels downstream to the MCA increased shear stress at the MCA that initiated the vasodilation. In addition, these

data suggest that the ICA is relatively insensitive to acute flow-mediated dilatory stimuli. Based on what has been documented about the time course of flow-mediated dilation in the periphery, and in particular the brachial artery, peak dilation is observed around 60 seconds after a stimulus in young subjects (2). It appears that this same flow-mediated mechanism does not play a role in stimulating dilation in the ICA. However, ICA dilation does appear to begin near the end of the five minute CO₂ stimulus (Figure 1B) consistent with the significant dilation observed in this vessel following 15 minutes of hypercapnia (21). Therefore, it seems unlikely that flow-mediated effects play a role in ICA dilation and at this point the reasons for this are unknown.

This study is limited by the fact that the current design could not rule out the effects of blood pressure on our estimates of CSA and Q. Dynamic cerebral autoregulation is reduced during HC (10) resulting in greater fluctuations in CBF with pressure. Thus, the increase in blood pressure during HC could contribute as a stimulus for increased flow and, perhaps, contribute to the apparent dilation at the MCA. However, such an impact of blood pressure is unlikely in the current study because the increase in MAP at the first minute of HC was small (from 82 ± 8 to 83 ± 8 mmHg) and a significant dilation was already observed. Another limitation is that the MRI and Lab sessions were performed on different days and on average, the interval between tests was 101 ± 74 days. In five subjects the two test days were separated by 22 days but an upgrade of our MRI system resulted in a delay for the remaining participants. To assess reproducibility, we determined CBFV CVR in one subject during HO and three subjects (all males) during HC on two durations separated by 29 ± 24 days. The ICC between test days was 0.81 ($p < 0.001$). Additionally, we have compared estimates of CBFV on separate days (TCD and phase contrast imaging) that were performed 53 ± 48 days apart and the ICC was 0.83 ($p < 0.001$) (4).

Additionally, we did not control for menstrual cycle in this study. Cerebrovascular resistance may change over the course of the menstrual cycle (8), but whether or not menstrual cycle phase alters the MCA CSA response to HC remains to be determined. Also, we did not clamp PO₂ during HC or HO. However, when measured independently of the current study end tidal PO₂ increased from 104 ± 8 to 136 ± 4

mmHg during HC (n=4) and during HO from 116 ± 4 to 136 ± 5 mmHg during HO (n=3). Based on the findings of Willie et al. (21) we speculate that this change in PO_2 would have little effect on CBFV or CSA outcomes because an increase in arterial PO_2 to 320 mmHg only decreased MCAv by ~ 4 cm/s on average and decreased ICA diameter by 0.03 cm. Lastly, the statistical power achieved for MCA CSA changes across minutes one to five are as follows: 0.42, 0.35, 0.71, 0.75, and 0.34, respectively. The differences in statistical power between the current and previous studies can be explained on the basis of the different methodological approach that minimized variability in the previous study. Specifically, in our previous work (4) the achieved power was 0.87 and was based on the peak response over a five minute stimulus. In contrast, the current study focused on effect sizes at each time point, increasing exposure to inter-individual differences in the rate of MCA dilation. During HO, the achieved powers are less than 0.6 at all time points due to a smaller overall response.

In summary, this study supports the conclusion that the CSA of the MCA increases by the first minute of HC. In contrast, the change in MCA CSA during HO was not detected until the fourth minute. Moreover, no changes in the CSA of the ICA were detected within the five minute stimulus period. Thus, in support of our previous findings, TCD MCAv underestimates changes in Q_{MCA} during HC but less so during HO (4). The similar relative changes in CBF between the ICA and MCA, suggest that the use of duplex ultrasound to evaluate ICA flow could be used as a surrogate measure of CVR when MCA diameters are not accessible.

3.5 References

1. Ainslie PN, Duffin J. Integration of cerebrovascular CO₂ reactivity and chemoreflex control of breathing: mechanisms of regulation, measurement, and interpretation. *Am J Physiol Integr Comp Physiol* 296: R1473–1495, 2009.
2. Black MA, Cable NT, Thijssen DHJ, Green DJ. Importance of measuring the time course of flow-mediated dilatation in humans. *Hypertension* 51: 203–210, 2008.
3. Bolduc V, Thorin-Trescases N, Thorin E. Endothelium-dependent control of cerebrovascular functions through age: exercise for healthy cerebrovascular aging. *Am J Physiol Heart Circ Physiol* 305: H620–633, 2013.
4. Coverdale NS, Gati JS, Opalevych O, Perrotta A, Shoemaker JK. Cerebral blood flow velocity underestimates cerebral blood flow during modest hypercapnia and hypocapnia. *J Appl Physiol* 117: 1090–1096, 2014.
5. Faraci FM, Heistad DD. Regulation of large cerebral arteries and cerebral microvascular pressure. *Circ Res* 66: 8–17, 1990.
6. Faul F, Erdfelder E, Lang AG, Buchner A. G*Power 3: a flexible statistical power analysis program for the social, behavioral, and biomedical sciences. *Behav Res Methods* 39: 175–191, 2007.
7. Kety SS, Schmidt CF. The effects of altered arterial tensions of carbon dioxide and oxygen on cerebral blood flow and cerebral oxygen consumption of normal young men. *J Clin Invest* 27: 484–492, 1948.
8. Krejza J, Rudzinski W, Arkuszewski M, Onuoha O, Melhem ER. Cerebrovascular reactivity across the menstrual cycle in young healthy women. *Neuroradiol J* 26: 413–419, 2013.
9. Liu J, Zhu YS, Hill C, Armstrong K, Tarumi T, Hodics T, Hynan LS, Zhang R. Cerebral autoregulation of blood velocity and volumetric flow during steady-state changes in arterial pressure. *Hypertension* 62: 973–979, 2013.

10. Panerai RB, Deverson ST, Mahony P, Hayes P, Evans DH. Effects of CO₂ on dynamic cerebral autoregulation measurement. *Physiol Meas* 20: 265–275, 1999.
11. Portegies ML, de Bruijn RF, Hofman A, Koudstaal PJ, Ikram MA. Cerebral vasomotor reactivity and risk of mortality: the Rotterdam Study. *Stroke* 45: 42–47, 2014.
12. Poulin M, Robbins P. Indexes of flow and cross-sectional area of the middle cerebral artery using Doppler ultrasound during hypoxia and hypercapnia in humans. *Stroke* 27: 2244–2250, 1996.
13. Schmetterer L, Findl O, Strenn K, Graselli U, Kastner J, Eichler H, Wolzt M. Role of NO in the O₂ and CO₂ responsiveness of cerebral and ocular circulation in humans. *Am J Physiol Integr Comp Physiol* 273: R2005–R2012, 1997.
14. Serrador JM, Picot PA, Rutt BK, Shoemaker JK, Bondar RL. MRI measures of middle cerebral artery diameter in conscious humans during simulated orthostasis. *Stroke* 31: 1672–1678, 2000.
15. Silvestrini M, Vernieri F, Pasqualetti P, Matteis M, Passarelli F, Troisi E, Caltagirone C. Impaired cerebral vasoreactivity and risk of stroke in patients with asymptomatic carotid artery stenosis. *JAMA* 283: 2122–2127, 2000.
16. Topcuoglu MA. Transcranial Doppler ultrasound in neurovascular diseases: diagnostic and therapeutic aspects. *J Neurochem* 123 Suppl : 39–51, 2012.
17. Tsivgoulis G, Alexandrov A V, Sloan MA. Advances in transcranial Doppler ultrasonography. *Curr Neurol Neurosci Rep* 9: 46–54, 2009.
18. Valdueza JM, Balzer JO, Villringer A, Vogl TJ, Kutter R, Einhaupl KM. Changes in blood flow velocity and diameter of the middle cerebral artery during hyperventilation: assessment with MR and transcranial Doppler sonography. *AJNR American J Neuroradiol* 18: 1929–1934, 1997.

19. Verbree J, Bronzwaer A-SGT, Ghariq E, Versluis MJ, Daemen MJ, van Buchem M a, Dahan A, Van Lieshout JJ, van Osch MJP. Assessment of middle cerebral artery diameter during hypocapnia and hypercapnia in humans using ultra high-field MRI. *J Appl Physiol* 117: 1084-1089, 2014.
20. Wang Q, Paulson OB, Lassen NA. Effect of Nitric Oxide Blockade by N^G -Nitro-L-Arginine on Cerebral Blood Flow Response to Changes in Carbon Dioxide Tension. *J Cereb Blood Flow Metab* 12: 947-953.
21. Willie CK, Macleod DB, Shaw AD, Smith KJ, Tzeng YC, Eves ND, Ikeda K, Graham J, Lewis NC, Day TA, Ainslie PN. Regional brain blood flow in man during acute changes in arterial blood gases. *J Physiol* 590: 3261–3275, 2012.

Chapter 4

4 Role of the middle cerebral artery and grey matter volume in cerebrovascular changes with healthy aging

4.1 Introduction

The cerebral vasculature is highly sensitive to alterations in the partial pressure of carbon dioxide ($P_a\text{CO}_2$) and in general, a lesser reactivity or change in cerebral blood flow velocity (CBFV) or cerebral blood flow (CBF) to a change in $P_a\text{CO}_2$ is indicative of increased risk of stroke and all-cause mortality and this measure is known as cerebrovascular reactivity (CVR) (98, 111). Age is currently the number one risk factor for development of cerebrovascular disease (41). It is generally well established that absolute CBFV as measured at the middle cerebral artery (MCA) with transcranial Doppler ultrasound (TCD) is reduced with healthy aging (11, 93, 134). However, there is conflicting evidence as to whether CVR is reduced with aging with some studies reporting decreased CVR with age (9, 11, 34, 132), while others reported no difference (35, 55, 88, 93). Some variability between studies can likely be attributed to different vasodilatory stimuli ranging from 5 to 7% CO_2 in room air (9, 11, 34, 35, 55, 88, 93, 132) or 5% CO_2 in 95% oxygen (9) and different modalities to acquire CBFV and CBF (TCD (9, 11, 34, 35, 88, 93), positron emission tomography (55), xenon inhalation (132)).

Examinations of CVR in healthy aging are further complicated by the fact that the majority of studies rely on estimates of CBFV rather than CBF. Many studies obtain these data using TCD that targets the MCA with the assumption that the diameter of the MCA does not change. However, we have documented with 3T magnetic resonance imaging (MRI) in two separate groups of young healthy subjects that the diameter of the MCA increases by approximately 8% during hypercapnia (HC) with 6% CO_2 (23, 24). Thus, at the end of five minutes of HC, CVR calculated with CBF was 58% greater than CVR calculated from CBFV (24). With 7T MRI, a MCA diameter change of 7% with HC of 15 mmHg above baseline has also been reported (121).

Previous studies using TCD to examine aging and CVR have not accounted for MCA dilation and a possible difference in the dilatory capacity of the cerebrovasculature between young and older groups as cerebrovascular conductance (CVC) is reduced with aging (2). There is evidence that the CBF response to HC is mediated by prostaglandins and/or nitric oxide (NO) (11, 71). Since both of these mediators decrease with age, at least in the periphery (36, 112), it is possible that older adults may not have the same dilatory response at the MCA as young subjects. If this is the case, quantifying CVR with CBF rather than CBFV may expose a difference between young and older groups that is masked when MCA diameter changes are not taken into account. Also, it is important to note that CVR alone does not quantify whether the dilatory capacity of the cerebrovasculature is intact with age. If the end tidal CO₂ (ETCO₂) change is equivalent between groups with HC then the change in CBF is the primary determinant of CVR. However, an increase in CBF could be a result of a change in mean arterial pressure (MAP) alone. Therefore, it is necessary to examine CVC in addition to CVR to quantify cerebrovascular health with age.

Additionally, with aging, brain atrophy occurs and is more pronounced in grey matter (GM) than white matter (WM) (67) with certain areas within GM and WM being more affected than others (4, 21). Thus, when CBF is compared in a young population to an older population it may be difficult to draw conclusions when the volume of the vascular bed being perfused is unknown. Chen et al. (2011) found that regional perfusion quantified with arterial spin labelling and cortical thickness were not closely related throughout much of the cortex (18). However, these measurements are based on voxel-level analysis and it is not clear whether this dissociation between CBF and GM volume holds with a more global measure of CBF, as with TCD. Therefore, the purposes of this study were to compare the change in cross-sectional area (CSA) of the MCA during HC in young adults (YA) to that in older healthy adults (OA) and to assess how these changes may impact estimates of CVR. We estimated brain volume, and more specifically GM volume, in order to determine if the reduction in CBFV and/or CBF with age is related to a reduction in GM volume.

4.2 Materials and Methods

Ten older subjects aged 59 to 75 years (66 ± 7 years, 5 females) and 12 younger subjects (24 ± 4 years, range 20 to 30 years, 6 females) gave informed consent to participate in this study that was approved by the Health Sciences Research Ethics Board at Western University and performed in accordance with the Declaration of Helsinki. Subjects were non-smokers who had no history of cardiovascular disease. A female OA was on 10 mg per day of Clobazam for seizures but had not had a seizure in 13 years. Additionally, an older male subject was on Warfarin for a blood clot that occurred five years prior. All other subjects were not on any type of medications. All subjects were recreationally active. Female OA reported that they were postmenopausal (and this was confirmed with sex hormone analysis (Table 4.3)) and not on hormone replacement therapy and young female subjects were studied in the early follicular phase of their menstrual cycle (days 1 to 6) or the low hormone phase of oral contraceptives (4 of 6 young female participants were taking oral contraceptives).

4.2.1 Experimental Protocols

All subjects participated in a familiarization session and two experimental sessions, including what will be referred to as an MRI day and a Lab day. During the familiarization session all experimental protocols were thoroughly explained, subjects practiced breathing 6% CO₂, and completed the Montreal Cognitive Assessment (MoCA: www.mocatest.org) and the Trail Making Test to assess cognitive abilities. The MoCA is a 10-minute test that covers eight cognitive domains and is scored out of 30 where a score less than 26 indicates mild cognitive impairment (19). The Trail Making Test consists of Parts A and B and in Part A 25 circles are numbered from 1 to 25 and the time is recorded while you connect the circles numerically as fast as possible. In Part B there is a combination of 25 consecutive numbers and letters that must be connected alternately (i.e., 1-A, 2-B, 3-C, etc.) as fast as possible. Times can then be stratified into percentiles based on normative data (26).

Prior to each experimental session subjects were asked to refrain from alcohol, physical activity, and caffeine for 12 hours prior to testing. For the Lab testing session, a blood sample was obtained after a 12-hour fast that was analyzed for blood glucose, hemoglobin, cholesterol, triglyceride, 17- β estradiol, progesterone, and testosterone concentrations. A small meal consisting of a granola bar and juice was then provided. For the MRI day subjects were permitted to eat a small breakfast before the testing session. For each day a HC trial was performed where subjects breathed air that consisted of 6% CO₂, 21% oxygen, and 72% nitrogen. Each of these HC periods consisted of approximately three minutes of baseline and five minutes of HC. During HC the partial pressure of oxygen was not clamped.

4.2.2 Measurements

4.2.2.1 Lab Session

Initially, three seated blood pressure (BP) measurements were taken (HEM-790-ITCAN, Omron, Lake Forest, IL, USA). Images of the right and left common carotid artery (10 MHz probe; Vivid 7 system, GE Healthcare Canada, Mississauga, ON, Canada) were then captured while seated in order to quantify intima-media thickness. Throughout, heart rate was acquired from standard ECG. Arterial BP was measured with finger cuff plethysmography (Finometer, Finapres Medical Systems BV, Amsterdam, The Netherlands) and the brachial BPs were derived from the finger pressure waveform corrected to manual sphygmomanometric values. Respiration rate and ET-CO₂ were monitored with a strain gauge and a gas analyzer (ML206, ADInstruments, Colorado Springs, CO, USA), respectively. In the supine position, the right MCA was insonated to measure CBFV (2 MHz pulsed wave TCD probe; Neurovision, Multigon Industries, Elmsford, CA, USA) with an average depth of insonation of 4.9 ± 0.4 cm in YA and 5.0 ± 0.5 cm in OA.

4.2.2.2 MRI Session

MRI was performed with a 3T system (Magnetom Prisma, Siemens Medical Solutions, Erlangen, Germany). A 3D time of flight pulse sequence was used to identify the location on the M1 segment of the MCA for application of a T2 fast spin echo sequence (8 slices,

repetition time = 3000 ms, echo time = 96 ms, flip angle = 120° , voxel dimensions = $0.4 \times 0.4 \times 2.0 \text{ mm}^3$). The pulse sequence was gated to the peak of the pulse wave measured at the third finger of the right hand with an MRI-compatible pulse oximeter (8600FO MRI, Nonin Medical Inc., Plymouth, MN, USA). Collection of an image took approximately 1.25 minutes. Respiration was monitored with a strain gauge around the upper abdomen and ETCO_2 data were collected as described during the Lab session. Additionally, a T1-weighted structural image was acquired with a 3D MPRAGE pulse sequence for determination of GM, WM, and cerebrospinal fluid volume (repetition time = 2.3 ms, echo time = 30 ms, flip angle = 9° , voxel dimensions = $1.0 \times 1.0 \times 1.0 \text{ mm}$).

4.2.3 Data Analysis

Baseline ETCO_2 values from the MRI were corrected to Lab values. The length of the hose to the CO_2 analyzer (located outside the MRI area) resulted in a damping of the signal that significantly diminished the baseline values. Since there was no difference in respiration rates between the Lab and MRI day we corrected MRI values to the average baseline Lab ETCO_2 . The MCA CSA was measured manually by two blinded observers using Osirix imaging software (Pixmeo, Bernex, Switzerland) and the data from both observers was averaged and reported. The agreement between the two observers was very good (intraclass correlation coefficient (ICC) was 0.987 ($p < 0.001$)). The reported CSA during HC is the maximal value from the five minute period and this is reported along with percent change ($\% \Delta$) from baseline. All other reported variables for HC correspond to this maximal CSA value. When reported, the MCA diameter was calculated from the measured CSA. Cerebral blood flow was calculated as $\text{CBF (ml/min)} = \text{CBFV (cm/s)} \times \text{CSA (cm}^2) \times 60 \text{ (s/min)}$. Cerebral blood flow velocity and CBF are also reported as $\% \Delta$. Cerebral blood flow velocity and MCA CSA were collected at the same time of day on separate days and, on average, the interval between each test was 11 ± 11 days.

Using SPM 8 (<http://www.fil.ion.ucl.ac.uk/spm/>), high-dimensional spatial normalization was performed with T1 images using the DARTEL toolbox. A template was created by averaging data from all subjects. Images were then segmented into GM, WM and cerebrospinal fluid. Total intracranial volume was calculated as the sum of these

three components. Since GM volume has been documented to change the most with age we normalized all measurements of CBFV, CBF, CVC, and CVR to GM volume and are reported as CBFV_{GM} , CBF_{GM} , CVC_{GM} , and CVR_{GM} .

Cerebrovascular conductance was calculated as the quotient of CBF_{GM} and MAP. Cerebrovascular reactivity indices were calculated both as the percent and absolute change in CBF_{GM} and CBFV_{GM} per mmHg change in ETCO_2 at approximately every 1.25 minutes during HC (to correspond with the timing of MCA images). The right and left common carotid artery intima-media thickness was quantified with calipers at three regions along the artery and averaged. An independent observer also completed the analysis and the ICC between the observers was 0.985 ($p < 0.001$). An average from the two investigators is reported.

4.2.4 Statistical Analysis

The effects of time (baseline versus hypercapnia) and group (YA versus OA) were assessed using a general linear mixed model ANOVA and a Holm-Sidak post hoc test for pairwise comparisons (SigmaStat 12.0; Systat Software, San Jose, CA) for heart rate, BP, ETCO_2 , respiration, MCA CSA, CBFV_{GM} , CBF_{GM} , CVC_{GM} , and CVR_{GM} . Unpaired t-tests were used to assess the impact of group on GM, WM and cerebrospinal fluid. The probability level for statistical significance was $p \leq 0.05$.

4.3 Results

On average, OA had greater systolic BP, fasting glucose, total and LDL cholesterol, triglycerides and hemoglobin A1C levels than YA but were still within the normal range (Table 4.1). On separate testing days (Lab and MRI) there were no differences in seated BP in YA or OA prior to beginning experimental protocols. Additionally, OA had greater intima-media thickness of the left and right common carotid arteries (Table 4.1). There were no differences in MoCA scores or Part B of the Trail Making Test between groups. Time to complete Part A of the Trail Making Test was 26 ± 10 s for the OA and 19 ± 6 s for the YA ($p = 0.07$). Testosterone levels in older postmenopausal women were greater than YA females ($p = 0.03$; Table 4.2) and 17- β estradiol levels were not detectable in 4 of

5 OA females. In the female with detectable estradiol the levels were within the postmenopausal range (<202 pmol/L).

A main effect of time (baseline to HC) was observed for heart rate and ETCO_2 in the Lab and MRI and diastolic BP in the Lab ($p<0.001$ for all) (Table 4.3). A group x time interaction was present for systolic BP where baseline ($p=0.03$) and HC ($p=0.002$) systolic BP values were greater in OA versus YA and there was a significant increase during HC ($p<0.001$) in OA that was not present in YA. There were also main effects of time ($p=0.003$) and group ($p=0.002$) for MRI respiration where respiration was greater in YA compared to OA.

There was a significant effect of time (baseline to HC) when absolute MCA CSA was compared to baseline but no effect of group was observed (Figure 4.1C). Specifically, in YA, MCA CSA increased from 6.5 ± 1.6 to 7.1 ± 1.4 mm² with HC while OA CSA changed from 7.0 ± 1.2 to 7.3 ± 1.4 mm² (Figure 4.1A and B). A significant difference between YA and OA was observed in $\% \Delta$ CSA ($p=0.04$; Figure 4.1D).

Grey matter volume was decreased in OA compared to YA ($p=0.008$) while WM volume was not different (Table 4.4). Compared to YA, cerebrospinal fluid volume was increased in OA ($p=0.02$) but the total intracranial volume was not different between groups. A main effect of time ($p<0.001$) but no effect of group was observed for CBFV_{GM} where HC was greater than baseline. Similarly, for CBF_{GM} there was a main effect of time ($p<0.001$) and no effect of group. There were significant differences in both YA ($p<0.001$) and OA ($p=0.04$; Figure 4.2C) when the $\% \Delta$ was compared for CBFV_{GM} and CBF_{GM} where CBFV_{GM} was lower than CBF_{GM} .

At baseline and during HC MAP was greater in OA than YA ($p=0.01$ at baseline and $p<0.001$ during HC; Figure 4.3A). Mean arterial pressure during HC was also greater than baseline levels within each group ($p=0.02$ in YA and $p<0.001$ in OA). At baseline there was no difference in CVC_{GM} between YA and OA (Figure 4.3B). During HC, CVC_{GM} was elevated in YA compared to OA ($p=0.02$). Additionally, within group differences in CVC_{GM} were present during HC compared to baseline where there was an increase in CVC_{GM} with HC (YA: $p<0.001$ and OA: $p<0.001$).

Cerebrovascular reactivity was determined in absolute and relative terms using both CBFV_{GM} and CBF_{GM} . There was no effect of group (YA versus OA) but a significant difference where CBFV_{GM} was lower when CBF_{GM} was used for absolute CVR_{GM} ($p < 0.001$; Figure 4.4A). Relative CVR_{GM} calculated with CBFV_{GM} was decreased compared to the same estimate calculated with CBF_{GM} in YA but not OA ($p = 0.001$; Figure 4.4B).

Table 4.1: Subject characteristics.

	YA	OA
n, male/female	12, 6/6	10, 5/5
Height (cm)	173 \pm 14	171 \pm 12
Weight (kg)	69 \pm 14	74 \pm 14
BMI (kg/m²)	23 \pm 3	25 \pm 3
Systolic BP (mmHg)	112 \pm 9	123 \pm 11*
Diastolic BP (mmHg)	72 \pm 6	75 \pm 11
Glucose (mmol/L)	4.8 \pm 0.5	5.4 \pm 0.4*
Total cholesterol (mmol/L)	3.92 \pm 0.50	5.00 \pm 0.77*
HDL cholesterol (mmol/L)	1.50 \pm 0.46	1.59 \pm 0.45
LDL cholesterol (mmol/L)	2.10 \pm 0.47	2.94 \pm 0.51*
Triglycerides (mmol/L)	0.70 \pm 0.27	1.05 \pm 0.48*
HbA1C (mmol/L)	0.053 \pm 0.002	0.057 \pm 0.003*
IMT (mm)		
Right	0.44 \pm 0.05	0.73 \pm 0.13*
Left	0.48 \pm 0.06	0.74 \pm 0.17*
MoCA score (out of 30)	28 \pm 1	28 \pm 2

Trail Making Test (s)

Part A	19 ± 6	26 ± 10
Part B	41 ± 13	61 ± 33

Values are mean ± standard deviation. BMI = body mass index; BP = blood pressure; HbA1C = hemoglobin A1C; HDL = high density lipoprotein; IMT = intima-media thickness; LDL = low density lipoprotein; MoCA = Montreal cognitive assessment; OA = older adults; YA = young adults. *p<0.05 versus YA.

Table 4.2: Sex hormones in young and older adults.

	YA		OA	
	Males	Females	Males	Females
	(n=6)	(n=6)	(n=5)	(n=5)
17- β Estradiol (pmol/L)	79 \pm 28	125 \pm 28	106 \pm 34	N/A*
Progesterone (nmol/L)	2.4 \pm 1.3	1.6 \pm 0.8	1.3 \pm 0.6	0.8 \pm 0.5
Testosterone (nmol/L)	18.5 \pm 6.3	0.9 \pm 0.4	18.3 \pm 7.8	0.5 \pm 0.2 \dagger

Values are mean \pm standard deviation. *Four of five postmenopausal women had 17- β estradiol levels lower than the assay could detect (<19 pmol/L) while the remaining woman was 47 pmol/L. OA = older adults; YA = young adults. \dagger p<0.05 versus YA females with t-test.

Table 4.3: Physiological characteristics at baseline and hypercapnia for Lab and MRI.

	YA		OA		<i>P</i> -value		
	Baseline	HC	Baseline	HC	Time	Group	Interaction
LAB							
Heart rate (bpm)	65 ± 9	71 ± 10	62 ± 11	68 ± 11	<0.001	0.49	0.97
SBP (mmHg)	114 ± 10	116 ± 12	124 ± 10*	132 ± 10*†	<0.001	0.07	0.04
DBP (mmHg)	68 ± 7	71 ± 7	73 ± 10	77 ± 10	<0.001	0.13	0.29
Respiration (breaths per minute)	13 ± 3	14 ± 5	11 ± 3	11 ± 3	0.62	0.07	0.93
ETCO ₂	38 ± 4	49 ± 4	39 ± 3	49 ± 4	<0.001	0.97	0.95

MRI

Heart rate (bpm)	71 ± 13	78 ± 13	69 ± 15	74 ± 15	<0.001	0.57	0.42
Respiration (breaths per minute)	15 ± 3	17 ± 4	10 ± 4	11 ± 4	0.003	0.002	0.83
ETCO ₂	38 ± 4	51 ± 2	38 ± 3	51 ± 3	<0.001	0.67	0.80

Values are mean ± standard deviation. DBP = diastolic blood pressure; ETCO₂ = end tidal carbon dioxide; HC = hypercapnia; OA = older adults; SBP = systolic blood pressure; YA = young adults. *p<0.05 compared to baseline. †p<0.05 compared to YA.

Table 4.4: Brain volume in young and older adults.

	YA	OA
Grey matter (ml)	719 ± 98	622 ± 50*
White matter (ml)	536 ± 60	545 ± 58
Cerebrospinal fluid (ml)	222 ± 37	266 ± 40*
Total intracranial volume (ml)	1476 ± 175	1432 ± 131

Values are mean ± standard deviation. OA = older adults; YA = young adults. *p<0.05 for baseline versus YA.

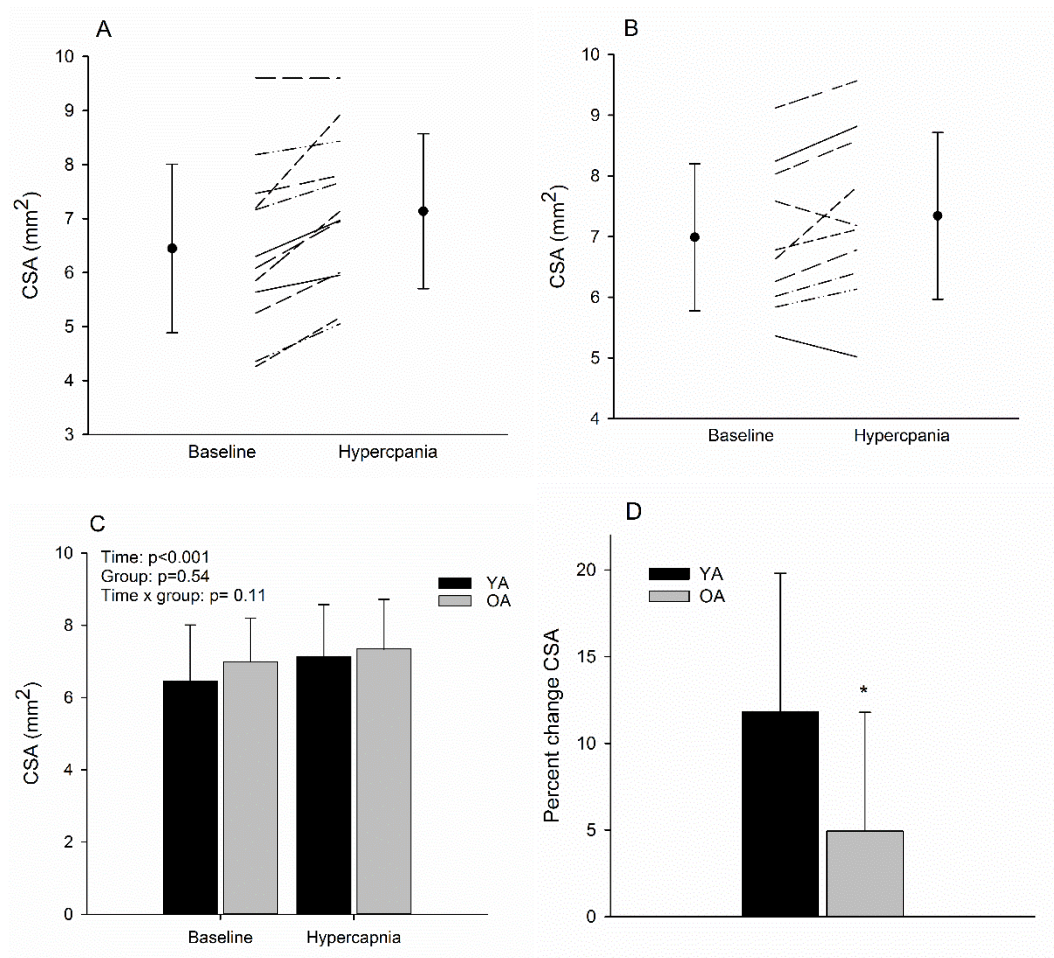


Figure 4.1: Middle cerebral artery cross-sectional area (CSA) during hypercapnia in young adults (YA) and older adults (OA). A: Mean and individual CSA at baseline and hypercapnia in YA. B: Mean and individual CSA at baseline and hypercapnia in OA. C: Mean CSA at baseline and hypercapnia in YA and OA. D: CSA percent change from baseline. * $p < 0.05$ versus YA.

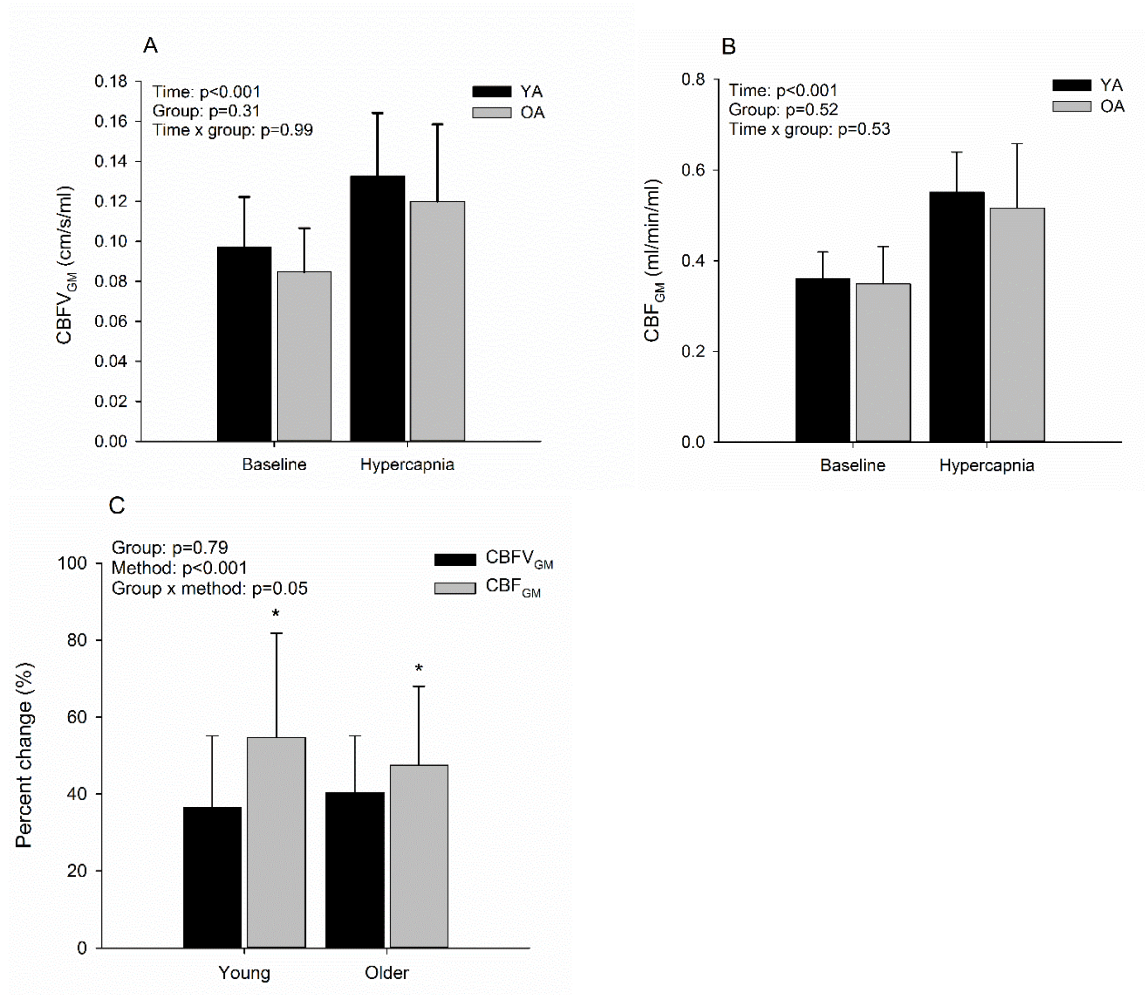


Figure 4.2: Cerebral blood flow velocity (CBFV) and cerebral blood flow (CBF) during hypercapnia in young adults (YA) and older adults (OA). A: CBFV at baseline and hypercapnia in YA and OA. B: CBF at baseline and hypercapnia in YA and OA. C: Percent change CBFV and CBF with hypercapnia in YA and OA. * $p < 0.05$ versus CBFV.

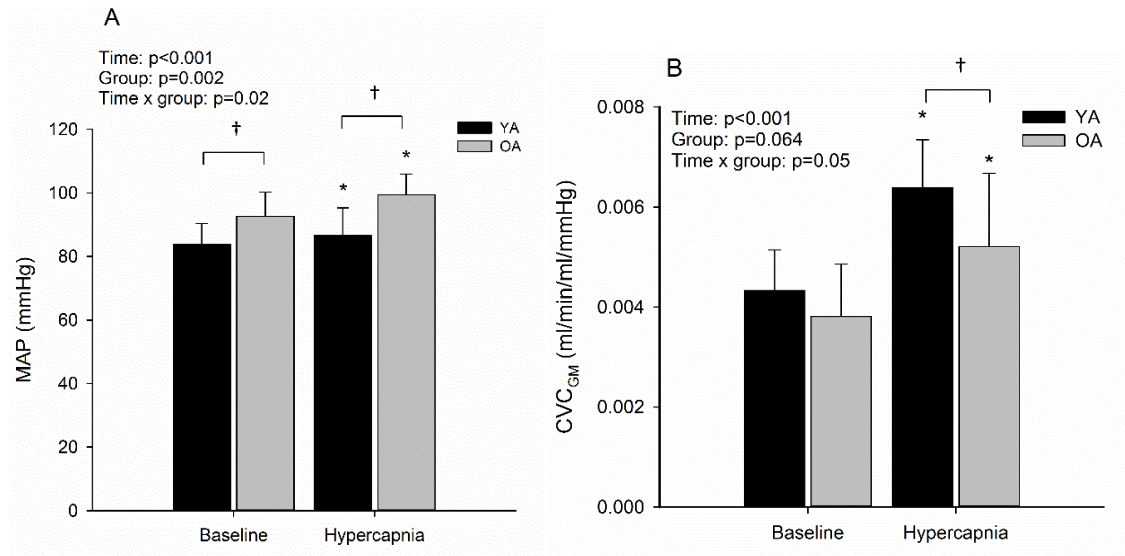


Figure 4.3: Mean arterial pressure (A) and cerebrovascular conductance (B) at baseline and hypercapnia in young adults (YA) and older adults (OA). * $p < 0.05$ versus baseline; † $p < 0.05$ versus YA.

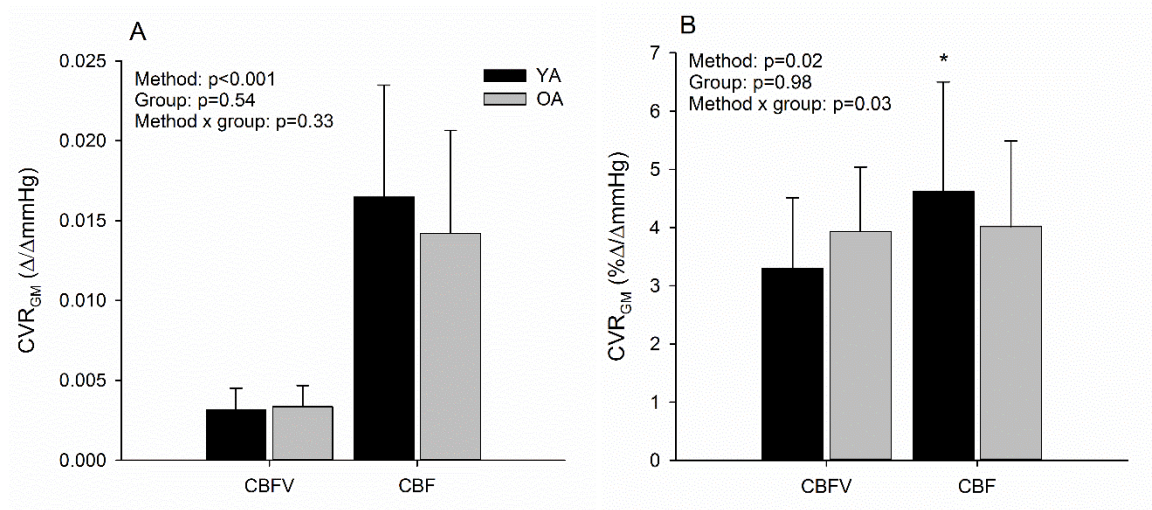


Figure 4.4: Cerebrovascular reactivity (CVR) at baseline and hypercapnia in young adults (YA) and older adults (OA). A: Absolute CVR in YA and OA. B: Relative CVR in YA and OA. * $p < 0.05$ compared to CBFV CVR.

4.4 Discussion

The main findings of this study are as follows: 1) The $\% \Delta$ in MCA CSA with HC was greater in YA than OA. 2) When corrected to GM volume, MCA flow velocity or blood flow were not different between YA and OA at baseline or during HC. 3) CBFV_{GM} underestimated the change in CBF_{GM} with HC in both YA and OA. 4) There was a greater change in CVC_{GM} during HC in YA than OA. 5) Despite the smaller dilatory response in OA versus YA, CVR was not different between the groups due to the compensatory central hemodynamic contributions to CBF through elevated BP in OA. Therefore, when studying MCA flow patterns, reductions in absolute baseline CBF in healthy aging are related to reductions in cortical mass. Furthermore, the aging process appears to include diminished cerebrovascular dilatory responsiveness in the MCA and its downstream vascular bed. In addition to exposing age-related decrements in CVC, these data outline the concern that the sole use of CVR to study cerebrovascular health may be misleading due to compensatory responses that can elevate CBF despite smaller dilatory responses.

A major finding of the current study was the smaller dilation of the MCA in OA in response to HC. The mechanism(s) involved in this impaired dilation is beyond the scope of this study but may include arterial stiffening or impaired endothelial function as it pertains to HC or shear stress stimuli. Extracellular pH of the cerebrovasculature is the main mediator of the HC-induced increase in CBF (64) via an effect on potassium channels (63) and it is unclear how aging may affect these channels. In addition, NO and prostaglandins may also play a role in this response (2, 17). Unfortunately, studying endothelial function in the intact, conscious human brain is difficult though drug studies have been employed to examine endothelial regulation of the cerebrovasculature. The hypercapnic increase in CBFV measured with TCD in humans (23) and CBF with the ^{133}Xe clearance method in rats (28) was impaired with NO synthase blockade, though not abolished. Additionally, administration of a NO donor to patients with endothelial dysfunction restores CVR measured with TCD to levels of healthy age-matched controls (71). However, other studies have found no effect of NO inhibition on the response to HC in humans (12, 29). It is possible that blockade of one pathway results in upregulation of

another (for example, the prostaglandin pathway) since it is not the NO pathway alone that is responsible for the hyperemic response to HC. Additionally, when indomethacin is administered to block the prostaglandin pathway in humans a difference in YA and OA in baseline TCD CBFV and CVR is abolished, which indicates that the prostaglandin-mediated response to HC is impaired with aging (11).

This study is the first to incorporate direct measures of MCA CSA and CBF scaled to GM volume in calculations of flow responses in a healthy aging model. A major outcome of this approach was the observation that healthy aging does not affect CVR. Previously, reports on the impact of age on CVR were based primarily on mean CBFV through the MCA (2, 9, 18, 20). Yet, even CVR calculated using CBFV was the same between groups when normalized to GM volume. Therefore, these data highlight the importance of considering contributing factors to the flow response. These findings are in line with other human studies that have reported no difference in CVR with age using TCD (9, 18). Galvin et al. (2010) and Murrell et al. (2013) found no difference in CVR between young and older groups with a very similar age range to our subjects. However, MAP during HC was not reported in either of these studies so it is unclear whether a greater pressor response played a role in maintaining CVR in OA as we suggest based on our data. These studies also reported an increase in cerebrovascular resistance in the older participants which is in line with the reduction in conductance during HC that we observed in OA.

The major outcome of this study was quantification of an age-related reduction in dilatory responsiveness at the MCA and the downstream vessels that it supplies. These data confirm the findings of Barnes et al. (2012) who drew similar conclusions based on TCD CBFV measures alone (11). Additionally, Barnes et al. (2012) found no differences in CVC between young and older adults when indomethacin was administered. These findings suggest that with age, one pathway that may be altered is cyclooxygenase-mediated dilation. Our results add to these findings because they confirm that CVC calculated based on CBF rather than CBFV is diminished in OA. Also, the impairment in dilation that results in decreased CVC is not limited to vessels downstream to the MCA,

but also to the MCA itself. Finally, changes in GM volume with aging cannot account for the difference in CVC between young and older groups.

The discussion above outlines the problem that measures of CVR_{GM} and CVC_{GM} support opposing conclusions in the context of studying human cerebrovascular health. These findings lead to the question of whether CVR or CVC is a more appropriate metric for examining the dilatory capacity of the cerebrovasculature. A major point here is that CVR does not measure vasodilation but only the flow response to a stimulus. In turn, changes in flow can be incurred by either a change in downstream conductance and/or by a change in the pressure gradient. The cerebrovascular pressure gradient is difficult to measure in humans but is formed to a large extent by the systemic BP. Nonetheless, rarely is BP measured or reported in CVR measures despite evidence that HC elevates BP (13, 20). The current study indicated that the pressor response to HC is greater in OA compared to YA. By accounting for changes in MAP, the current calculation of CVC_{GM} exposed the reduced dilatory response in the OA. The effect of MAP on CBFV has been examined and reported that above a threshold $ETCO_2$, increases in MAP with $ETCO_2$ have a linear relationship with CBFV (13). As well, Claassen et al. (2007) found that the magnitude of increase in an index of CVC with a rebreathing challenge was greater than the magnitude of change in CBFV which suggests that MAP has a direct effect on CBFV (20). Based on these findings and the fact that the change in MAP during HC was different between groups, we suggest that the best way to rationalize these findings is to calculate a CVC reactivity index as the change in CVC divided by the change in $ETCO_2$. When this is done as a percent change in CVC_{GM} there is no difference between YA ($4.22 \pm 1.60 \text{ \%/mmHg}$) and OA ($3.18 \pm 1.34 \text{ \%/mmHg}$, $p=0.11$). However, the difference is significant using the absolute change in CVC_{GM} (YA: $1.8 \times 10^{-4} \pm 0.69 \times 10^{-4}$ ml/min/ml/mmHg and OA: $1.2 \times 10^{-4} \pm 0.56 \times 10^{-4}$ ml/min/ml/mmHg, $p=0.04$).

We examined the relationship between GM volume and cerebrovascular indices based on the idea that there is a linkage between CBF and tissue atrophy. Previous studies have reported decreased CBFV in OA compared to YA (2, 20, 31) and when we normalized CBFV to GM volume we did not see differences in $CBFV_{GM}$, CBF_{GM} , or CVR_{GM} . However, a difference in CVC between groups was present during HC even

when normalized to GM volume. One limitation of this normalization approach is that we used total GM volume though the MCA is not responsible for perfusion of all the GM and the exact portion of tissue that it supplies is unknown. This estimate was used because it is difficult to determine exactly which regions are supplied by the MCA due to individual variation. The challenge of our approach is exposed by Chen et al. (2011) who examined voxel-wise measures of cortical blood flow using MRI perfusion methods (arterial spin labelling) and cortical thickness and reported that, on that small scale, reductions in CBF with aging were dissociated from the concurrent process of cortical atrophy (18). Therefore, our results suggest that an overall relationship exists between CBF and GM volume; however, the pattern becomes dissociated at the voxel scale. Additionally, with this cross-sectional approach we are unable to determine if initial atrophy results in the flow reduction or a flow impairment leads to atrophy.

In conclusion, this study was the first to show that the MCA and its vascular bed display impaired dilation to hypercapnia in healthy aging. Our studies indicate that the measure of CVC and/or CVC reactivity to CO₂ is a more appropriate estimate of the dilatory capacity of the cerebrovasculature than a traditional estimate of CVR. Additionally, we confirm that there is a relationship between GM volume and MCA CBF so that a reduction in MCA CBFV and/or CBF with age may be a result of global GM tissue atrophy, or impaired flow leads to atrophy, and this should be accounted for when making comparisons between groups.

4.5 References

1. Bakker SL, de Leeuw FE, den Heijer T, Koudstaal PJ, Hofman A, Breteler MM. Cerebral haemodynamics in the elderly: the rotterdam study. *Neuroepidemiology* 23: 178–184, 2004.
2. Barnes JN, Schmidt JE, Nicholson WT, Joyner MJ. Cyclooxygenase inhibition abolishes age-related differences in cerebral vasodilator responses to hypercapnia. *J Appl Physiol* 112: 1884–1890, 2012.
3. Battisti-Charbonney A, Fisher J, Duffin J. The cerebrovascular response to carbon dioxide in humans. *J Physiol* 589: 3039–3048, 2011.
4. Chen JJ, Rosas HD, Salat DH. Age-associated reductions in cerebral blood flow are independent from regional atrophy. *Neuroimage* 55: 468–478, 2011.
5. Claassen JA, Zhang R, Fu Q, Witkowski S, Levine BD. Transcranial Doppler estimation of cerebral blood flow and cerebrovascular conductance during modified rebreathing. *J Appl Physiol* 102: 870–877, 2007.
6. Coverdale NS, Gati JS, Opalevych O, Perrotta A, Shoemaker JK. Cerebral blood flow velocity underestimates cerebral blood flow during modest hypercapnia and hypocapnia. *J Appl Physiol* 117: 1090–1096, 2014.
7. Coverdale NS, Lalande S, Perrotta A, Shoemaker JK. Heterogeneous patterns of vasoreactivity in the middle cerebral and internal carotid arteries. *Am J Physiol Heart Circ Physiol*. (February 27, 2015). doi: 10.1152/ajpheart.00761.2014.
8. Fluck D, Beaudin AE, Steinback CD, Kumarpillai G, Shobha N, McCreary CR, Peca S, Smith EE, Poulin MJ. Effects of aging on the association between cerebrovascular responses to visual stimulation, hypercapnia and arterial stiffness. *Front Physiol* 5: 49, 2014.

9. Galvin SD, Celi LA, Thomas KN, Clendon TR, Galvin IF, Bunton RW, Ainslie PN. Effects of age and coronary artery disease on cerebrovascular reactivity to carbon dioxide in humans. *Anaesth Intensive Care* 38: 710–717, 2010.
10. Gerhard M, Roddy M, Creager S, Creager M. Aging progressively impairs endothelium-dependent vasodilation in forearm resistance vessels of humans. *Hypertension* 27: 849–853, 1996.
11. Goldstein LB, Bushnell CD, Adams RJ, Appel LJ, Braun LT, Chaturvedi S, Creager MA, Culebras A, Eckel RH, Hart RG, Hinchey JA, Howard VJ, Jauch EC, Levine SR, Meschia JF, Moore WS, Nixon JVI, Pearson TA. Guidelines for the primary prevention of stroke: a guideline for healthcare professionals from the American Heart Association/American Stroke Association. *Stroke* 42: 517–584, 2011.
12. Ide K, Worthley M, Anderson T, Poulin MJ. Effects of the nitric oxide synthase inhibitor L-NMMA on cerebrovascular and cardiovascular responses to hypoxia and hypercapnia in humans. *J Physiol* 584: 321–332, 2007.
13. Ito H, Kanno I, Ibaraki M, Hatazawa J. Effect of aging on cerebral vascular response to $P_a\text{CO}_2$ changes in humans as measured by positron emission tomography. *J Cereb Blood Flow Metab* 22: 997–1003, 2002.
14. Kitazono T, Faraci F, Taguchi H, DD H. Role of potassium channels in cerebral blood vessels. *Stroke* 26: 1713–1723, 1995.
15. Kontos HA, Raper AJ, Patterson JL. Analysis of vasoactivity of local pH, PCO_2 and bicarbonate on pial vessels. *Stroke* 8: 358–360, 1977.
16. Kruggel F. MRI-based volumetry of head compartments: normative values of healthy adults. *Neuroimage* 30: 1–11, 2006.
17. Lavi S, Gaitini D, Milloul V, Jacob G. Impaired cerebral CO_2 vasoreactivity: association with endothelial dysfunction. *Am J Physiol Circ Physiol* 291: H1856–1861, 2006.

18. Murrell CJ, Cotter JD, Thomas KN, Lucas SJ, Williams MJ, Ainslie PN. Cerebral blood flow and cerebrovascular reactivity at rest and during sub-maximal exercise: effect of age and 12-week exercise training. *Age* 35: 905–920, 2013.
19. Nasreddine ZS, Phillips NA, Bédirian V, Charbonneau S, Whitehead V, Collin I, Cummings JL, Chertkow H. The Montreal Cognitive Assessment, MoCA: A brief screening tool for mild cognitive impairment. *J Am Geriatr Soc* 53: 695–699, 2005.
20. Oudegeest-Sander MH, van Beek AHEA, Abbink K, Olde Rikkert MGM, Hopman MTE, Claassen JAHR. Assessment of dynamic cerebral autoregulation and cerebrovascular CO₂ reactivity in ageing by measurements of cerebral blood flow and cortical oxygenation. *Exp Physiol* 99: 586–598, 2014.
21. Pfefferbaum A, Rohlfing T, Rosenbloom M, Chu W, Colrain I, Sullivan E. Variation in longitudinal trajectories of regional brain volumes of healthy men and women (ages 10 to 85 years) measured with atlas-based parcellation of MRI. *Neuroimage* 65: 176–193, 2013.
22. Portegies ML, de Bruijn RF, Hofman A, Koudstaal PJ, Ikram MA. Cerebral vasomotor reactivity and risk of mortality: the Rotterdam Study. *Stroke* 45: 42–47, 2014.
23. Schmetterer L, Findl O, Strenn K, Graselli U, Kastner J, Eichler H, Wolzt M. Role of NO in the O₂ and CO₂ responsiveness of cerebral and ocular circulation in humans. *Am J Physiol Integr Comp Physiol* 273: R2005–R2012, 1997.
24. Silvestrini M, Vernieri F, Pasqualetti P, Matteis M, Passarelli F, Troisi E, Caltagirone C. Impaired cerebral vasoreactivity and risk of stroke in patients with asymptomatic carotid artery stenosis. *JAMA* 283: 2122–2127, 2000.
25. Singh N, Prasad S, Singer DRJ, MacAllister R. Ageing is associated with impairment of nitric oxide and prostanoid dilator pathways in the human forearm. *Clin Sci (Lond)* 102: 595–600, 2002.

26. Tombaugh TN. Trail Making Test A and B: normative data stratified by age and education. *Arch Clin Neuropsychol* 19: 203–214, 2004.
27. Verbree J, Bronzwaer A-SGT, Ghariq E, Versluis MJ, Daemen MJAP, van Buchem MA, Dahan A, van Lieshout JJ, van Osch MJP. Assessment of middle cerebral artery diameter during hypocapnia and hypercapnia in humans using ultra-high-field MRI. *J Appl Physiol* 117: 1084–1089, 2014.
28. Wang Q, Paulson OB, Lassen NA. Effect of nitric oxide blockade by N^G-Nitro-L-Arginine on cerebral blood flow response to changes in carbon dioxide tension. *J Cereb Blood Flow Metab* 12: 947–953, 1992.
29. White RP, Deane C, Vallance P, Markus HS. Nitric oxide synthase inhibition in humans reduces cerebral blood flow but not the hyperemic response to hypercapnia. *Stroke* 29: 467–472, 1998.
30. Yamamoto M, Meyer JS, Sakai F, Yamaguchi F. Aging and cerebral vasodilator responses to hypercarbia: responses in normal aging and in persons with risk factors for stroke. *Arch Neurol* 37: 489–496, 1980.
31. Zhu YS, Tarumi T, Tseng BY, Palmer DM, Levine BD, Zhang R. Cerebral vasomotor reactivity during hypo- and hypercapnia in sedentary elderly and Masters athletes. *J Cereb Blood Flow Metab* 33: 1190–1196, 2013.

Chapter 5

5 General Discussion

5.1 Perspectives

A literature search in PubMed using the search term “transcranial Doppler ultrasound” elicits a response of almost 8,000 papers. A majority of these papers examine the MCA and all assume that the diameter of the MCA does not change or that the change is negligible so CBFV is the same as CBF. Hypercapnia and/or hypocapnia are commonly used to examine cerebrovascular health where a greater increase in CBFV with HC and/or a greater decrease in CBFV with HO is a healthier response. Based on evidence that MCA diameter may not be constant combined (2, 4) with a greater availability of MRI technology with enhanced resolution we designed this series of studies to examine how MCA CSA changes with HC or HO. Additionally, we wanted to quantify how changes in MCA CSA impact estimates of CBF and CVR in young and older populations. Finally, we examined how changes in MCA CSA compare to those at the ICA with HC and HO.

5.2 Major Findings

The main finding of this series of studies were that MCA CSA increased during HC and decreased during HO. When the findings from all three studies using HC (n=36) and the two studies with HO (n=24) for young adults were combined the average increase was $15 \pm 8\%$ during HC and the average decrease was $9 \pm 6\%$ during HO (Figure 5.1). When CBFV was compared to CBF during HC, CBFV underestimated the change in CBF. Also, CVR during HC was underestimated if CBFV was used. In the first study of this series we documented similar results with HO where CBFV underestimated the change in CBF and CVR. However, in the second study of this series the difference between CBF and CBFV was not significant during HO. Additionally, even in OA where the change in CSA was smaller during HC, this still resulted in a greater change in CBF versus CBFV.

When the CSA data from all studies are combined (Figure 5.1) an important observation is that there is variability in the data both in baseline CSA and in the response HC and HO. Initially, we were hopeful that a universal correction factor could be applied so that TCD users could correct CBFV measurements based on the amount of change in ETCO_2 to more closely estimate CBF; however this is not practical because of the variability in the response. For example, in the subject with the largest baseline CSA (who also had the smallest response to HC), during HC there was no diameter change so CBFV is equivalent to CBF. However, in the subject with the greatest hypercapnic response, the MCA CSA change was almost 29% resulting in a 42% difference in estimates of CBFV and CBF. During HO, there were also subjects who had almost no constriction at the MCA while the greatest change was a 22% decrease which resulted in an 11% difference in CBFV and CBF.

Comparison of diameter changes at the MCA to the ICA during HC and HO revealed that the dilation/constriction response is greater at the MCA as no change was observed in ICA diameter. This difference was not expected as Willie et al. (2012) had documented changes in ICA diameter with HO and HC (5). Different exposure times to HC and HO likely played a role in these observations as we did HC and HO for five minutes while Willie et al. (2012) applied each stimulus for 12 to 15 minutes before measurement for CBFV (5). Future studies could examine MCA CSA over longer exposure to HC and HO. Another notable finding from this study was that at the end of five minutes, CVR calculated with ICA CBF produced similar estimates to those from MCA CBF. Since ICA CBF can be quantified with duplex ultrasound and does not require MRI technology this method of determining CVR is likely more feasible than performing TCD to determine CBFV and then MRI to determine MCA CSA.

Lastly, CBFV, CBF, and CVR normalized to GM volume were not different between young and older adults while CVC_{GM} and the percent change in MCA CSA was greater in YA during HC. In this study, during HC there was a greater pressor response in OA (7 ± 5 mmHg) versus YA (3 ± 3 mmHg) which we believe compensated for decreased dilation at the MCA to equalize CBF between groups. Based on these findings, we suggest that CVC or CVC reactivity ($\Delta\text{CVC}/\Delta\text{ETCO}_2$) is a more appropriate measure

to examine the dilatory capacity of the cerebrovasculature as it accounts for changes in MAP. Even with 4% CO₂, Barnes et al. (2012) reported, on average, a change in MAP from 81 ± 5 to 84 ± 5 mmHg which suggests that even with a smaller stimulus a change in pressure cannot be avoided (1). Examining the mechanism behind reduced cerebrovascular dilation was beyond the scope of this research. However, previous work has implicated a lack of production or utilization of prostaglandins and/or NO in the response to HC by examining CBFV with TCD (1, 3). Therefore, this same study design could be used to examine CVC in populations with poor endothelial health, such as those with atherosclerosis.

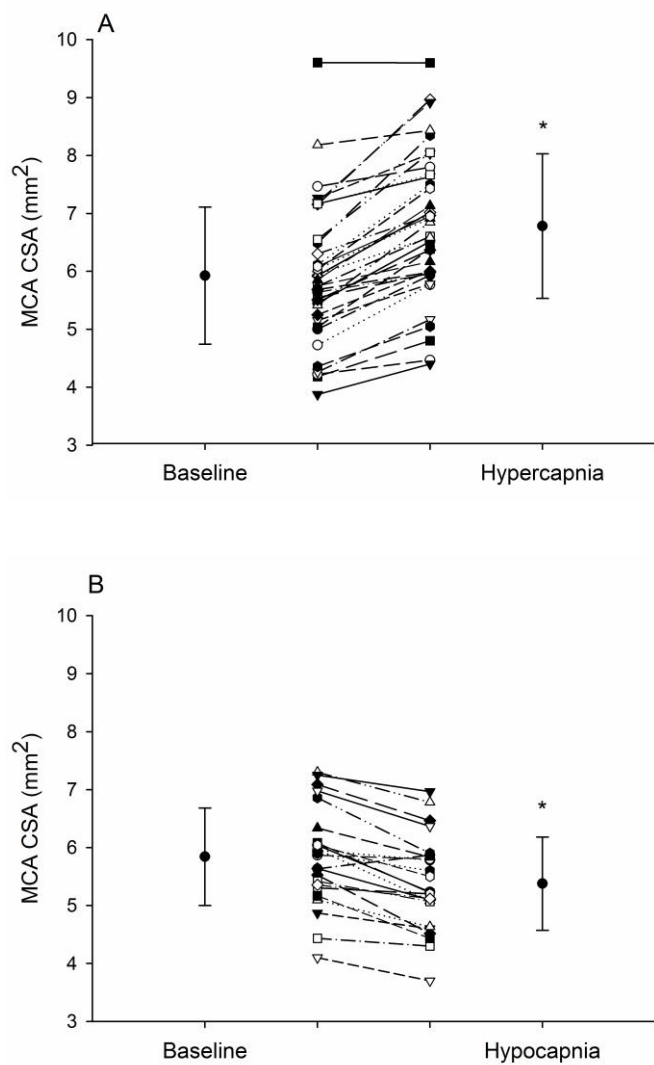


Figure 5.1: Change in middle cerebral artery (MCA) cross-sectional area (CSA) during hypercapnia (A) and hypocapnia (B).

5.3 Utility of Transcranial Doppler Ultrasound

It is important to identify how these changes in MCA CSA during HC and HO may impact the findings of many TCD studies as MRI technology is not as widely accessible or feasible. When examining differences between groups and/or experimental conditions that involve HC or HO it is important to recognize that measured changes in CBFV likely underestimate actual changes in CBF. However, this is more of a problem when comparing groups that likely have differences in arterial health. For example, in the third study in this thesis young and older adults did not have the same dilatory response at the MCA to HC so we cannot say that CBFV underestimates CBF by the same amount in each group. Based on our findings in OA we speculate that other groups of older adults such as those with cardiovascular disease likely have a similar, or possibly even greater, impairment in MCA dilation. Therefore, when comparing such a group to a young population it is more important to keep in mind that changes in the MCA are likely different between groups. In terms of HO, the constrictor response at the MCA was smaller than the dilatory response to HC so changes at the MCA have less of an impact on CBF with HO. For instance, in the second study of this thesis when the changes in CBFV versus CBF were compared over five minutes, no significant changes in HO CSA were detected until minute four. Therefore, for the first three minutes of HO there is little difference between CBFV and CBF. Consequently, employing HO protocols that are shorter in duration is the best way to minimize differences in CBFV versus CBF. Additionally, if the study population consists of all OA then we have established that there is less CSA change even with HC so in this case CBFV is a better indicator of CBF.

Finally, TCD is unmatched in its time resolution. In our studies, a difference in MCA CBFV could be observed within 30 seconds of initiation of HC or HO and tracked beat-by-beat. This is in contrast to our MRI measurement of phase contrast CBFV that took approximately 2.5 minutes to create the velocity profile over one cardiac cycle or our measurement of CSA that could be captured every 1 to 1.25 minutes. Therefore, the aim of these studies was not to imply that TCD is not a useful tool but to encourage examination into some of the basic assumptions of the technique. Application of TCD during changes in ETCO_2 can still be encouraged though possible changes in diameter

should be considered in terms of designing a study that minimizes the impact of these changes so that CBFV more closely predicts CBF.

5.4 Conclusions

In young adults, the MCA dilates by the first minute of hypercapnia and this dilation means that CBFV underestimates both CBF and CVR. In contrast, the MCA does not constrict during hypocapnia until the fourth minute and the impact of this constriction on estimates of CBF and CVR is less than that of hypercapnia. In addition, constriction and dilation at the MCA is unmatched by similar responses at the ICA. Finally, the CVR response to hypercapnia is preserved in healthy older adults, compared to young. However, impaired MCA dilation and CVC in older adults suggests that the dilatory capacity of the cerebrovasculature is impaired in comparison to young adults. Therefore, we suggest that CVC or CVC reactivity is a more telling estimate of the health of the cerebrovasculature than CVR.

5.5 References

1. Barnes JN, Schmidt JE, Nicholson WT, Joyner MJ. Cyclooxygenase inhibition abolishes age-related differences in cerebral vasodilator responses to hypercapnia. *J Appl Physiol* 112: 1884–1890, 2012.
2. Clark JM, Skolnick BE, Gelfand R, Farber RE, Stierheim M, Stevens WC, Beck G, Lambertsen CJ. Relationship of ^{133}Xe Cerebral Blood Flow to Middle Cerebral Arterial Flow Velocity in Men at Rest. *J Cereb Blood Flow Metab*
3. Lavi S, Gaitini D, Milloul V, Jacob G. Impaired cerebral CO_2 vasoreactivity: association with endothelial dysfunction. *Am J Physiol Circ Physiol* 291: H1856–1861, 2006.
4. Valdueza JM, Draganski B, Hoffmann O, Dirnagl U, Einhaupl KM. Analysis of CO_2 vasomotor reactivity and vessel diameter changes by simultaneous venous and arterial Doppler recordings. *Stroke* 30: 81–86, 1999.
5. Willie CK, Macleod DB, Shaw AD, Smith KJ, Tzeng YC, Eves ND, Ikeda K, Graham J, Lewis NC, Day TA, Ainslie PN. Regional brain blood flow in man during acute changes in arterial blood gases. *J Physiol* 590: 3261–3275, 2012.

Appendix A: Ethics Approval



Research Ethics

Use of Human Participants - Ethics Approval Notice

Principal Investigator: Dr. Kevin Shoemaker

File Number: 103083

Review Level: Full Board

Approved Local Adult Participants: 60

Approved Local Minor Participants: 0

Protocol Title: Examining flow and diameter in the middle cerebral artery during different levels of carbon dioxide, lower body negative pressure and nitroglycerin.

Department & Institution: Health Sciences\Kinesiology, Western University

Sponsor: Canadian Institutes of Health Research

Ethics Approval Date: November 13, 2012

Ethics Expiry Date: September 30, 2014

Documents Reviewed & Approved & Documents Received for Information:

Document Name	Comments	Version Date
Letter of Information & Consent	LOI - clean copy	2012/10/18
Western University Protocol		

This is to notify you that the University of Western Ontario Health Sciences Research Ethics Board (HSREB) which is organized and operates according to the Tri-Council Policy Statement: Ethical Conduct of Research Involving Humans and the Health Canada/ICH Good Clinical Practice Practices: Consolidated Guidelines; and the applicable laws and regulations of Ontario has reviewed and granted approval to the above referenced study on the approval date noted above. The membership of this HSREB also complies with the membership requirements for REB's as defined in Division 5 of the Food and Drug Regulations.

The ethics approval for this study shall remain valid until the expiry date noted above assuming timely and acceptable responses to the HSREB's periodic requests for surveillance and monitoring information. If you require an updated approval notice prior to that time you must request it using the University of Western Ontario Updated Approval Request form.

Member of the HSREB that are named as investigators in research studies, or declare a conflict of interest, do not participate in discussions related to, nor vote on, such studies when they are presented to the HSREB.

The Chair of the HSREB is Dr. Joseph Gilbert. The HSREB is registered with the U.S. Department of Health & Human Services under the IRB registration number IRB 00000940.

Signature

Ethics Officer to Contact for Further Information

Janice Sutherland (jsuther@uwo.ca)	Grace Kelly (grace.kelly@uwo.ca)	Shantel Walcott (swalcol@uwo.ca)
---------------------------------------	-------------------------------------	-------------------------------------

This is an official document. Please retain the original in your files.



**Western
Research**

Research Ethics

**Western University Health Science Research Ethics Board
HSREB Amendment Approval Notice**

Principal Investigator: Dr. Kevin Shoemaker
Department & Institution: Health Sciences\Kinesiology, Western University

HSREB File Number: 103083

Study Title: Examining flow and diameter in the middle cerebral artery during different levels of carbon dioxide, lower body negative pressure and nitroglycerin.

Sponsor: Canadian Institutes of Health Research

HSREB Amendment Approval Date: September 10, 2014

HSREB Expiry Date: September 30, 2015

Documents Approved and/or Received for Information:

Document Name	Comments	Version Date
Revised Study End Date		

The Western University Health Science Research Ethics Board (HSREB) has reviewed and approved the amendment to the above named study, as of the HSREB Amendment Approval Date noted above.

HSREB approval for this study remains valid until the HSREB Expiry Date noted above, conditional to timely submission and acceptance of HSREB Continuing Ethics Review. If an Updated Approval Notice is required prior to the HSREB Expiry Date, the Principal Investigator is responsible for completing and submitting an HSREB Updated Approval Form in a timely fashion.

The Western University HSREB operates in compliance with the Tri-Council Policy Statement Ethical Conduct for Research Involving Humans (TCPS2), the International Conference on Harmonization of Technical Requirements for Registration of Pharmaceuticals for Human Use Guideline for Good Clinical Practice Practices (ICH E6 R1), the Ontario Personal Health Information Protection Act (PHIPA, 2004), Part 4 of the Natural Health Product Regulations, Health Canada Medical Device Regulations and Part C, Division 5, of the Food and Drug Regulations of Health Canada.

Members of the HSREB who are named as Investigators in research studies do not participate in discussions related to, nor vote on such studies when they are presented to the REB.

The HSREB is registered with the U.S. Department of Health & Human Services under the IRB registration number IRB 00000940.

Ethics Officer, on behalf of Dr. Joseph Gilbert, HSREB Chair

Ethics Officer to Contact for Further Information

Erika Basile ebasile@uwo.ca	Grace Kelly grace.kelly@uwo.ca	Mina Mekhail mmekhail@uwo.ca	Vikki Tran vikki.tran@uwo.ca
--------------------------------	-----------------------------------	---------------------------------	---------------------------------

This is an official document. Please retain the original in your files.

Appendix B: Letters of Information and Consent Forms

LETTER OF INFORMATION

Project Title: Examining flow and diameter in the middle cerebral artery during different levels of carbon dioxide, lower body negative pressure and nitroglycerin.

Principal Investigator: J. Kevin Shoemaker, Ph.D.

Research Coordinator: Nicole Coverdale, M.Sc.

Katelyn Norton, M.Sc.

Carly Barron, M.Sc.

Sponsor: CIHR team grant in physical activity, mobility and neural health

This letter of information is part of the process of informed consent. It should give you an understanding of the research being conducted and what your participation will involve. If you would like more details regarding something mentioned in this letter, or information not included here, please ask. Take time to read this carefully and to know the following information. You will receive a copy of this form to keep as your own.

Introduction

You are invited to voluntarily participate in a research study that examines how blood vessels in your brain respond to different protocols by using imaging techniques. A variety of stressors change blood flow in the brain and it is currently unclear whether this is because the large blood vessels are changing diameter in response to such stressors. Therefore, the main purpose of the study is to measure the diameter of and flow through larger brain vessels with magnetic resonance imaging (MRI). As well, a type of ultrasound called transcranial Doppler (TCD) is commonly used to study brain blood flow often based on the assumption that large vessel diameter does not change. Therefore, a secondary purpose of this study is to validate TCD measures of blood flow velocity against MRI measures. The study contains three parts that will be conducted on three separate days. A total of 60 participants will be recruited in this study. If you agree to participate, you will be required to come to the laboratory approximately three hours following a light meal and after having avoided alcohol, Nicorette gum, coffee, tea, soft drinks and chocolate for at least 12 hours.

Participant Inclusion/Exclusion Criteria

You will not be included in the study if you are not within the age ranges of 18 and 80 years of age or if you have any of the following: Raynaud's disease, respiratory illnesses, glaucoma, claustrophobia, metallic implants or objects in or under your skin. You will not be included in the study if you are a smoker. In addition, you will not be included in the study if you are, or think you might be, pregnant. Also, you will not be included in the study if you have taken phosphodiesterase type 5 inhibitors within the last 24 hours. This class of drugs includes Viagra, Cialis, and Levitra and are used for the treatment of erectile dysfunction. There is a risk for decreased blood pressure due to the

administration of nitroglycerin in this study and ingestion of these types of drugs magnify this risk. Additionally, since MRI is used in this study, you will not be included in the study if you are not suitable for MRI based on the following criteria:

MRI exclusion criteria

If you have any history of head or eye injury involving metal fragments, if you have some type of implanted electrical device (such as a cardiac pacemaker), if you have severe heart disease (including susceptibility to heart rhythm abnormalities), you should not have an MRI scan unless supervised by a physician. Additionally you should not have a MRI scan if you have conductive implants or devices such as skin patches, body piercing or tattoos containing metallic inks because there is a risk of heating or induction of electrical currents within the metal element causing burns to adjacent tissue.

Research Tests

If you take part in this study, you will report to the laboratory on separate occasions to complete two phases (and 3 Days) of the study. The following addresses what will happen on each day of testing.

Day 1 Instrumentation: Laboratory for Brain and Heart Health, Room 402, Labatt Health Sciences Building.

For the tests that occur at the Laboratory for Brain and Heart Health you will have the following devices attached to you/tests performed for data collection:

1. A button ultrasound probe will be held against the temple region of your head that will determine how fast the blood is flowing through one of the larger vessels in the brain. This process is known as transcranial Doppler ultrasound.
2. Small electrodes will be placed on your chest to record the electrocardiogram (ECG, the heart rate tracing).
3. A small cuff will be placed around one finger and a blood pressure cuff will be placed around the upper portion of the same arm. These cuffs are used to measure your blood pressure. When activated, the finger cuff will inflate with air and you should feel a pulsating sensation on your finger. During a recording session your finger may turn slightly blue and feel numb but this quickly goes away when the cuff pressure is reduced.
4. An elastic strap will be placed around your chest to monitor changes in breathing rate and depth. No discomfort or risks are associated with this procedure.
5. You will be fitted with a small mouthpiece so that you can breathe a mixture of gas that is mostly oxygen but contains a higher than normal level of carbon dioxide. Breathing the carbon dioxide will last a minimum of 7 to 8 minutes.
6. You will be asked to breathe faster than normal, in time with a metronome.
7. You will undergo a procedure called “lower body negative pressure (LBNP)”. In this procedure your legs and hips are sealed in a box and a vacuum will create suction around your lower body to mimic the effects of gravity. This lower body

suction mimics the effect of upright posture and, depending on the degree of suction, unloads baroreceptors in the heart and/or in the aortic arch and carotid sinus. The level of suction that will be used is equivalent to the effect of gravity when sitting up.

8. An anesthetist will insert a small plastic tube (catheter) into a large vein in your arm or hand. This catheter will be connected to an intravenous tube through which the anesthetist will infuse a drug called nitroglycerin (used to treat angina) or a saline solution that simply mimics the water portion of your blood. Any infusion will last up to 15 minutes.
9. You will be asked to breathe through an inspiratory impedance threshold device (ITD) attached to a tube. You will experience some resistance while inhaling through this device.

Day 1 Experimental Procedures (Summarized in Figure 1)

You will undergo 5 experimental tasks: 1) Breathing higher-than-normal carbon dioxide (6% CO₂, 21% oxygen and balanced nitrogen), 2) hyperventilating (to reduce carbon dioxide in your blood), 3) LBNP 4) nitroglycerin administration and 5) ITD. Tossing a coin will randomize the order of the first three protocols.

1. Carbon dioxide: a facemask will be attached through which you will breathe air with the same amount of oxygen as with normal air but with more carbon dioxide. Carbon dioxide levels will be monitored from a line attached to the facemask. After 5 minutes of rest, you will breathe CO₂ until end tidal partial pressure of CO₂ (PETCO₂) reaches 50 mmHg (about 2-3 minutes), after which you will continue breathing the gas for 5 minutes for a total of 7 to 8 minutes. This level of CO₂ will make you breathe faster and deeper. Five minutes recovery will then allow your levels of carbon dioxide to return to normal.
2. Hyperventilation: after a 5 minutes rest period, you will be asked to breathe in time with a metronome at a rate that is faster than your normal breathing rate. You will then be given 5 minutes to recover.
3. LBNP: after 5 minutes of rest, suction will be turned on for 5 minutes and this will be followed by 5 minutes of recovery.
4. Saline and nitroglycerin: in a random assignment (like the tossing of a coin) saline or nitroglycerine will be infused. Saline will be infused for 5 minutes and nitroglycerine (0.5 µg/kg/min) will continue for 15 minutes. Five minutes of recovery will end the test.
5. ITD: You will be asked to breathe through a tube with an attached ITD for 1-5 minutes at rest and during LBNP.

The protocols will take approximately 75 minutes for the actual experiment plus time for equipment setup, insertion of the catheter, familiarization with the protocol and recovery from the nitroglycerin. Also, it is expected that the TCD probe will continually need to be adjusted slightly to maximize the quality of the signal. Therefore, the entire test time is expected to be about 3 hours.

Days 2 and 3 Instrumentation: Robarts Research Institute at Western University

For the tests that occur at the Robarts Research Institute you will have the following devices attached to you/tests performed for data collection:

1. The blood vessels in your brain will be imaged, which means that you will lie on a table that enters the bore of a 3.0 Tesla whole-body MRI. It can be noisy during the MRI procedure so you will wear hearing protection (head phones).
2. A small cuff will be placed around one finger and will measure heart rate.
3. An elastic strap will be placed around your chest to monitor changes in breathing rate and depth. No discomfort or risks are associated with this procedure.
4. You will be fitted with a small mouthpiece so that you can breathe a mixture of gas that is mostly oxygen but contains a higher than normal level of carbon dioxide. Breathing the carbon dioxide will last a minimum of 7 to 8 minutes.
5. You will be asked to breathe faster than normal, in time with a metronome.
6. You will undergo a procedure called “lower body negative pressure (LBNP)”. In this procedure your legs and hips are sealed in a box and a vacuum will create suction around your lower body to mimic the effects of gravity. This lower body suction mimics the effect of upright posture and, depending on the degree of suction, unloads baroreceptors in the heart and/or in the aortic arch and carotid sinus. The level of suction that will be used is equivalent to the effect of gravity when sitting up.
7. An anesthetist will insert a small plastic tube (catheter) into a large vein in your arm or hand. This catheter will be connected to an intravenous tube through which the anesthetist will infuse a drug called nitroglycerin (used to treat angina) or a saline solution that simply mimics the water portion of your blood. Any infusion will last up to 15 minutes.
8. You will be asked to breathe through an inspiratory impedance threshold device (ITD) attached to a tube. You will experience some resistance while inhaling through this device.

Days 2 and 3 Experimental Procedures (Summarized in Figure 1)

You will undergo 5 experimental tasks: 1) Breathing higher-than-normal carbon dioxide (6% CO₂, 21% oxygen and balanced nitrogen), 2) hyperventilating (to reduce carbon dioxide in your blood), 3) LBNP, 4) nitroglycerin administration and 5) ITD. Tossing a coin will randomize the order of these tasks.

1. Carbon dioxide: a facemask will be attached through which you will breathe air with the same amount of oxygen as with normal air but with more carbon dioxide. Carbon dioxide levels will be monitored from a line attached to the facemask. After 5 minutes of rest, you will breathe CO₂ until end tidal partial pressure of CO₂ (PETCO₂) reaches 50 mmHg (about 2-3 minutes), after which you will continue breathing the gas for 5 minutes for a total of 7 to 8 minutes. This level of CO₂ will make you breathe faster and deeper. Five minutes recovery will then allow your levels of carbon dioxide to return to normal.
2. Hyperventilation: you will continue wearing the facemask during this protocol. After a 5 minutes rest period, you will be asked to breathe in time with a metronome at a rate that is faster than your normal breathing rate. You will then be given 5 minutes to recover.
3. LBNP: after 5 minutes of rest, suction will be turned on for 5 minutes and this will be followed by 5 minutes of recovery.
4. Saline and nitroglycerin: in a random assignment (like the tossing of a coin) saline or nitroglycerine will be infused. Saline will be infused for 5 minutes and nitroglycerine (0.5 µg/kg/min) will continue for 15 minutes. Five minutes of recovery will end the test.
5. ITD: You will be asked to breathe through a tube with an attached ITD for 1-5 minutes at rest and during LBNP.

The protocols will take approximately 75 minutes for the actual experiment plus time for equipment setup, insertion of the catheter, familiarization with the protocol and recovery from the nitroglycerin. Therefore, the entire test time is expected to be about 2 hours.

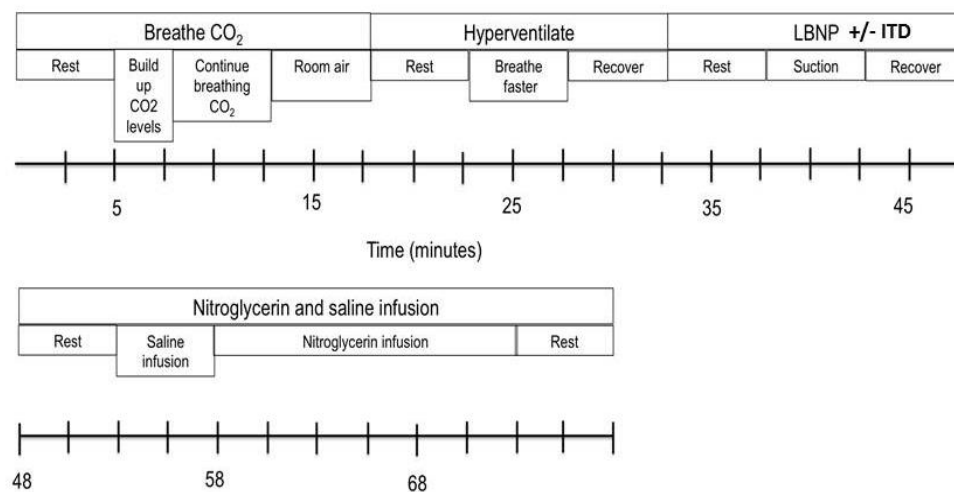


Figure 1. Study protocol.

Risks

MRI

Part of your participation in this study will involve a research test with Magnetic Resonance Imaging (MRI) system, a common medical diagnostic tool that uses a strong magnetic field, a low frequency magnetic field, and a radio frequency field. No X-rays are used. As with any technology there is a risk of death or injury. For MRI the risk of death is less than 1 in 10 million and the risk of injury is less than 1 in 100,000. These risks do not arise from the MRI process itself, but from a failure to disclose or detect MRI incompatible objects in or around the body of the subject or the scanner room. It is therefore very important that you answer all the questions honestly and fully on the MRI screening questionnaire.

Almost all the deaths and injuries related to MRI scans have occurred because the MRI operator did not know that surgically implanted metal hardware (such as a cardiac pacemaker) was present inside the subject during the MRI scan. Other remote risks involve temporary hearing loss from the loud noise inside the magnet. This can be avoided with ear headphone protection that also allows continuous communication between the subject and staff during the scan.

For comparison, the risk of death in an MRI is similar to travelling 10 miles by car, while the risk of injury during an MRI is much less than the risks associated with normal daily activities for 1 hour.

You may not be allowed to continue in this research study if you are unable to have a MRI scan because, for example, you have some MRI incompatible metal in your body, you may be pregnant or attempting to become pregnant, or you may have a drug patch on your skin that contains a metal foil. Should you require a medically necessary MRI scan in the future, the final decision as to whether you can be scanned will be made by a qualified physician considering all the risks and benefits.

Venous Catheter

There is a small risk of bruising or infection when inserting the catheter into your vein. Some patients may experience mild pain and discomfort and some may feel nauseated or dizzy when blood is taken.

ECG

The adhesive on the electrodes used to measure your heart rate may cause a small rash to develop under the electrode. However, this rash should disappear in a day or two.

Blood pressure cuff

There are no known risks of using the finger cuff methods (Finometer) of examining arterial blood pressure. With the finger cuff the fingertip may turn a little blue and feel numb during the prolonged test sessions but this resolves immediately when the cuff is

removed. Standard arm cuff blood pressure measures of arterial pressure will also be obtained periodically, a method that has no known risks.

Transcranial Doppler ultrasound

There are no known harmful effects with standard diagnostic ultrasound and tonometry as used in this study.

CO₂ Breathing

Breathing a slightly higher level of carbon dioxide may give you a small headache and it may make you feel breathless. These feelings vanish quickly when you start breathing room air again.

Lower Body Negative Pressure

As an orthostatic stress, LBNP carries a risk of fainting (syncope). This is particularly important during prolonged levels (i.e., 5-10 minutes). To reduce the risk of syncope you will be instructed to inform the experimenters if you feel any of the symptoms of presyncope (i.e. nausea, light headedness, tunnel vision, blurry vision, excessive heat and sweat). You will also be monitored throughout the test for the following termination criteria: systolic blood pressure less than 90 mmHg, sudden reductions in systolic blood pressure of >20 mmHg, sudden decrease in heart rate or heart rate less than 30 bpm and symptoms suggestive of impending syncope. There is minimal risk to you for the duration and level of LBNP used here because mean arterial pressure is minimally threatened and there is no additional challenge to cerebral perfusion. Also note that syncope does not develop immediately even in full head-up tilt tests. Moreover, the signs of imminent syncope generally develop 1-2 minutes prior to the event (i.e., generally, there is a progressive reduction in blood pressure prior to the sudden hypotension that marks presyncope). We will monitor you for these symptoms and stop the suction upon their first appearance.

Inspiratory impedance Threshold Device

There are no known harmful effects associated with breathing through the ITD as used in this study.

Nitroglycerin

Nitroglycerin may induce headache. A headache occurs in up to 50% of patients as a result of dilation of brain blood vessels. The headache usually disappears within several days with continued treatment. Acetaminophen (Tylenol) may be used to treat nitrate headaches. Other adverse reactions that occur in less than 1% of patients include allergy: itching, wheezing, tracheobronchitis (inflammation of lower respiratory tract); cardiovascular: hypotension (low blood pressure), reflex tachycardia (increased heart rate), palpitations (abnormality of regular heart rhythm), bradycardia (slowed heart rate), syncope due to nitrate vasodilation has rarely been reported; central nervous system: headache, weakness, dizziness, apprehension, restlessness; gastrointestinal: nausea,

vomiting, diarrhea, and abdominal pain; genitourinary: dysuria (difficulty urinating), urinary frequency, impotence; metabolic: methemoglobinemia (abnormal amount of a form of hemoglobin is produced); musculoskeletal: arthralgia (joint pain), muscle twitching; ophthalmologic: blurred vision; respiratory: bronchitis, pneumonia, upper respiratory symptoms.

Staying still

During the experiment, you have to remain still in a lying down position for 3 hours. You may develop a sore back in the middle of the experiment. These sensations will diminish very quickly when you sit up from the bed after the experiment.

Alternatives to Participating

You may choose not to participate in this study.

Benefits to You if You Take Part in the Study

There are no direct benefits to you as a result of the study.

Voluntary Participation

You are encouraged to ask questions regarding the purpose of this study and the outcome of your testing. Participation in this study is voluntary. You may refuse to participate, refuse to answer any questions, or withdraw from the study at any time with no effect on your academic or employment status. We ask that you do not get involved in any other study while you are involved in this study. However, participation in this study will not stop you from being involved in future studies. You do not waive any legal rights by signing the consent form.

Incidental Findings

An incidental finding refers to any unexpected observation made during the course of the study that may require attention by your doctor. Examples could include high blood pressure, irregular heart rhythm or a mass observed with MRI. Should an abnormality be detected during testing, you will be informed and will be encouraged to share this information with your doctor.

Confidentiality

All information that you provide will be kept strictly confidential. No information that could reveal your identity will be released to anyone unless disclosure is required legally. All of the information collected for this study will be stored in a locked filing cabinet that will only be accessible to the research team. To further protect your anonymity, your name will be replaced with a subject ID number on all documents. Representatives of The University of Western Ontario Health Sciences Research Ethics Board may require access to your study-related records or may follow up with you to monitor the conduct of the research.

Compensation

You will be compensated for parking expenses.

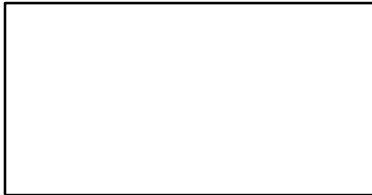
Publication of Results

Published results from this study will not identify you by name. New findings from this study may be forwarded to each interested participant upon request. You may keep a copy of this letter of information.

Contact Persons

If you have any questions regarding this study, please feel free to contact:

Dr. Kevin Shoemaker



If you have any questions about your rights as a participant or about the conduct of the study you may contact The University of Western Ontario Office of Research Ethics,

or email



LETTER OF INFORMED CONSENT

Project Title:

Examining flow and diameter in the middle cerebral artery during different levels of carbon dioxide, lower body negative pressure and nitroglycerin.

Principal Investigator:

J. Kevin Shoemaker, Ph.D.

I have read the letter of information, have had the nature of the study explained to me and I agree to participate. All questions have been answered to my satisfaction.

SIGNATURES

In the event that abnormal findings are observed during any of the tests, or upon my wishes, I consent to the release of my medical information to my family doctor or medical clinic.

Name of Doctor or Clinic

I agree _____

(initial)

OR

I disagree _____

(initial)

Name of participant (Please print)

Signature of participant

Date

Name of person obtaining consent

Signature of person obtaining consent

Date

Appendix C: Rights of Authors of APS Articles

The APS Journals are copyrighted for the protection of authors and the Society. The Mandatory Submission Form serves as the Society's official copyright transfer form.

Rights of Authors of APS Articles

For educational purposes only, authors may make copies of their own articles or republish parts of these articles (e.g., figures, tables), without charge and without requesting permission, provided that full acknowledgement of the source is given in the new work. Authors may not post a PDF of their published article on any website; instead, links may be posted to the article on the APS journal website.

Posting of articles or parts of articles is restricted and subject to the conditions below:

- ***Theses and dissertations.*** APS permits whole published articles to be reproduced without charge in dissertations and posted to thesis repositories. Full citation is required.
- ***Open courseware.*** Articles, or parts of articles, may be posted to a public access courseware website. Permission must be requested from the APS. A copyright fee will apply during the first 12 months of the article's publication by the APS. Full citation is required.
- ***Institutional websites.*** The author's published article (in whole or in part) may not be posted to an institutional website, neither at the institutional nor departmental level. This exclusion includes, but is not limited to, library websites and national government websites. Instead, a link to the article on the APS journal website should be used. (See also the APS [Policy on Depositing Articles in PMC](#).)
- ***Institutional repositories (non-theses).*** The author's published article (in whole or in part) may not be posted to any institutional repository. This exclusion includes, but is not limited to, library repositories and national government repositories. Instead, a link to the APS journal website should be used. (See also the APS [Policy on Depositing Articles in PMC](#).)
- ***Author's article in presentations.*** Authors may use their articles (in whole or in part) for presentations (e.g., at meetings and conferences). These presentations may be reproduced (e.g., in monographs) on any type of media including, but not limited to, CDs, DVDs, and flash drives, for educational use only in materials arising from the meeting or conference such as the proceedings of a meeting or conference. A copyright fee will apply if there is a charge to the user or if the materials arising are directly or indirectly commercially supported.
- ***Reuse in another journal before final publication is prohibited.*** Permission for reuse of an article (whether in whole or in part) in another publication is restricted to the final-published version of the article. If an article is currently published on the APS "publish ahead of print" website (Articles in Press), then the author must wait to request permission to reuse the article, or any part of the article, until such time when the article appears in final-published form on the APS journal website.

Authors who do not have access to a subscription and/or who are not APS members may:

- purchase the article through the pay-per-view option, or
- purchase a Toll-Free Link from APS, which will allow them to post a link to the APS journals website (directly to the article) enabling unlimited free downloads for any user accessing the article via this Toll-Free Link.

Curriculum Vitae

Nicole S. Coverdale

EDUCATION

The University of Western Ontario: 2010 – 2015 (expected)

PhD Integrative Physiology of Exercise

Thesis: Reactivity of the middle cerebral artery to carbon dioxide

Advisor: Dr. J. Kevin Shoemaker, PhD

Brock University: 2008 – 2010

MSc Applied Health Sciences

Thesis: Baroreflex sensitivity in children with Developmental Coordination Disorder

Advisor: Dr. Deborah O’Leary, PhD

Brock University: 2003 – 2007

BSc Health Sciences

Thesis: Examination of differences between mitochondrial and whole tissue fatty acids in plantaris, red gastrocnemius and soleus

Advisor: Dr. Paul LeBlanc, PhD

HONOURS & AWARDS

- | | |
|-------------|---|
| 2014 | Panerai Award for Best Oral Presentation <ul style="list-style-type: none"> • Changes in cerebral blood flow velocity and cross-sectional area of the middle cerebral artery in response to manipulations of end-tidal carbon dioxide. <i>Experimental Biology</i>, San Diego, CA, USA. April 26-30, 2014. |
| 2012 – 2014 | Canadian Institutes of Health Research Doctoral Research Award
Frederick Banting and Charles Best Canada Graduate Scholarship (\$70,000) |
| 2011 – 2012 | Ontario Graduate Scholarship (\$15,000) |
| 2010 – 2011 | Ontario Graduate Scholarship (\$15,000) |
| 2009 – 2010 | Canadian Institutes of Health Research Master’s Award Canada Graduate Scholarship (\$17,500) |
| 2009 – 2010 | Dean of Graduate Studies Excellence Scholarship (\$5,500) |
| 2009 | Ontario Graduate Scholarship (declined) |

2009	Oded Bar-Or Graduate Travel Award in Pediatric Exercise Medicine (\$460)
2008 – 2009	Ontario Graduate Scholarship in Science and Technology (\$12,978)
2008	Dean of Graduate Studies Entrance Scholarship (\$4,000)
2007	Brock Undergraduate Student Research Award (\$3,250)
2003 – 2007	Dean's Honours List
2003 – 2007	Brock Entrance Scholarship (\$2,500)

RESEARCH CONTRIBUTIONS

Articles in Peer Reviewed Journals:

1. **Coverdale NS**, Lalande S, Perrotta A, Shoemaker JK. Heterogeneous patterns of vasoreactivity in the middle cerebral and internal carotid arteries. *Am J Physiol Heart Circ Physiol* 2015 Feb 27:ajpheart.00761.2014. doi: 10.1152/ajpheart.00761.2014. [Epub ahead of print]
2. Usselman CW, Gimon TI, Nielson CA, Luchyshyn TA, **Coverdale NS**, Van Uum SH, Shoemaker JK. Menstrual cycle and sex effects on sympathetic responses to acute chemoreflex stress. *Am J Physiol Heart Circ Physiol* 2014 Dec 19:ajpheart.00345.2014. doi: 10.1152/ajpheart.00345.2014. [Epub ahead of print]
3. Phillips AA, Chirico D, **Coverdale NS**, Fitzgibbon LK, Shoemaker JK, Wade TJ, Cairney J, O'Leary DD. The association between arterial properties and blood pressure in children. *Appl Physiol Nutr Metab* 40: 72-80, 2015.
4. **Coverdale NS**, Gati JS, Opalevych O, Perrotta A, Shoemaker JK. Cerebral blood flow velocity underestimates cerebral blood flow during modest hypercapnia and hypocapnia. *J Appl Physiol* 117: 1090-1096, 2014.
 - Selected for an editorial: Ainslie, PN, Hoiland RL. Transcranial Doppler ultrasound: valid, invalid, or both? *J Appl Physiol* 117: 1081-1083, 2014.
 - Selected for a podcast: December, 2014.
<http://jappl.podbean.com/e/cerebral-blood-flow-velocity-underestimates-cerebral-blood-flow-during-modest-hypercapnia-and-hypocapnia/>
5. Zamir M, **Coverdale NS**, Barron CC, Sawicki CP, Shoemaker JK. Baroreflex variability and "resetting": A new perspective. *J Biomech* 47: 237-244, 2014.

6. **Coverdale NS**, O'Leary DD, Faught BE, Chirico D, Hay J, Cairney J. Baroreflex sensitivity is reduced in adolescents with probable developmental coordination disorder. *Res Developmental Disabil* 33: 251-257, 2012.
7. **Coverdale NS**, Wade TJ, Reid GJ, Fitzgibbon LK, Cairney J, O'Leary DD. Baroreflex sensitivity is associated with sleep-related breathing problems in adolescents. *J Pediatr* 160: 610-614, 2012.
8. Fitzgibbon LK, **Coverdale NS**, Phillips A, Shoemaker JK, Klentrou P, Wade TJ, John Cairney, O'Leary DD. The association between baroreflex sensitivity and blood pressure in children. *Appl Physiol Nutr Metab* 37: 301-307, 2012.
9. Chirico D, O'Leary DD, Cairney J, Haluka K, **Coverdale NS**, Klentrou P, Hay J, Faught BE. Longitudinal assessment of left ventricular structure and function in adolescents with developmental coordination disorder. *Res Developmental Disabil* 33: 717-725, 2011.
10. Stefanyk LE, **Coverdale NS**, Roy BD, Peters SJ, LeBlanc PJ. Skeletal muscle type comparison of subsarcolemmal mitochondrial membrane phospholipid fatty acid composition in rat. *J Membr Biol* 234: 207-215, 2010.

Abstracts in Peer Reviewed Conference Proceedings:

1. **Coverdale NS**, Badrov MB, Shoemaker JK. Examining cerebrovascular reactivity in healthy aging. *Experimental Biology*, Boston, MA, USA. March 28-April 1, 2015.
2. **Coverdale NS**, Lalande S, Perrotta A, Shoemaker JK. Time course of changes in middle cerebral artery cross-sectional area and blood flow during hypercapnia and hypocapnia. *Canadian Society of Exercise Physiology*, St. John's, NL, Canada. October 22-25, 2014.
3. **Coverdale NS**, Gati JS, Opalevych O, Perrotta A, Shoemaker JK. Changes in cerebral blood flow velocity and cross-sectional area of the middle cerebral artery in response to manipulations of end-tidal carbon dioxide. *Experimental Biology*, San Diego, CA, USA. April 26-30, 2014.
4. **Coverdale NS**, Gati JS, Opalevych O, Perrotta A, and Shoemaker JK. Cross-sectional area of the middle cerebral artery changes during manipulations of end-tidal carbon dioxide. *Canadian Society of Exercise Physiology*, Toronto, ON, Canada. October 16-19, 2013.
5. **Coverdale NS**, Usselman CW, Gimon TI, Nielsen CA, Luchyshyn TA, Shoemaker JK. Sympathoinhibition in men during paced breathing at 0.25 Hz. *Experimental Biology*, Boston, MA, USA. April 20-24, 2013.

6. Chirico D, **Coverdale NS**, Wade TJ, Cairney J, O'Leary D. Cardiovagal baroreflex sensitivity in children with elevated blood pressure. *Canadian Society of Exercise Physiology*, Regina, SK, Canada. October 10-13, 2012
7. **Coverdale NS**, Faught B, Klentrou P, Chirico D, Cairney J, Hay J, O'Leary DD. Baroreflex sensitivity is reduced in children with probable DCD. *Developmental Coordination Disorder International Conference IX*, Lausanne, Switzerland. June 23-25, 2011.
8. **Coverdale N**, Banach A, O'Leary DD. Autonomic indices in overweight and obese pre- and early pubescent children. *Canadian Society of Exercise Physiology*, Toronto, ON, Canada. November 3-6, 2010.
9. McMeekin L, Fajardo VA, **Coverdale N**, Hajna S, Stefanyk LE, Roy BD, Peters SJ, LeBlanc PJ. Influence of high-fat diet on subsarcolemmal and intermyofibrillar mitochondrial membrane phospholipid fatty acid composition: examining the conformer-regulator paradigm. *Canadian Society of Exercise Physiology*, Toronto, ON, Canada. November 3-6, 2010.
10. **Coverdale NS**, Fitzgibbon LK, Wade TJ, Reid GJ, Cairney J, O'Leary DD. The effect of sleep-related breathing problems and obesity on baroreflex gain in children. *Second Joint Meeting of the North American Society for Pediatric Exercise Medicine (NASPEM) and the European Group for Pediatric Work Physiology (PWP)*, Niagara-on-the-Lake, ON, Canada. September 22-26, 2010.
11. **Coverdale NS**, Wade TJ, Reid GJ, Fitzgibbon LK, Cairney J, O'Leary DD. Sleep-related breathing problems and pediatric blood pressure regulation. *Pediatric Academic Societies*, Baltimore, MD, USA. May 2-5, 2009.
12. Fitzgibbon LK, Peralta-Huertas J, Phillips AA, **Coverdale NS**, Klentrou P, Cairney J, Wade TJ, O'Leary DD. Baroreflex gain and blood pressure in children. *Pediatric Academic Societies*, Baltimore, MD, USA. May 2-5, 2009.
13. Phillips AA, Peralta-Huertas J, Fitzgibbon LK, Rodrigue E, **Coverdale NS**, Wade TJ, Cairney J, O'Leary DD. Common carotid artery distensibility and high blood pressure in children. *Pediatric Academic Societies*, Baltimore, MD, USA. May 2-5, 2009.
14. Stefanyk LE, **Coverdale NS**, Roy BD, Peters SJ, LeBlanc PL. Skeletal muscle fibre-type comparison of mitochondrial and whole tissue phospholipids and fatty acids. *Canadian Society of Exercise Physiology*, London, ON, Canada. November 14-17, 2007.

TEACHING AND MENTORSHIP EXPERIENCE

Guest Lectures:

The University of Western Ontario, Kinesiology 3347: Human Growth and Development

- Invited lecture for a third year undergraduate course of 100 students.

The University of Western Ontario, Kinesiology 4432: Physiology of Exercise.

Regulation of cerebral blood flow. November 27, 2014.

- Invited lecture for a fourth year undergraduate course of approximately 100 students.

Teaching Assistantships:

KIN4432: Physiology of Exercise (Fall 2013)

School of Kinesiology, The University of Western Ontario

Duties: Grading of assignments, providing teaching support after lectures and during office hours for undergraduate students.

KIN 3330: Laboratory in Exercise Physiology (Fall 2010)

School of Kinesiology, The University of Western Ontario

Duties: Instructing and supervising exercise physiology lab sections for undergraduate students; grading lab reports and exams.

CHSC 2F95: Human Anatomy (Fall & Winter 2007-2008, 2008-2009, 2009-2010)

Faculty of Applied Health Sciences, Brock University

Duties: Course coordinator and teaching assistant. Developed practice questions for all lab groups, served as the contact person between the instructor and other teaching assistants.

CHSC 1F90: Introduction to Community Health Sciences (Fall & Winter 2007-2008)

Faculty of Health Sciences, Brock University

Duties: Seminar Leader. Evaluated student presentations and led discussion.

CHSC 2P07: Biostatistics I (Fall 2005)

Faculty of Health Sciences, Brock University

Duties: Assisted students using a statistical computer program (SAS).

Mentorship:

2014 – Present

Co-supervised the fourth year undergraduate projects of two students. Taught the students ultrasound, data analysis methods, and assisted with developing a presentation and paper on their projects.